

**Spatial sensitivity of midbrain lateral line units
of the goldfish, *Carassius auratus***

Dissertation
zur
Erlangung des Doktorgrades (Dr. rer. nat.)
der
Mathematisch-Naturwissenschaftlichen Fakultät
der
Rheinischen Friedrich-Wilhelms-Universität Bonn

vorgelegt von
Gunnar Meyer
aus Emsbüren

Bonn 2010

Angefertigt mit Genehmigung der Mathematisch-Naturwissenschaftlichen Fakultät der Rheinischen Friedrich-Wilhelms-Universität Bonn

1. Gutachter: Prof. Dr. H. Bleckmann
Institut für Zoologie
Rheinische Friedrich-Wilhelms-Universität Bonn

2. Gutachter: PD Dr. J. Mogdans
Institut für Zoologie
Rheinische Friedrich-Wilhelms-Universität Bonn

Tag der Disputation: 26.03.2010

Diese Dissertation ist auf dem Hochschulschriftenserver der ULB Bonn unter der Adresse http://hss.ulb.uni-bonn.de/diss_online elektronisch publiziert.

Erscheinungsjahr 2010

Contents

List of figures	VII
Abbreviations	VIII
Zusammenfassung	X
Summary	XII
1 Introduction	1
1.1 The mechanosensory lateral line	1
1.2 Periphery of the mechanosensory lateral line	2
1.3 Afferent lateral line pathways	5
1.4 Hydrodynamic stimulation	6
2 Materials & Methods	10
2.1 Experimental animals	10
2.2 Preparation	10
2.3 Experimental setup	11
2.4 Stimulation	13
2.4.1 Stimulus generation	13
2.4.2 Search stimulus	14
2.4.3 Characterisation of unit modality	15
2.4.4 Stimulus protocol	15
2.4.5 Stimulus calibration	17
2.5 Recording	18
2.6 Data analysis	19
2.6.1 Data reduction	19
2.6.2 Response patterns of evoked neural activity	21
2.6.3 Phase histograms	21
2.7 Histology	21
3 Results	23
3.1 Anatomy	23
3.2 Electrophysiology	26
3.2.1 Ongoing activity	26
3.2.2 Response patterns of evoked neural activity	26
3.2.3 Spatial excitation patterns	26
3.2.4 Phase locking	35
3.2.5 Plots of average phase angles and average Z-values	38
3.2.6 Topography	41
4 Discussion	43
4.1 Aims of research	43

4.2	Anatomy	43
4.3	Electrophysiology	44
4.3.1	Ongoing activity	45
4.3.2	Response patterns of evoked neural activity	46
4.3.3	Spatial excitation patterns	47
4.3.4	Phase locking	51
4.4	Topography	55
4.5	Limitations of this study and suggested methodical improvements	56
4.6	Conclusion	56
5	Bibliography	58
	Appendix A - Recipes	70
	Appendix B - Tabular overview of units	73
	Appendix C - Phase histograms	75
	Anhang laut Promotionsordnung - Erklärung des Verfassers	77

List of Figures

1	Schematic drawing of a longitudinal and horizontal section through a superficial neuromast. Schematic drawing of a longitudinal section through a canal neuromast.	3
2	Spatial distribution of lateral line canal pores and superficial neuromasts in the goldfish, <i>Carassius auratus</i>	4
3	Line drawing of the dorsal surface of a goldfish brain.	5
4	Side view of an immobilised, fixed and artificially respired fish.	11
5	Top view of an immobilised, fixed and artificially respired fish.	12
6	Visualisation of respiratory water flow through the gills of a goldfish.	13
7	Block diagram of components of stimulus generation setup.	14
8	Schematic drawing of a vibrating sphere with corresponding isobars and water flow.	16
9	Results of stimulus calibration.	17
10	Block diagram of components of recording setup.	19
11	Example of data reduction.	20
12	Dorsal view of the surface of the optic tectum and a part of the cerebellum.	23
13	Electrolytic lesions of the recording sites of units 1–6.	24
14	Electrolytic lesions of the recording sites of units 8, 10–14.	25
15	Response patterns of units 1–16.	27
16	Spatial excitation patterns and ongoing activity of midbrain lateral line units 1–8	28
17	Spatial excitation patterns and ongoing activity of midbrain lateral line units 9–16	29
18	Widths of spatial excitation patterns of units 1–4	31
19	Widths of spatial excitation patterns of units 5–8	32
20	Widths of spatial excitation patterns of units 9–12	33
21	Widths of spatial excitation patterns of units 13–16	34
22	Phase locked responses of unit 3.	35
23	Selected phase histograms of units 3 and 15.	37
24	Plots of average phase angles and average Z-values of midbrain lateral line units 1–8.	39
25	Plots of average phase angles and average Z-values of midbrain lateral line units 9–16.	40

26 Rostro-caudal position of half maximum widths plotted relative to the medio-lateral and the
 rostro-caudal positions of electrode penetrations 41

27 Rostro-caudal positions of half maximum widths plotted against recording depths. 42

28 Modelled pressure gradients and spatial excitation patterns of a primary afferent unit. . . . 49

29 Effects of sphere positions and sphere vibration directions on the shape of phase histograms 54

Abbreviations

ALLN = anterior lateral line nerve

C = cerebellum

CC = corpus cerebelli

CN = canal neuromast

CNS = central nervous system

HMW = half maximum width

ISIH = inter spike interval histogram

LL = lateral lemniscus

MO = medulla oblongata

MON = medial octavolateral nucleus

OA = ongoing activity

OB = olfactory bulb

OT = optic tectum

PLLN = posterior lateral line nerve

PSTH = peri stimulus time histogram

RPC = response pattern coefficient

SD = standard deviation

SEP = spatial excitation pattern

SN = superficial neuromast

T = telencephalon

TL = torus longitudinalis

TTL = transient transistor level

TS = torus semicircularis

VC = valvula cerebelli

VL = vagal lobe

Zusammenfassung

Das mechanosensorische Seitenliniensystem der Fische antwortet auf Wasserbewegungen und Druckgradienten, die von biotischen Faktoren wie z.B. Beutetieren, Fressfeinden, Artgenossen oder abiotischen Faktoren hervorgerufen werden. Theoretische und elektrophysiologische Arbeiten zeigen, dass die von einer vibrierenden Kugel verursachten Reizmuster entlang des Kanalsystems der Seitenlinie Informationen über die Position und Vibrationsrichtung der Kugel enthalten. Diese Reizmuster werden von primären Seitenlinienafferenzen abgebildet. Unklar ist bislang, ob und wie diese Informationen entlang der aufsteigenden Bahn der Seitenlinie weiter verarbeitet werden.

In der Medulla, dem ersten Kern in der aufsteigenden Seitenlinienbahn, wurde keine Repräsentation der Position und/oder Vibrationsrichtung einer stationären vibrierenden Kugel gefunden. Die vorliegende Arbeit untersucht, ob Seitenlinienneurone im zweiten Kern der aufsteigenden Seitenlinienbahn, dem Torus semicircularis, die Position und/oder Vibrationsrichtung einer stationären vibrierenden Kugel abbilden. Dazu wurde eine vibrierende Kugel (Dipol, Durchmesser 10 mm, Frequenz 50 Hz, Dauer 500 ms) an verschiedenen Positionen entlang eines Fisches positioniert. Die Vibrationsrichtung der Kugel betrug 0° (parallel zur Längsachse des Fisches), 45° , 90° (im rechten Winkel zur Längsachse und zur dorso-ventralen Achse des Fisches) oder 135° . Die maximale Amplitude der Kugelbewegung lag zwischen 124 und 237 μm . Die minimalen Abstände zwischen Fisch und Kugeloberfläche betragen 5, 10, 15, 20, 30 oder 40 mm.

Insgesamt wurde 98 unimodale torale Seitenlinienneurone abgeleitet. Für 16 Neurone konnte das komplette, bis zu vier Stunden dauernde Reizprotokoll durchgeführt werden. Dieser Studie liegen deshalb nur diese 16 Neurone zu Grunde. Die Ableitorte von 12 Neuronen konnten nachgewiesen werden, sie lagen im ventrolateralen Kern des Torus semicircularis. Dieses Gebiet erhält ausschließlich Eingang von der Seitenlinie.

Die Spontanaktivität von 14 der untersuchten Neurone lag bei $\leq 0,44$ Hz (Mittelwert \pm SD $0,44 \pm 0,45$ Hz, Median 0,32 Hz, Bereich 0,01–1,40 Hz). Zwei Neurone wiesen durchschnittliche Spontanraten von 12,37 Hz bzw. 51,72 Hz auf. Die Antworten eines Neurons waren phasisch, neun Neurone

antworteten phasisch-tonisch und sechs Neurone tonisch. Sofern eine Antwort erfolgte, antworteten 15 Neurone bei allen Kugelpositionen mit einer Erhöhung der Spikerate. Ein Neuron antwortete je nach Kugelposition mit einer Erhöhung oder einer Abnahme der Entladungsrate.

Im Hinblick auf Antwortrate und Phasenkopplung war kein torales Neuron raumsensitiv. Bei einigen Neuronen reichte aber eine Positionsänderung der Kugel von 5 mm aus, um eine signifikante Veränderung der evozierten Antwortrate, des Phasenwinkels der Antwort und/oder der Phasenkopplung hervor zu rufen. Ähnliche Effekte konnten bei einigen Neuronen auch durch Veränderung der Vibrationsrichtung der Kugel ausgelöst werden.

Drei Neurone zeigten bei mehreren nebeneinander liegenden Positionen der Kugel eine signifikante Phasenkopplung. Während zwei Neurone nur auf eine Hälfte jeder Sinuswelle antworteten, reagierte ein Neuron auf beide Hälften jeder Sinuswelle mit Exzitation.

Die räumlichen Erregungsmuster von drei Neuronen waren unabhängig von der Vibrationsrichtung der Kugel. Die räumlichen Erregungsmuster von vier Neuronen änderten sich je nach Vibrationsrichtung der Kugel und waren relativ zueinander verschoben. Mit zunehmendem Vibrationswinkel der Kugel relativ zum Fisch verlagerte sich das Maximum der räumlichen Erregungsmuster in Richtung rostral. Die räumlichen Erregungsmuster der restlichen neun Neurone zeigten keine systematischen Veränderungen auf unterschiedliche Vibrationsrichtungen der Kugel.

Im Rahmen dieser Arbeit wurden keine toralen Seitenlinienneurone gefunden, die für sich genommen die Position und/oder die Vibrationsrichtung einer stationären vibrierenden Kugel abbilden. Daher postuliere ich, dass Seitenlinieninformationen zu Position und Vibrationsrichtung einer stationären vibrierenden Kugel mittels eines Ratencodes verarbeitet werden. Wenn es raumsensensitive Neurone gibt, welche die Position und Vibrationsrichtung einer Kugel abbilden, können sie möglicherweise im optischen Tectum (der nächsten Stufe der Verarbeitung von Seitenlinieninformation in der aufsteigenden Seitenlinienbahn) gefunden werden, wo etwa beim afrikanischen Krallenfrosch *Xenopus laevis* oder dem Axolotl *Ambystoma mexicanum* schon neuronale Karten der Seitenlinie nachgewiesen wurden.

Summary

The mechanosensory lateral line system of fish responds to water motions and pressure gradients caused by biotic factors (e.g. prey, predators or conspecifics) or abiotic factors. Theoretical and neurophysiological data show that a stationary vibrating sphere creates a spatial stimulus pattern along the lateral line. This spatial stimulus pattern contains information about the stimulus, i.e. sphere position and sphere vibration direction, and is represented in primary lateral line afferents. Up to now it is not clear how the excitation patterns of primary lateral line afferents are processed along the ascending lateral line pathway.

In the medulla, the first nucleus of the ascending lateral line pathway, no representation of the position and/or vibration direction of a stationary vibrating sphere was found. The present study examines if lateral line units in the second nucleus of the ascending lateral line pathway, the torus semicircularis, encode the position and/or vibration direction of a stationary vibrating sphere. To do so, a stationary vibrating sphere (dipole, diameter 10 mm, frequency 50 Hz, duration 500 ms) was positioned at different positions along the rostral-caudal axis of a fish. Sphere vibration directions were 0° (parallel to the long axis of the fish), 45°, 90° (perpendicular to the long axis and the dorso-ventral axis of the fish) and 135°. The maximum peak-to-peak sphere displacement was 124–237 µm. The minimum distances between the fish and the surface of the sphere were 5, 10, 15, 20, 30 or 40 mm.

A total of 98 unimodal toral lateral line units were recorded. 16 of these units could be examined with the complete stimulation protocol, that lasted up to four hours. This study examines only the responses of these 16 units. The recording sites of 12 out of these 16 units were verified, they were located in the ventrolateral nucleus of the Torus semicircularis, which is known to receive only lateral line input.

The ongoing activity of 14 units was $\leq 0,44$ Hz (mean \pm SD 0,44 \pm 0,45 Hz, median 0,32 Hz, range 0,01–1,40 Hz). Two units had mean ongoing activities of 12,37 Hz and 51,72 Hz. The responses of one unit were phasic, nine units responded phasic-tonic and six units showed tonic responses. 15 units responded with an increase in evoked neural activity at all sphere positions. One unit showed

an increase in evoked neural activity or a decrease in evoked neural activity inhibition, depending on the sphere position.

None of the examined toral lateral line units was space sensitive in terms of evoked spike rates or phase locking. In some units a small change (5 mm) in sphere position led to a significant change of the evoked frequency, the phase angle of the response and/or the phase-locking. Similar effects were observed for changes in the direction of sphere vibration.

Three units showed significant phase-locking at multiple side by side sphere positions. Two of these units responded to only one half of a full wave cycle. One unit, however, responded to both halves of a full wave cycle.

Spatial excitation patterns of three units were independent from sphere vibration direction. The spatial excitation patterns of four units were systematically and continuously displaced towards the snout of the fish with increasing sphere vibration angles. The spatial excitation patterns of nine units showed no systematic changes to changes of sphere vibration direction.

In this study no toral lateral line units were found that single-handedly encode the position and/or vibration direction of a stationary vibrating sphere. I therefore assume that lateral line information on the position and vibration direction of a stationary vibrating sphere is encoded in a population code. If space sensitive lateral line units exist, that encode sphere position and vibration direction, they can possibly be found in the optic tectum (the next level of processing of lateral line information in the ascending lateral line pathway), where computed lateral line maps have been proven in other animals with a lateral line.

1 Introduction

1.1 The mechanosensory lateral line

The commonly known senses of vision, olfaction, taste, hearing and touch are, along with thermoreception, nociception, proprioception and the sense of balance, widespread in the animal kingdom (for review, see Martin and Jessell 1996). In addition, other senses have developed, such as the mechanosensory lateral line (Dijkgraaf 1952; for review, see Bleckmann 1994), magnetoreception (Lohmann 2000; Wiltschko and Wiltschko 2005), electroreception (von der Emde 1990; Manger and Pettigrew 1995; for review, see Bullock 1982) and infrared vision (Ebert et al. 2006; Schmitz et al. 2007).

The mechanosensory lateral line is evident in approximately 30,000 extant fish species and many aquatic amphibians (for reviews, see Bleckmann 1994; Nelson 2006). It is capable of detecting minute water motions, that are elicited by prey, predators, conspecifics or abiotic factors like wind or gravity (for reviews, see Bleckmann 1993, 1994). Lateral line information plays an important role in different behaviours (for reviews, see Bleckmann 1993, 1994) like for example prey detection and capture (Hoekstra and Janssen 1985; Montgomery and Hamilton 1997; Coombs et al. 2001; Pohlmann et al. 2001, 2004), predator (Kaus 1986; for review, see Blaxter and Fuiman 1989) and obstacle avoidance (for review, see Hassan 1989), spatial mapping (van Campenhausen et al. 1981; Teyke 1989; Burt de Perera 2004), shoaling (Partridge and Pitcher 1980), entrainment (Liao 2006, 2007) and rheotaxis (Montgomery et al. 1997; Montgomery and Baker 1997; Baker and Montgomery 1999).

Most hydrodynamic stimuli have a dipole component (for review, see Bleckmann 1994). Due to the physical properties of dipole water motions most hydrodynamic stimuli decrease rapidly with distance (Kalmijn 1988; for review, see Bleckmann 1994). Therefore the mechanosensory lateral line is limited to a distance of at most a few body lengths (Kalmijn 1989). Consequently the lateral line system is often referred to as „distant touch“ (Dijkgraaf 1952).

1.2 Periphery of the mechanosensory lateral line

The smallest functional unit of the lateral line system is the neuromast (for review, see Münz 1989). A single neuromast consists of a gelatinous cupula (Nortcutt 1989) with a circular or elliptical base and sensory hair cells (Flock and Wersäll 1962; Flock and Duvall 1965; Schmitz et al. 2008; for review, see Coombs et al. 1988)(Fig. 1A). The hair cells are separated by supporting cells and differentiated from the surrounding tissue by mantle cells (for review, see Münz 1989). The macula, i.e. the area covered by sensory cells, consists of up to 10,000 hair cells in a single neuromast (for review, see Denton and Gray 1989). In goldfish 14–32 hair cells occur in each neuromast (Schmitz et al. 2008). Each neuromast features two equally large groups of antagonistically oriented hair cells, that bear apical ciliary hair bundles. Hair bundles extend into the cupula and are composed of up to 150 stereovilli, that grow longer from one edge of the bundle to the other and a single true 9+2 kinocilium at the tall edge of the hair bundle (Flock and Duvall 1965; Flock 1971). Within a single neuromast hair cells are aligned nearly parallel to each other with respect to their longitudinal axis, i.e. the long axis of the sensory epithelium (Schmitz et al. 2008)(Fig. 1B). Single hair cells are innervated by afferent and efferent nerve fibres (Münz 1979; Puzdrowski 1989). While primary lateral line afferents relay information into the central nervous system (CNS), the efferent pathway can probably actively reduce the sensitivity of neuromasts, e.g. to compensate for self-produced hydrodynamic stimuli that occur during active swimming movements (for review, see Bleckmann 1994).

There are two types of neuromasts that differ in terms of morphology and response properties. Superficial neuromasts (SN) are situated in the epidermis with their cupulae protruding into the water surrounding the fish (for review, see Münz 1989). They occur in lines or clusters across the whole epidermis, but are absent on the scales on the ventral side of the trunk, on the lips and on all fins except the tail fin (Puzdrowski 1989; Bensouilah and Denizot 1991; Schmitz et al. 2008). Canal neuromasts (CN) are located in subepidermal fluid filled canals with their cupulae looming into the canal fluid that is usually connected with the outside medium by means of pore-like openings (for review, see Münz 1989). In general a CN is positioned between two adjacent pores (for review, see Münz 1989)(Fig. 1C). In most fish species CN are organised in a supraorbital canal above the eye,

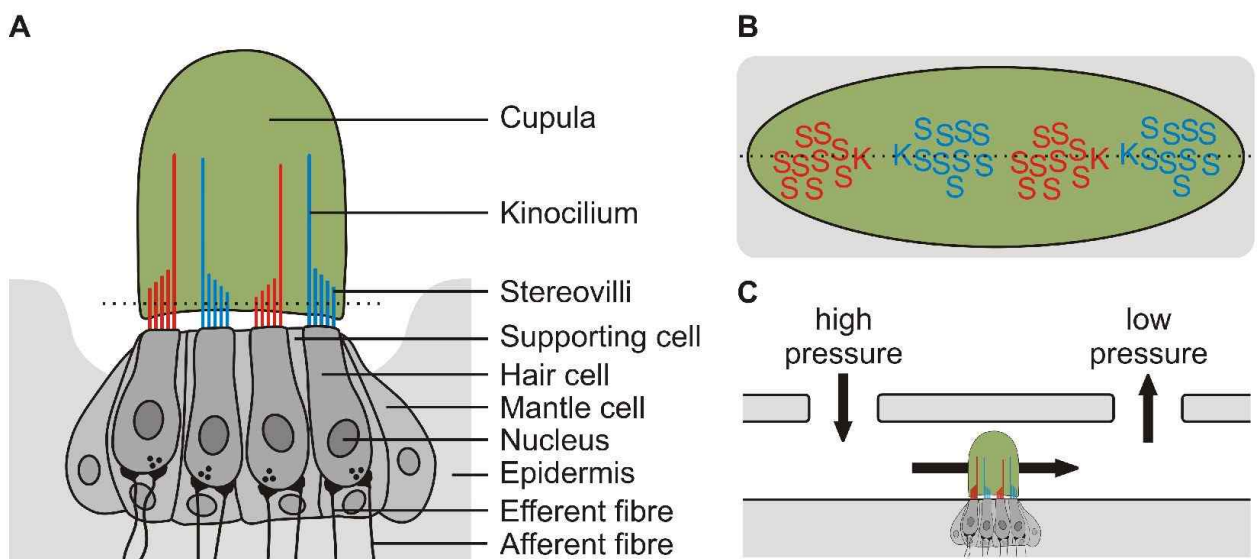


Fig. 1A, B, C. **A** Schematic drawing of a longitudinal section through a SN. Characteristic properties of a neuromast are the gelatinous cupula and the hair cells, each with an apical hair bundle consisting of one kinocilium and numerous stereovilli. Ciliary bundles with the same orientation are drawn in the same color. The size of neuromasts differs considerably between species and among neuromast types (see text). Note that only four exemplary hair cells each with four stereovilli are shown. The dotted line marks the section plane of Fig. 1B. **B** Schematic drawing of a horizontal section through the SN depicted in Fig. 1A. Only cupula, stereovilli, kinocilia and epidermis are shown. Hair cells occur in pairs whose ciliary bundles have a common axis of best sensitivity but antagonistic directional orientation. Note that only four exemplary hair cells each with nine stereovilli are shown. K = Kinocilium, S = Stereovilli. The dotted line marks the section plane of Fig. 1A **C** Schematic drawing of a longitudinal section through a canal neuromast. The pressure difference between two adjacent pores leads to flow in the canal and thus to a stimulation of the canal neuromast. Modified and redrawn, with kind permission, from W. E. Bemis.

an infraorbital canal below the eye, a mandibular canal on the lower jaw and a trunk lateral line canal (Nortcutt 1989; for review, see Bleckmann 2008)(Fig. 4).

The adequate stimulus for both types of neuromasts is a shearing or gliding movement of the cupula (Flock 1971; van Netten and Kroese 1987) that results in shearing of the ciliary bundles of the hair cells in the stimulated neuromast. The hair cells are physiologically polarized to respond maximally to a shearing of the ciliary bundles along their axis of alignment (Flock and Wersäll 1962). Shearing of the ciliary bundle towards the kinocilium leads to a depolarization, while shearing in the opposite direction leads to a hyperpolarization of the hair cell (for reviews, see Hudspeth 1983; Kroese and van Netten 1989). This morphological feature leads to a directional sensitivity of the hair cell and therefore consequently to a directional sensitivity of the neuromast (Flock and Duvall 1965). The main orientation of the sensory epithelium in SN located on the trunk and the tail fin is rostro-caudal. The axes of best sensitivity on the head are variable, while the orientation of SN on the trunk

lateral line scales is mainly rostro-caudal or dorso-ventral. The alignment of hair cells in CN differs depending on their location. Cephalic CN occur in all orientations while CN of the trunk lateral line are primarily oriented in the rostro-caudal axis (Schmitz et al. 2008). Depending on the species the lateral line consists of hundreds or even thousands of neuromasts. Goldfish possess 120–160 CN and about 2,000 SN per body side (Puzdrowski 1989; Schmitz et al. 2008)(Fig. 2). SN have diameters from 20–100 μm , while CN can be much larger with diameters ranging from 100 to more than 700 μm (for review, see Münz 1989). If stimulated with sinusoidal stimuli, SN respond largely in proportion to the net velocity between the fish and the surrounding water. CN, on the other hand, detect pressure gradients between adjacent canal pores, i.e. the net acceleration of water outside the canal (Kalmijn 1989).

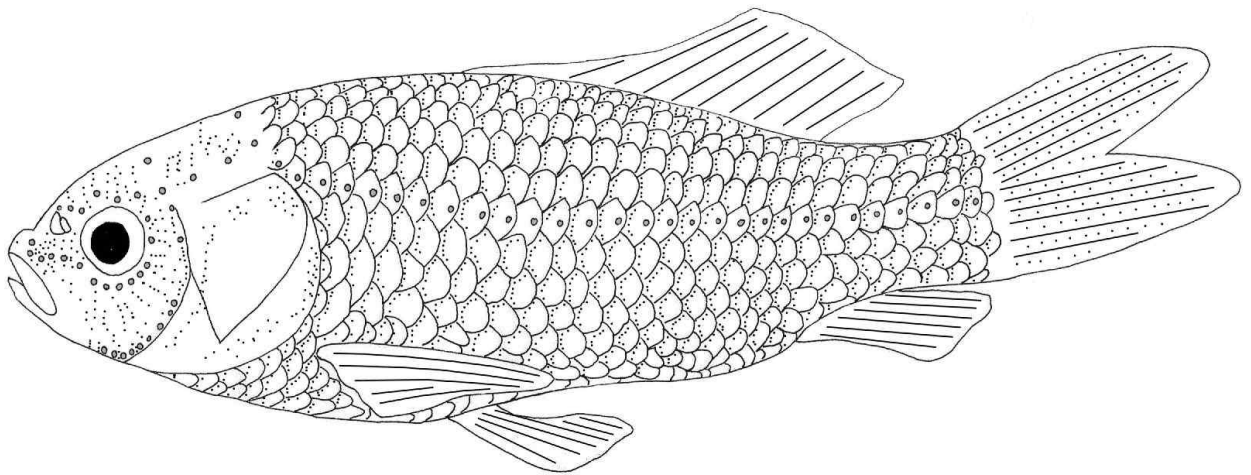


Fig. 2. Spatial distribution of lateral line canal pores (circles) and superficial neuromasts (dots) in the goldfish, *Carassius auratus*. Canal neuromasts are not visible due to their subcutaneous location. The drawing was gratefully provided by A. Schmitz.

Total number, spatial distribution, location, shape, size and orientation of neuromasts as well as the ratio of SN to CN can differ substantially among species (e.g. Münz 1979; Schmitz et al. 2008; van Trump and McHenry 2008; for reviews, see Coombs et al. 1988; Denton and Gray 1988; Schellart and Wubbels 1998). These morphological variations may be adaptations to environmental circumstances. Fish that are slow swimmers or live in stillwater tend to have many SN. Fish that are fast swimmers or inhabit turbulent waters possess few SN but a well developed canal system (Schellart and Wubbels 1998; for review, see Bleckmann 1994). The non-predatory goldfish lives in still or slow moving waters and has thousands of SN. However, the predatory trouts, who live in

turbulent running water, have only about 40 SN (Engelmann et al. 2002). *Xiphister atropurpureus*, who lives in the turbulent waters of the surge in shorelines, does not possess a single SN but has a highly branched and zigzag shaped canal system (Bleckmann and Münz 1990).

1.3 Afferent lateral line pathways

Lateral line information originating from cephalic neuromasts is routed into the CNS via the anterior lateral line nerve (ALLN), while information from the trunk is relayed via the posterior lateral line nerve (PLLN)(McCormick 1982; Northcutt 1997; for review, see Northcutt 1989). Some species feature a middle lateral line nerve (MLLN), that innervates SN and CN caudal to the eye (for review, see Bleckmann 1994). Primary lateral line afferents terminate predominantly in the ipsilateral medial octavolateralis nucleus (MON) in the medulla (e.g. Puzdrowski 1989; Bleckmann et al. 1991). The majority of second order cells in the MON projects to the contralateral torus semicircularis (TS) and optic tectum (OT)(for review, see Wullimann 1998; Bleckmann and Zelick 2009). The TS consists of two nuclei, the nucleus centralis that receives input from the inner ear and the nucleus ventrolateralis that receives input from the lateral line (Knudsen 1977; Schellart et al. 1987; McCormick and Hernandez 1996; for review, see McCormick 1989). The TS is located in the midbrain, ventral to the optic tectum (McCormick and Hernandez 1996; Rupp et al. 1996; for review, see McCormick et al. 1989)(Fig. 3). Fibres originating in the TS terminate in the nucleus praeeminentialis and are relayed to the telencephalon via the nucleus praeglomerulosus in the diencephalon (for review, see Wullimann 1998).

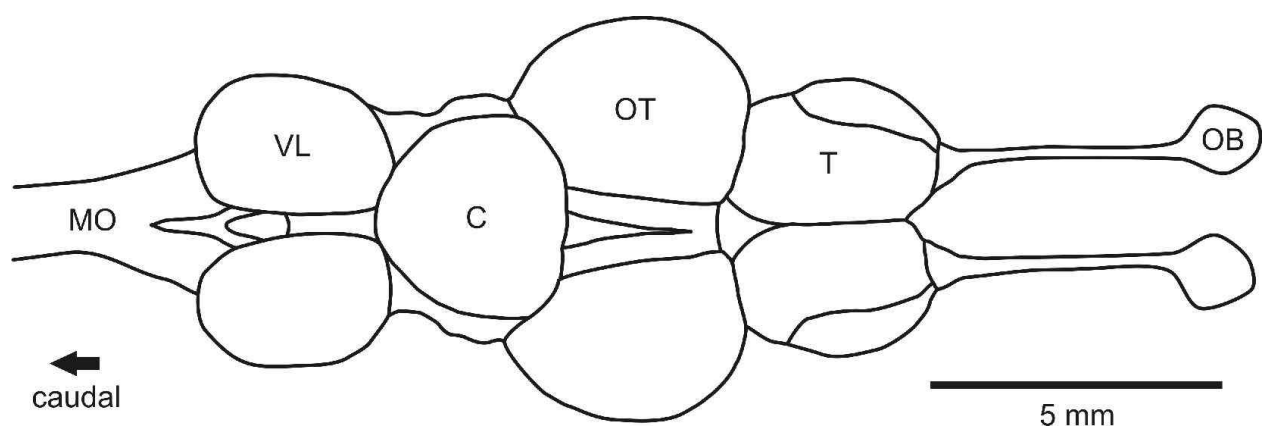


Fig. 3. Line drawing of the dorsal surface of a brain removed from a goldfish that had a body length of 124 mm. The brain was fixed in 4 % paraformaldehyde (see appendix A) for five days. The torus semicircularis is located in the caudal part of the midbrain, ventral to the dorsal surface of the optic tectum (McCormick and Hernandez 1996; Rupp et al. 1996; for review, see McCormick et al. 1989), are marked by the stippled lines. OB = Olfactory bulb, C = Cerebellum, MO = Medulla oblongata, T = Telencephalon, TS = Torus semicircularis, VL = Vagal lobe

Findings suggest that SN and CN are innervated by different primary lateral line afferents (Münz 1985). Thus at least two parallel ascending lateral line pathways exist. One pathway, innervating exclusively SN, holds information on the velocity of the water surrounding the fish's body. The other pathway relays information from the CN about the pressure gradient pattern across the surface of the fish (for review, see Bleckmann 2008).

1.4 Hydrodynamic stimulation

A stimulus that was often used by lateral line researchers in still water experiments is a stationary or slowly moving sphere that vibrates sinusoidally under water (e.g. Harris and van Bergeijk 1962; Sand 1981; Münz 1985; Coombs and Janssen 1990; Coombs and Montgomery 1992; Montgomery and Coombs 1992; Wubbels 1992; Coombs et al. 1996; Coombs et al. 1998; Mogdans and Kröther 2001; Engelmann et al. 2002; Kröther et al. 2002; Engelmann and Bleckmann 2004; Künzel 2009; for review, see Bleckmann and Bullock 1989). A submerged vibrating sphere generates defined water motions and a defined pressure gradient pattern on the body surface of an experimental animal (e.g. Coombs et al. 1996).

For a sphere with a given diameter and peak-to-peak displacement amplitude the shape of the pressure gradient pattern depends on the location of the sphere (azimuth, elevation and distance between fish and sphere) and its vibration direction relative to the fish (e.g. Sand 1981; Kalmijn 1988; Coombs et al. 1996; Coombs and Conley 1997a, 1997b; Coombs et al. 2000, 2002; Ćurčić-Blake and van Netten 2006; Goulet et al. 2008; Coombs and Patton 2009). The rostro-caudal position of a sphere is determined by the pressure gradient maximum (e.g. Coombs et al. 1996)(cf. Fig. 28). The stimulus distance, i.e. the distance between fish and sphere, relates directly to the zero crossings of the pressure gradients. For a sphere vibrating parallel to the rostro-caudal axis of the fish, the stimulus distance relates directly to the positions of the zero crossings of the pressure gradients. With all other parameters being equal, the distance between these two points increases with increasing distance between fish and sphere (e.g. Coombs et al. 1996). Lastly, the orientation of the sphere relative to the fish, i.e. sphere vibration direction, is reflected in the spatial pattern of the pressure gradient. A sphere vibrating parallel to the rostro-caudal axis of the fish results in a tri-phasic pattern,

whereas a sphere vibrating perpendicular to the fish evokes a bi-phasic pattern (e.g. Sand 1981; Kalmijn 1989; Coombs et al. 1996; Coombs and Patton 2009)(cf. Fig. 28).

Electrophysiological experiments have shown that pressure gradient patterns of a stationary vibrating sphere are unambiguously encoded in the spatial excitation patterns of primary lateral line afferents (Sand 1981; Coombs et al. 1996; Goulet et al. 2008)(Fig. 28). Hence the information contained in peripheral excitation patterns can theoretically be relayed to and used by central lateral line units to unequivocally compute the location and the vibration direction of a stationary or slowly moving vibrating sphere. In fish, up to now, no units that code the location and vibration direction of a sphere have been found in the MON (e.g. Mogdans and Kröther 2001) or TS (e.g. Wojtenek et al. 1998; Plachta et al. 1999; Engelmann and Bleckmann 2004). However, the aforementioned researchers did not systematically look for space sensitive units, but rather focused on other aspects of lateral line information processing. Lately, in the first systematic search for space sensitive lateral line units, Künzel (2009) did not find MON units that were highly sensitive to sphere position and/or sphere vibration direction. It is therefore not even known if or how the information of peripheral excitation patterns is used by the CNS to compute the location of a stimulus source or its vibration direction.

However, the following indications make it likely that central lateral line units of fish could extract information out of the peripheral pressure gradient patterns in order to localize a vibrating sphere and detect the sphere vibration direction.

The lateral line system of amphibians is more simple than the lateral line system of fish since it only consists of SN which have a smaller response range (e.g. 0.1–40 Hz in *Xenopus laevis*; for review, see Elepfandt 1996). Nevertheless Claas and Münz (1996) showed that *Xenopus laevis* uses lateral line information to extract information on both, the direction and the distance to a water surface wave source. Lateral line units that are tuned to the direction of an impinging water surface wave were discovered in electrophysiological experiments (*Xenopus laevis*: Zittlau et al. 1986; Behrend et al. 2006; *Ambystoma mexicanum*: Bartels et al. 1990). Zittlau et al. (1986) and Bartels et al. (1990) found that midbrain lateral line units of *Xenopus laevis* and *Ambystoma mexicanum* form computational maps, while Behrend et al. (2006) could neither prove nor exclude the existence of a map due to a limited data set. Claas et al. (1989) showed, that tectal lateral line units of *Xenopus*

laevis only respond to a surface wave stimulus if the distance between the stimulus source and the animal was 6 cm. These results suggest that in these amphibians the distance of a concentric water surface wave source can be derived from the direction and/or the curvature of a surface wave stimulus. In fish, the distance of a stationary vibrating sphere is encoded in the distance between the zero crossings of the pressure gradients along the lateral line canal (see above). In addition, it has to be kept in mind that the physical properties of midwater waves and surface water waves differ fundamentally (Kalmijn 1988; for review, see Bleckmann 1994).

Furthermore, the distance to a visual or acoustic stimulus is represented in computational maps in the CNS (for review, see Bleckmann 1994). In the auditory and visual system of vertebrates, the location of a stimulus source is encoded by the activity of central neurons that are highly sensitive to stimulation at a specific spatial location (e.g. Knudsen 1982). For example, the peripheral hair cells in the ear of the barn owl receive acoustic stimuli and relay their information to space sensitive midbrain neurons. These units fire only if a sound is presented at a particular location (Knudsen and Konishi 1978).

The midbrain TS of fish contains at least a crude topographical organisation of electrosensory (e.g. Knudsen 1977), auditory (e.g. Schellart et al. 1987; Wubbels et al. 1995; Wubbels and Schellart 1998) and lateral line information (e.g. stimulus = stationary vibrating sphere: Bleckmann et al. 1987, 1989; stimulus = sphere passed alongside the fish: Plachta et al. 2003).

Taking into account that no space sensitive units were found in the first lateral line nucleus, the MON, a promising locus for the search of space sensitive lateral line units (azimuth and distance) is the TS. In addition, the vibration direction of a stimulus could also be encoded in the TS. Admittedly, medullary and midbrain lateral line units in *Ancistrus* and *Apteronotus* showed no coding of object distance, as an increasing stimulus distance always led to an decreasing rate of evoked action potentials (for review, see Bleckmann 1994).

In order to systematically search for space sensitive units I determined the spatial excitation patterns (SEPs, also often referred to as receptive fields) of lateral line units recorded in the midbrain TS of goldfish. To do so the lateral line system was stimulated with a sphere that was placed at various

locations and distances alongside the fish. In addition, the sphere vibrated at various angles with respect to the body surface of the fish. Space sensitive units would - irrespective of the attenuation of dipole induced water motions (Kalmijn 1988) - show a maximum response (in terms of action potential frequency or phase locking) at a certain sphere distance. A central lateral line unit that is sensitive to stimulation with a certain sphere vibration direction would exhibit a maximum response if it is stimulated with a sphere vibrating at a certain angle relative to the fish.

A possible encoding of the elevation of a stimulus by midbrain lateral line units was not examined in this study since the dorso-ventral position of the sphere was not altered during an experiment. In this study goldfish (*Carassius auratus*, Superclass: Osteichthyes (bony fish), Class: Actinopterygii (ray-finned fishes), Order: Cypriniformes, Family: Cyprinidae) were used as experimental animals.

2 Materials & Methods

2.1 Experimental animals

Data were collected from 132 goldfish (*Carassius auratus*) ranging from 8.1–12.8 cm in standard body length and 14–33 g in weight. Only the common variety of the goldfish (for reviews, see Piechocki 1990; Sterba 1990) was used, because multiple specimen of other varieties, e.g. those with a deeply forked and long tail fin („Comet“) or multiple colors with black dots („Shubunkin“) showed obvious mutations of the central nervous system (CNS), like a malformed or missing OT. Animals were acquired from german retailers, kept in 300 l communal tanks (water temperature 16–19 °C, light-dark cycle 10:14 hours, substrate layer 5 cm coarse gravel, aquatic plants), and fed standard fish food (Pond Vario, JBO GmbH & Co. KG, Neuhofen, Germany).

2.2 Preparation

Fish were initially anaesthetised by immersion in MS-222 (1:10,000 in tap water, Sigma Aldrich, Seelze, Germany) for 2–5 minutes or ice water (4 °C) for 15–30 minutes, until movements of operculi stopped for a minimum of 10 s. Animals were immobilised with injections of 50 µl Pancuroniumbromide (1:20 in physiological salt solution (see appendix A), Pancuronium Organon®, Organon, Oss, The Netherlands) into the back muscles right of the dorsal fin. Occasionally, a second injection was necessary to fully tranquilise a fish. For preparation animals were fixed on a surgical setup made of Styrodur®. During preparation and experiment fish were artificially respired with tap water (flow rate 80–100 ml/min) by means of a water loop. It consisted of a submerged pump (Tauchpumpe Typ 03, Conrad Electronic, Hirschau, Germany) placed in a bucket full of tap water and an overflow in the surgical setup or the experimental tank, respectively, that piped superfluous water back into the bucket. To prevent drying of the skin during preparation, fish were continuously rinsed with fresh water. To minimise mechanical stress during handling, fish were invariably handled with forceps and only taken hold of on the first ray of the dorsal fin. The skin on the dorsal surface of the skull was infused with the local anesthetic lidocaine hydrochloride (Xylocain®, AstaZeneca GmbH, Wedel, Germany). After the drug took effect (10–15 min), an area of skin (approximately 8 × 8 mm), dorsal to the right OT, was scraped off with a scalpel. A hole (about 6 × 6 mm) was made into the cranial

bone with a dental drill (rose-head bur in FBS 240/S, Proxxon GmbH, Niersbach, Germany). Fluids and adipose tissue were removed to expose the right OT and the very rostral part of the C (cf. Fig. 12). Preparations were performed under a binocular (Leica M655, Leica Microsystems GmbH, Wetzlar, Germany).

The dorsal surface of each brain was photographed and positions of electrode penetrations were plotted on the respective photograph. Positions of electrode penetrations that resulted in a successful recording of a midbrain lateral line unit were normalised to an OT with a width of 1,000 μm . The rostro-caudal and dorso-ventral borders of the OT were used as landmarks.

Physiological salt solution was applied into the cranial cavity. Occasionally occurring bleedings were stopped by placing gelatine foam (Gelastyp[®], Ferrosan, Soeborg, Denmark) in the cavity for a few minutes. To prevent water from entering the cranial cavity, a plastic cylinder (\varnothing 12 mm, height 17–24 mm) was glued (Vetbond[™], 3M Animal Care Products, St. Paul, MN, USA) to the dried skin around the opening in the skull. Leaks were sealed with cotton wool and glue. After sufficient leak tightness of the cylinder was obtained, fish were transferred to the experimental tank (50 \times 50 \times 22 cm, water level 21.5 cm), that rested on a vibration isolated table (Micro-g[®], TMC, Peabody, MA, USA) and was filled with tap water (16–23 $^{\circ}\text{C}$).

2.3 Experimental setup

The snout of the fish was put over a stainless steel pipe (Fig. 4) that delivered respiratory water.

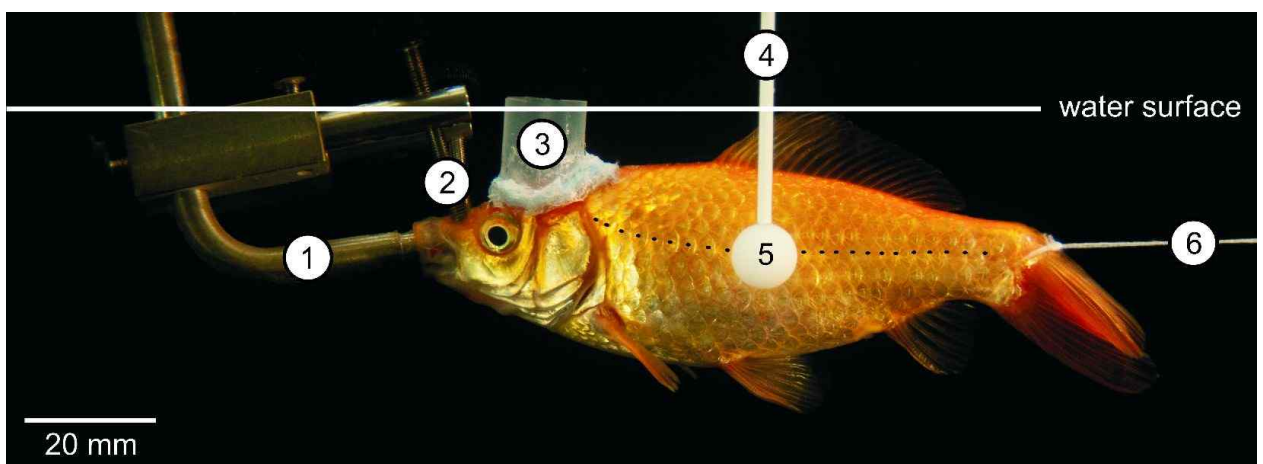


Fig. 4. Side view of an immobilised, fixed and artificially respired fish. Black stipples indicate the pores of the trunk lateral line canal. 1 = respiratory pipe (flow rate 80–100 ml/min), 2 = screws clamping the skull to the pipe, 3 = plastic cylinder to prevent water from entering the cranial cavity, 4 = rigid steel wire, 5 = sphere, 6 = twine, attached to the rear wall of the tank.

The skull was clamped in a stable position with two screws. Animals were completely submerged in the experimental tank, leaving only the top of the plastic cylinder above the water surface. In addition, a piece of twine was tied through the locally anaesthetised base of the tail fin and affixed to the rear wall of the fish tank by means of modelling clay. The fish was aligned in such a way that the distance between the sphere and the left side of the fish remained approximately constant for different sphere positions (Fig. 5). The position of the fish was left unaltered during the entire experiment.

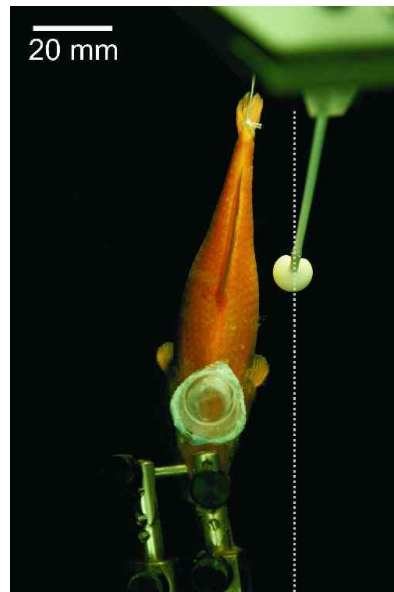


Fig. 5. Top view of an immobilised, fixed and artificially respired fish. The sphere is positioned at various locations along the dashed line. The minimum distance between the surface of the sphere and the surface of the fish was 5 mm in this case.

To examine a possible influence of the respiratory water flow on evoked neural activity the flow of respiratory water through the gills of a fish was visualised in two ways. Either black ink or hollow glass spheres (mean particle \varnothing 50 μm , PSP-50, Dantec Dynamics, Skovlunde, Denmark), with the same density as water and therefore floating in it, were added to the respiratory water. While the dispersion of the ink dyed water in the clear water of the experimental tank could be observed with the naked eye, the glass spheres needed to be illuminated with a sheet of laser light (laser diode, wavelength 650 μm , output power 50 mW) in a darkened surrounding. The laser sheet was either aligned parallel to the water surface, virtually dissecting the fish at the level of the lateral line, or parallel to the rostro-caudal axis of the fish. Flow visualisation was recorded with a high speed camera (HighSpeedStar 4, LaVision, Göttingen, Germany) at a resolution of $1,024 \times 1,024$ pixels

at 10 frames/s. Examples of flow visualisation with hollow glass spheres and ink, respectively, are depicted in Fig. 6.

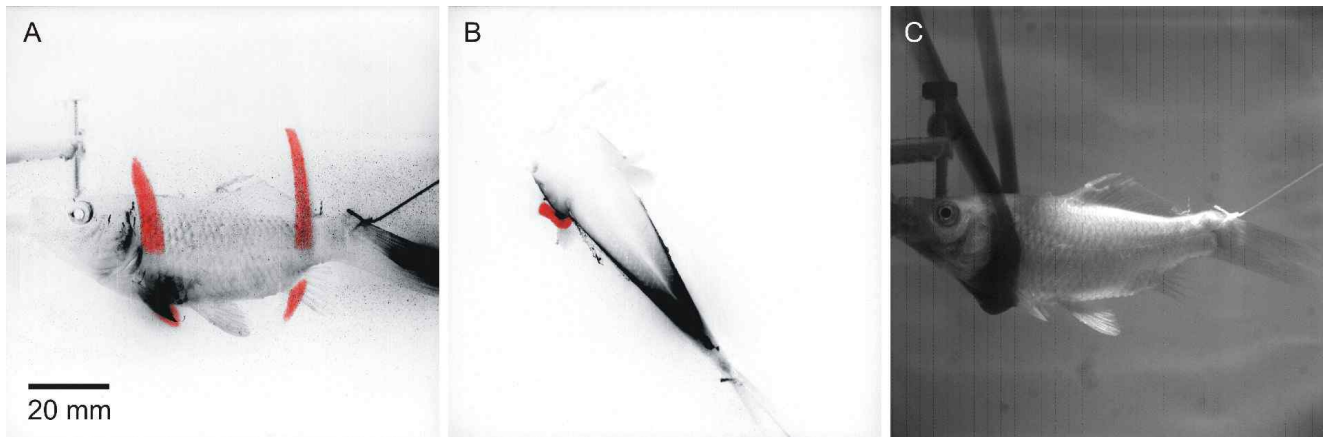


Fig. 6A, B, C. Visualisation of respiratory water flow through the gills of a goldfish. Side view (**A**) and top view (**B**) of particles illuminated by a laser sheet. Images were black-white inverted. Locations of high particle density were manually coloured in red after the recording. Note that a horizontal extent of the caudal water current was not visible in terms of particle movement. **C** Side view of the flow of ink dyed water through the gills of the same experimental animal as depicted in A and B. Note that the water flow close to the base of the anal fin shown in A is not visible. Evenly spaced vertical lines result from a defect in the CCD chip of the digital camera.

2.4 Stimulation

2.4.1 Stimulus generation

Fish were stimulated with water motions generated by a stationary, sinusoidally vibrating, chemically inert plastic sphere (\varnothing 10 mm). Stimuli (50 Hz, 500 ms duration, 100 ms rise and fall time, starting phase 0° , cf. Fig. 11) were software generated on a PC (Spike 2 v5.16, Cambridge Electronic Design (CED), Cambridge, UK), DA converted (Power 1401, CED), monitored on an oscilloscope (DL 1300A, Yokogawa, Tokyo, Japan), amplified (KAF-1010, Kenwood, Heusenstamm, Germany) and passed to a permanent magnet electrodynamic minishaker (Model V101, Ling Dynamic Systems (LDS), Royston, GA, USA). A plastic rod to which the sphere was attached by means of a rigid stainless steel wire (length 100 mm, \varnothing 1.58 mm) was mounted perpendicular to the minishakers diaphragm to generate sinusoidal oscillations in the horizontal plane. The minishaker was attached to a custom-made rail system (machine shop, Institute of Zoology, University of Bonn) that allowed to alter the distance between fish and sphere and the position of the sphere along the rostro-caudal axis of the fish, respectively. The stimulus setup rested on a free-standing platform, to prevent the

direct transmission of vibrations from the minishaker to the experimental animal. For a block diagram of the stimulus generation setup, see Fig. 7.

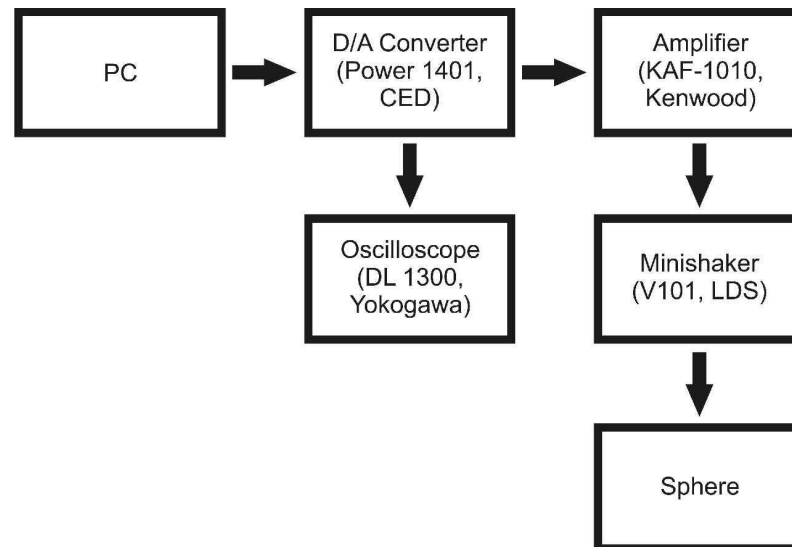


Fig. 7. Block diagram of components of stimulus generation setup. Boxes show the names of the components, brackets contain model name and manufacturer.

Since the majority of second order projections from the MON terminates in the contralateral TS (for review, see Bleckmann 2008), hydrodynamic stimulation leads to an excitation of the contralateral TS. Therefore, the sphere was positioned on the left side of the fish during all experiments, while recordings were exclusively made from the right hemisphere of the midbrain. At the beginning of an experiment, the sphere was positioned in the middle of the rostro-caudal axis (or long axis) and at the level of the trunk lateral line canal (Fig. 4). The dorso-ventral position of the sphere was not changed during the entire experiment. The initial distance between fish and sphere was 10 mm. All denoted distances between fish and sphere relate to the distance between the surface of the fish and the surface of the sphere. In addition to changing the sphere position, the minishaker could be turned in steps of 45° , leaving the position of the sphere unaltered but resulting in a change of the sphere vibration direction of 45° . Initial sphere vibration direction was 0° , i.e. sphere vibration direction was parallel to the long axis of the fish.

2.4.2 Search stimulus

Units responding to water motions were found by simultaneously advancing the electrode through the OT into the TS in steps of $3\ \mu\text{m}$ and presenting search stimuli. For this purpose, water motions were

generated by a stationary vibrating sphere (peak-to-peak displacement of 237 μm) and a pipette that was moved alongside the rostro-caudal axis on the left side of the fish at a distance of 5–15 mm to the surface of the fish.

2.4.3 Characterisation of unit modality

The TS of fish receives not only lateral line input but also visual, acoustic and somatosensory information (and electrosensory input in certain species)(Knudsen 1977; Nederstigt and Schellart 1986; Schellart et al. 1987; McCormick and Hernandez 1996; for review, see McCormick et al. 1989). The OT is located dorsal to the TS and receives and processes visual information (Meek and Schellart 1978). It was therefore critical to assure that the units responding to the search stimuli did exclusively react to lateral line stimuli and not to auditory, vestibular or optic stimuli. Units that responded to shouting and/or handclapping were assumed to receive auditory input. Units that responded to changes in illumination were supposed to receive visual input. Units that were sensitive to tapping on the edge of the experimental tank with the thin end of a pasteur pipette or to stomping with a feet on the ground were assumed to receive vestibular (vibratory) input. Units that received acoustic, visual or vestibular input were not further investigated. Similarly, units that did not respond to acoustic, vibratory or optic stimuli but answered if the non-vibrating sphere was moved along the rostro-caudal axis of the fish were also not further examined. Only units that responded exclusively to the stationary vibrating sphere were defined as unimodal lateral line units and examined in this study.

2.4.4 Stimulus protocol

For unimodal lateral line units the position at which the sphere elicited the strongest response was determined. At this position, the dynamic range of the units was curtailed by altering the peak-to-peak displacement of the vibrating sphere. Used peak-to-peak displacements were 124, 160, 176, 220 or 237 μm . The stimulus amplitude that lay approximately in the middle of the unit's dynamic range was used throughout the entire experiment. The small differences between the stimuli with peak-to-peak displacements of 160 and 176 μm and 220 and 237 μm , respectively, resulted from the usage of two different minishakers. One minishaker broke during the early stages of data acquisition for this study

and the initially used displacements of 160 and 220 μm were not exactly reproducible with the new minishaker.

Fish were stimulated with eight successive single stimuli (50 Hz, 500 ms duration, 100 ms rise and fall time, cf. Fig. 11, offset 3s, inter stimulus interval 5s, total time 47s) at each sphere position, starting at the initial sphere position (cf. Fig. 4). After recording the unit's responses to the stimulus, the sphere was relocated along the rostro-caudal axis of the fish in steps of 5 mm (10 mm during the stimulation of one fish). This was repeated until the vibrating sphere elicited no changes in ongoing activity at a minimum of two consecutive sphere positions both in the anterior and the posterior direction, meaning the stimulus protocol for a given sphere vibration direction was completed. Thereafter, the axis of sphere vibration was altered and the aforementioned stimulus protocol was repeated for the sphere vibration directions of 45°, 90° (sphere vibrating perpendicular to the rostro-caudal axis of the fish) and 135° (cf. Fig. 8). If the stimulus protocol could be presented for all four vibration directions, the distance between sphere and fish was increased in steps of 5 or 10 mm. The minimum distances between the fish and the surface of the sphere were 5, 10, 15, 20, 30 or 40 mm. For each distance, the units responses were again mapped for the sphere vibration directions of 0°, 45°, 90° and 135°. Measurements were continued until a unit was lost. Recordings for a certain distance between fish and sphere were only analysed if the stimulus protocol was completed for all four sphere vibration directions.

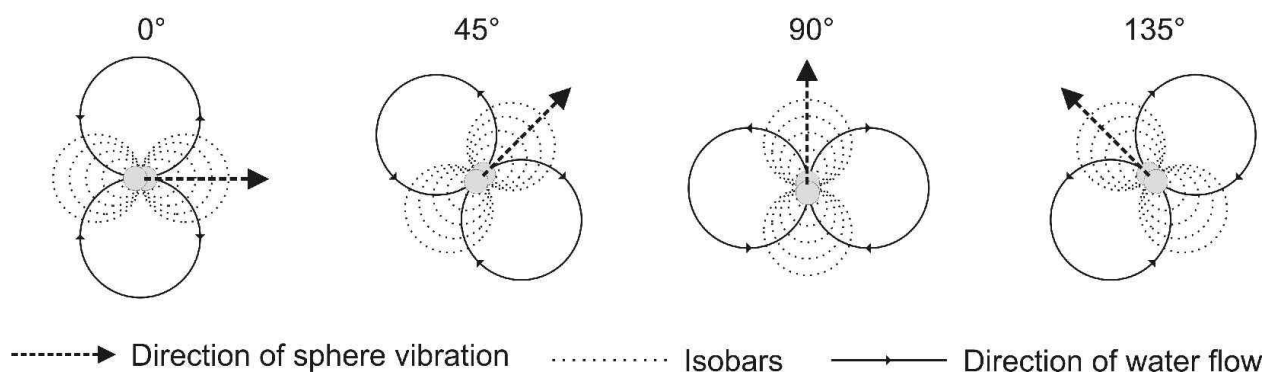


Fig. 8. Schematic drawing of a vibrating sphere with corresponding isobars and water flow. Isobars are depicted for the plane that bisects the source along its axis of oscillation. At 0° the sphere vibrated parallel to the rostro-caudal axis of the fish. At 90° the sphere vibrated perpendicular to the rostro-caudal and the dorso-ventral axis of the fish. Modified and redrawn after Coombs et al. (1996).

2.4.5 Stimulus calibration

Peak-to-peak sphere displacements were calibrated in the absence of a fish with a capacitive displacement transducer (4810, LOT-Oriel GmbH & Co. KG, Darmstadt, Germany), that measures displacements between the stationary sensor and a reference object (brass disc, \varnothing 6 mm, thickness 0.12 mm). Since the transducer can not be operated under water, the displacement of the sphere could only be measured indirectly. Therefore the disc was attached to the steel wire, approximately 15 mm above the centre of the sphere, while the sphere vibrated under water. Results are depicted in Fig. 9. Due to noise the sphere permanently vibrated with a peak-to-peak displacement of up to 3 μm .

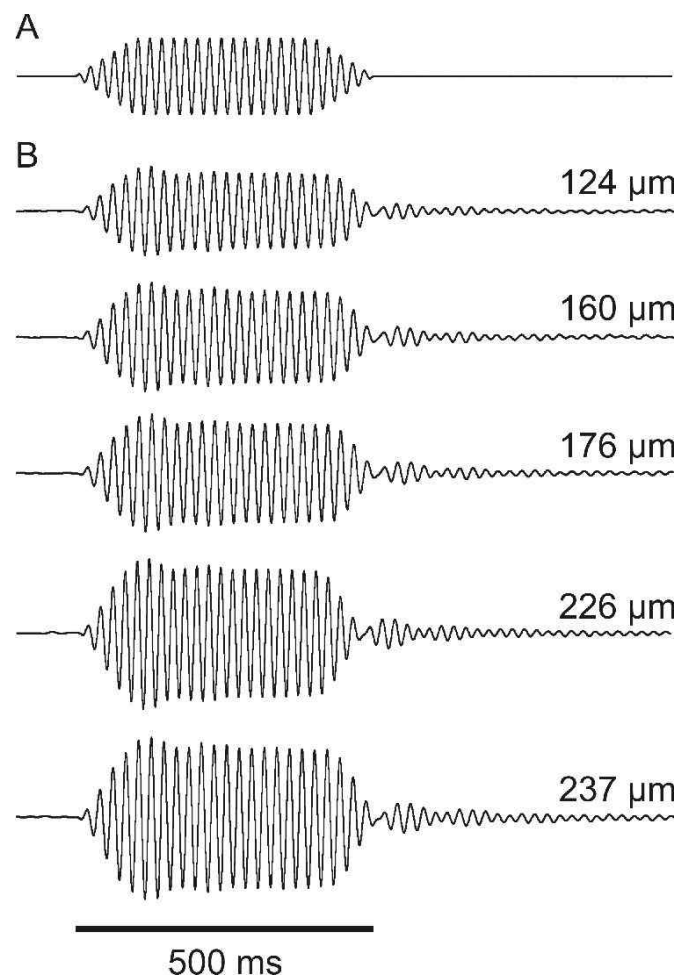


Fig. 9 A, B. Results of stimulus calibration. **A** Software generated voltage fed into the minishaker. **B–F** Outputs of the displacement transducer for the peak-to-peak displacement amplitudes of the sphere indicated on the right. The fluctuations of the baselines in B before the onset of the stimulus result from noise that causes the sphere to vibrate permanently with a peak-to-peak displacement of up to 3 μm . The fluctuations after the end of the software generated voltage fed into the minishaker result from post-oscillations of the sphere.

2.5 Recording

During recording the physiological status of the animal was evaluated by monitoring the blood flow through the blood vessels on top of the OT. Extracellular responses of single midbrain lateral line units were recorded with metal-filled glass micropipettes (Dowben and Rose 1953), that were fabricated by pulling single barrel borosilicate glass without filament (GB150-8P, Science Products, Hofheim, outer \varnothing 1.5 mm, inner \varnothing 0.86 mm) on a horizontal puller (P-80, Sutter Instrument Company, USA). Tips were broken off to a diameter of 1–2 μm . Micropipettes were filled with an indium-alloy (LMA-117, Small Parts Inc., Miramar, CA, USA). Micropipette tips were electrolytically plated with gold (0.2 % Hydrogen Tetrachloroaurate Trihydrate ($\text{AuHCl}_4 \cdot 3 \text{H}_2\text{O}$, Carl Roth GmbH + Co. KG, Karlsruhe) in distilled water) and platinum (4 % Hexachloroplatinic acid hydrate ($\text{Cl}_6\text{H}_2\text{Pt} \cdot x \text{H}_2\text{O}$, Sigma-Aldrich, Seelze)) for 2–5 s each, resulting in a spherical or clubbed swelling (\varnothing 2–8 μm) on top of the electrode tip. Electrodes had an impedance of 0.8–1.1 $\text{M}\Omega$ determined with an ohmmeter (Ω mega-Tip-Z, World Precision Instruments Inc., Sarasota, USA) with a resolution of 10 $\text{k}\Omega$ and an accuracy of ± 20 %. A chlorinated silver wire (\varnothing 0.8 mm) was used as a reference electrode. Its tip was placed in the cranial cavity, about 3–5 mm away from the recording electrode. For a block diagram of the recording setup, see Fig. 10.

Initially, the recording electrode was positioned with its tip on top of the rostro-lateral part of the OT, dorsal to the TS (cf. Fig. 12) under visual control through binoculars. While search stimuli were presented, the electrode was advanced vertically into the midbrain in steps of 3 μm with a microdrive (accuracy 0.1 nm; IW-800 and Controller 8200, Exfo, Mississauga, Ontario, Canada). The depth of the electrode tip relative to the surface of the midbrain was monitored on the microdrive display. Unit responses were differentially amplified thousandfold (DAM80, World Precision Instruments, Sarasota, FL, USA), band-pass filtered (DAM80, 300–3,000 Hz) and monitored on an oscilloscope (DL 1300A, Yokogawa) and an audio monitor. Data were A/D converted (Power 1401, Spike 2, sampling rate 30 KHz, time resolution 16.7 μs) and stored on a PC for offline analysis.

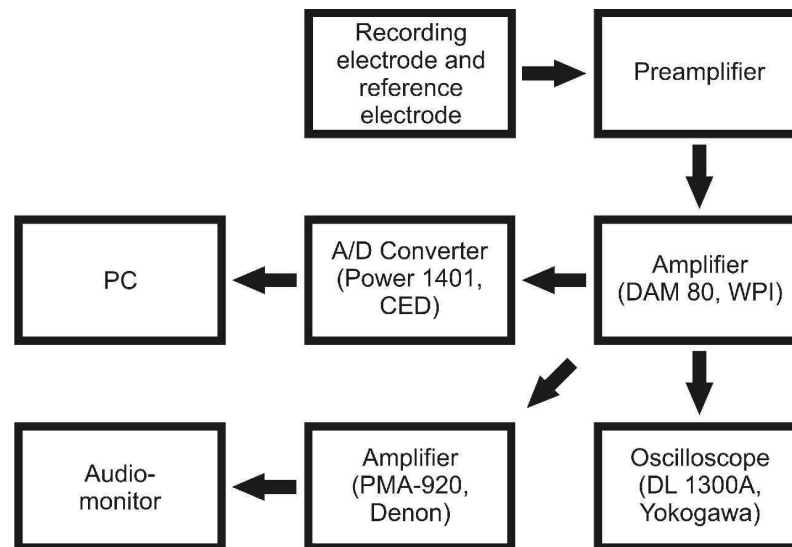


Fig. 10. Block diagram of components of recording setup. Boxes show the names of the components, brackets contain model name and manufacturer.

2.6 Data analysis

Only the responses of single units were analysed. Two parameters were used to determine single units from multi units. Inter spike interval histograms (ISIH) were plotted, in which the time intervals between successive spikes were sorted into bins (width 1 ms). If no spikes were present in the first two bins, i.e. no spike occurred within at least 2 ms after one another, and the amplitudes of action potentials did not differ by more than 150% of the noise, the recorded unit was defined as a single unit.

2.6.1 Data reduction

Data were analysed offline with Spike 2 software controlled by a custom-made script. A threshold was used to create transient transistor level (TTL) pulses (Fig. 11).

For every sphere position and vibration angle five values were calculated. Mean frequency of ongoing activity was computed from the number of TTL pulses during the inter stimulus time intervals. Mean evoked activity was calculated from the total number of TTL pulses during all eight stimuli presented at each sphere position.

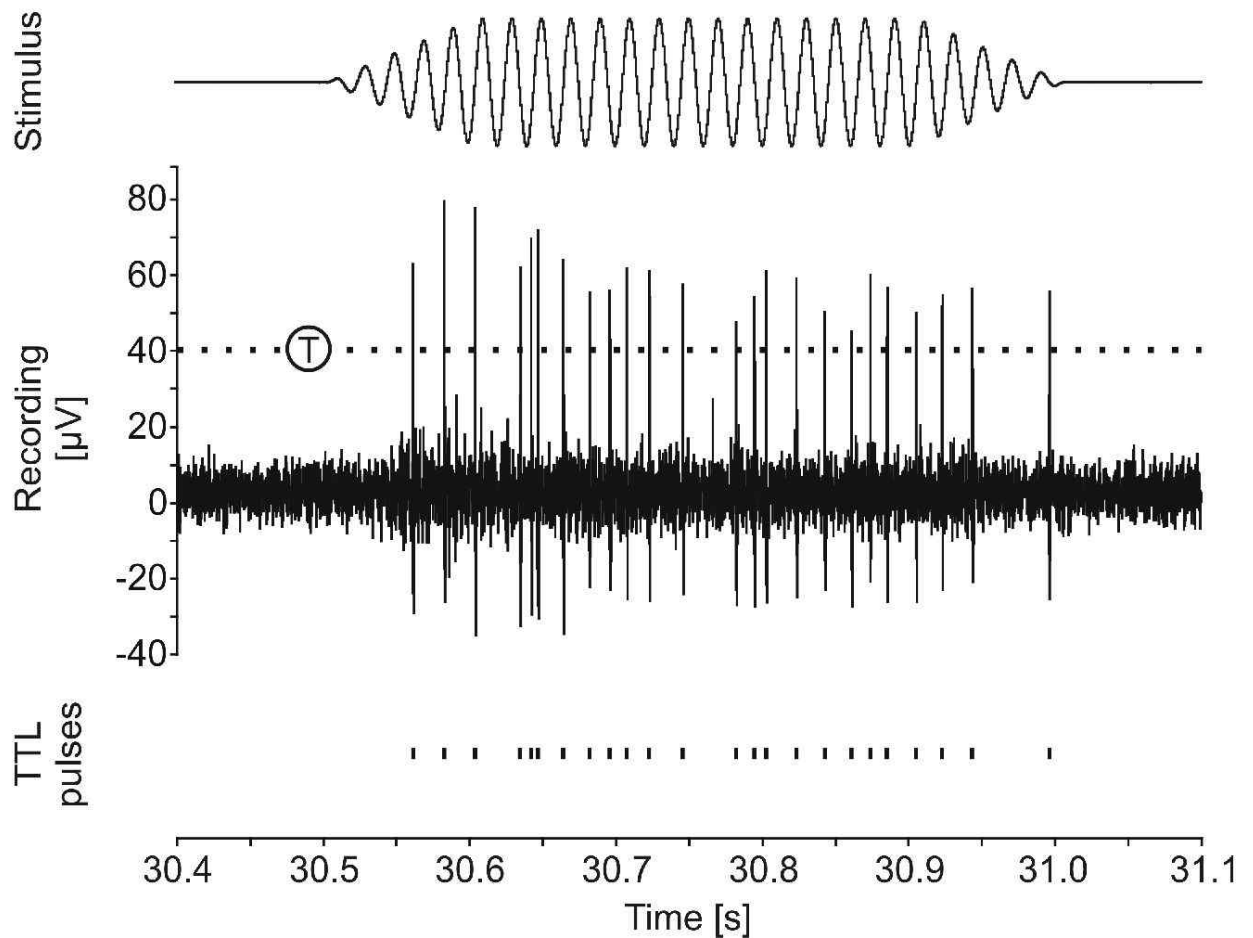


Fig. 11. Example of data reduction. Response of a midbrain lateral line unit (middle trace) to a vibrating sphere stimulus (voltage input to minishaker, top trace). T marks the threshold used to compute the TTL pulses (bottom trace).

The phase angles of spike times were determined with respect to each cycle, i.e. each full sine wave, of the 50 Hz stimulus. The average phase angle of spike times was computed along with the strength of phase-locking by means of the synchronisation coefficient R (vector strength, after Goldberg and Brown, 1969). A synchronisation coefficient of 1 indicates that all spikes occurred at the same phase angle. The Rayleigh statistic Z ($Z = R * 2N$, with N being the total number of spikes; Batschelet, 1981) was used as a measure of the statistical significance of the strength of phase-locking. Z -values > 4.6 indicate a probability of < 0.01 that action potentials were randomly distributed over a full sine wave. The mean Z -value, averaged over all full sine waves of a stimulus and all stimulus iterations, was calculated for every sphere position. The mean frequencies of ongoing and evoked activity were, as well as the average phase angles and average Z -values, plotted as function of sphere position for all examined sphere vibration angles and stimulus distances.

Plots based on evoked discharge rate were named spatial excitation patterns (SEPs). For each SEP its half maximum width (HMW; Weisstein EW 1998) was determined. A HMW was calculated from the width of a SEP at 50 % of the SEP's maximum evoked neural activity after subtraction of the mean ongoing activity. In addition to the HMWs, the widths of the SEPs were also determined for 30 % and 70 % of the maximum evoked neural activity of the SEP after subtraction of the mean ongoing activity. HMWs and the positions of the peaks of neural activity were normalised with respect to a 10 cm long fish. For each unit the maximum distance between its peaks of neural activity of SEPs of sphere vibration directions of 0°, 45°, 90° and 135° was calculated for a stimulus distance of 10 mm.

2.6.2 Response patterns of evoked neural activity

Response patterns were determined by initially plotting a unit's strongest answer (action potential frequency) for the sphere distance 10 mm in form of a peri-stimulus time histogram (PSTH, bin width 20 ms). Ongoing activity and its standard deviation were calculated from the number of events in each bin. For each unit the threshold was defined as the units mean ongoing activity plus two times the standard deviation. Bins during the stimulus (duration 500 ms) with values at or above this threshold were counted and divided by 25, i.e. the total number of bins during a single stimulus. The result was defined as response pattern coefficient (RPC). The response properties of units with a $RPC < 0.4$ were classified as phasic, a $RPC \geq 0.4$ but < 0.9 was rated phasic-tonic, and units showing an $RPC \geq 0.9$ were categorised as tonic.

2.6.3 Phase histograms

For units that showed average Z-values > 4.6 phase histograms (bin width 10°) were computed and plotted as function of sphere position.

2.7 Histology

At the end of each successful experiment the location of the electrode tip inside the brain was marked with an electrolytic lesion by successively passing DC currents of both polarities through the electrode for 15 s each. The electrode was removed 30–45 minutes after the lesion. Fish were

decapitated and the opening in the skull was widened. Heads were fixed in 4 % paraformaldehyde (see appendix A) for a minimum of six days. Brains were removed, postfixed for at least three days in paraformaldehyde, embedded in paraffin and cut in 15 μm sections in a transverse plane parallel to the electrode penetration. Sections were stained with cresyl violet (see appendix A), that stains the Nissl bodies, and analysed microscopically. Locus and extent of lesions were identified by a dark stained area and, in some cases, damaged tissue. The approximate locus of a possible lesion was curtailed by the recording depth of the respective unit. The locating of a lesion was facilitated by tissue damage resulting from electrode penetrations that led to the recording of the respective unit. Digital images of verified lesions were stored. Since brains shrunk considerably during histological processing (Simmons and Swanson 2009), the recording depths (relative to the surface of the OT) displayed on the microdrive during experiments differed from the positions of the lesions relative to the surface of the OT in the brain sections. Only the recording depths read from the microdrive were used in this study.

3 Results

For this study 98 single unimodal lateral line units were recorded from 78 goldfish. Out of these 98 units a total of 16 units could be recorded for a minimum of one hour, so that at least one SEP could be mapped for each of the four tested directions of sphere vibration. Thus the results of this study are based on 16 unimodal lateral line units that were recorded from 16 goldfish, that ranged from 9.5–12 cm in standard body length and 18–31 g in weight. Recording depths ranged from 971–2,088 μm , relative to the dorsal surface of the OT. For a tabular overview of all units see appendix B.

3.1 Anatomy

The positions of electrode penetrations of 14 out of 16 units are plotted in Fig. 12. Positions of penetrations of unit 15 and 16 were not determined.

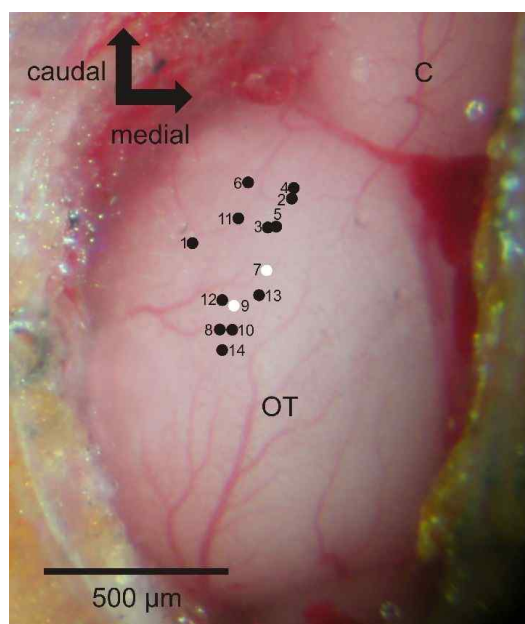
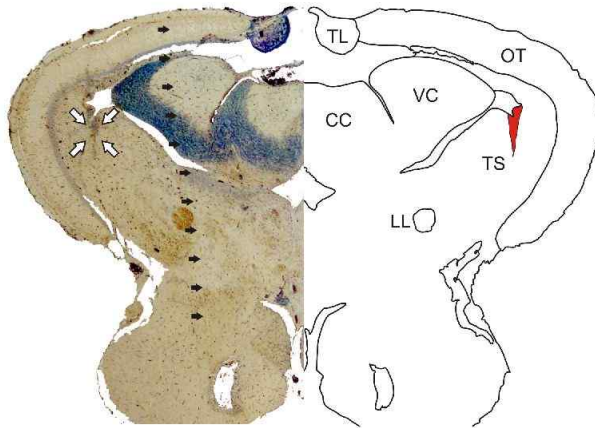


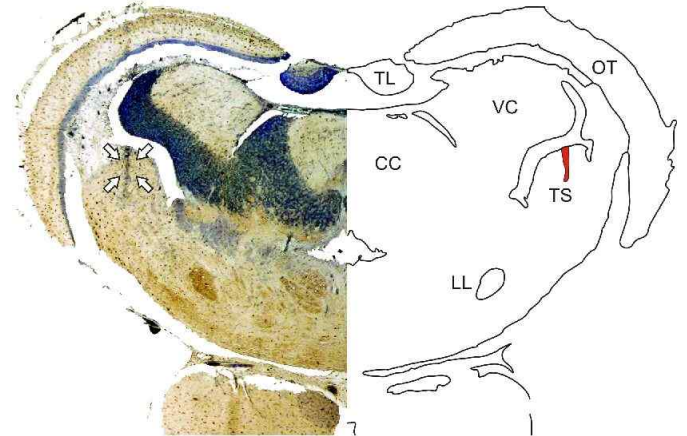
Fig. 12. Dorsal view of the surface of the optic tectum and a part of the cerebellum after removal of a fraction of the cranial bone and adipose tissue. The torus semicircularis lies ventral to the dorsal surface of the OT (McCormick and Hernandez 1996; Rupp et al. 1996; for review, see McCormick et al. 1989). C = Cerebellum, OT = Optic tectum. Dots indicate electrode penetrations that led to a successful recording of a unimodal midbrain lateral line unit. Black dots indicate penetrations where recording sites could be verified by a lesion. White dots represent penetrations with unverified recording sites. Positions of electrode penetrations of units 15 and 16 could not be determined.

12 of 16 lesions were located in the nucleus ventrolateralis of the TS (Fig. 13, Fig. 14). Lesions were roundish (\varnothing 25–170 μm) or longish (20×130 – $120 \times 340 \mu\text{m}$).

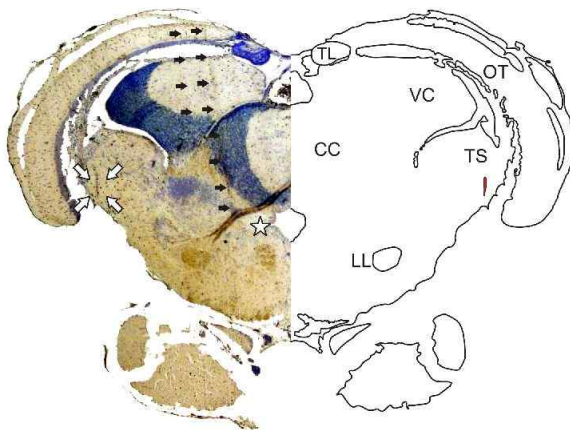
A - Unit 1



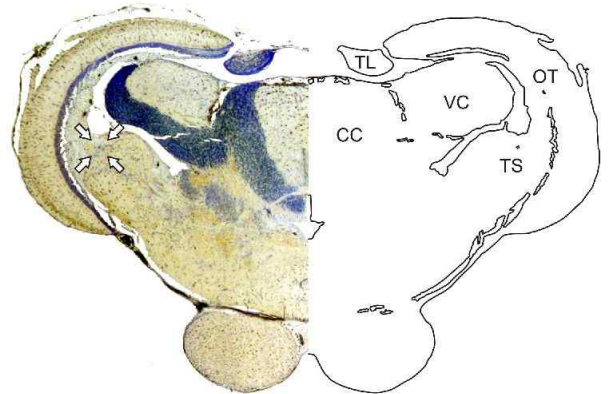
B - Unit 2



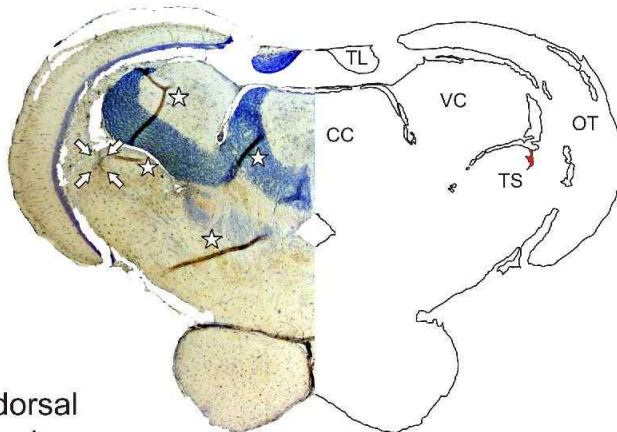
C - Unit 3



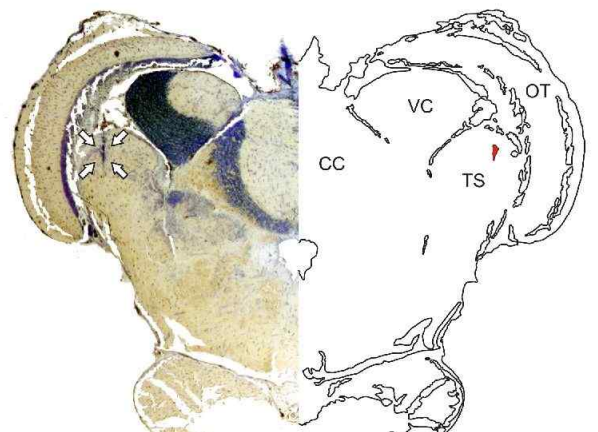
D - Unit 4




E - Unit 5



F - Unit 6

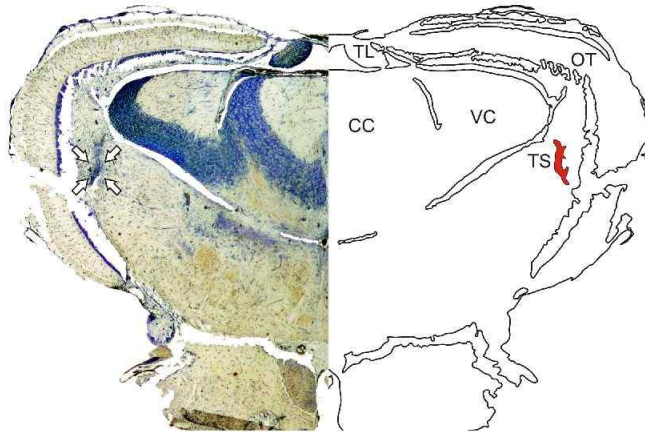


dorsal
 medial

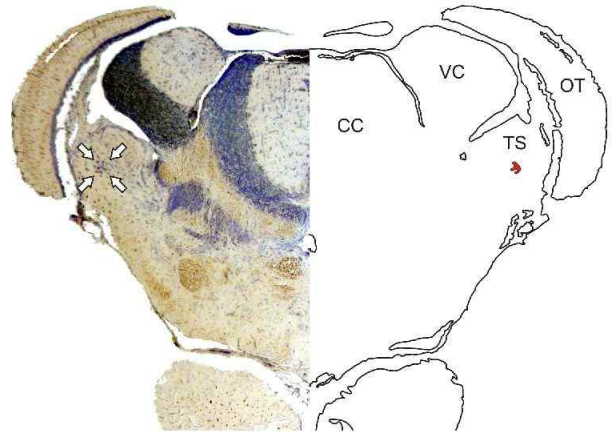
1.000 μm

Fig. 13, A–F. Electrolytic lesions in the midbrain of goldfish for verification of the recording sites of units 1–6. Paraffin-sectioned (15 μm) cresyl-violet stained transverse hemisections and horizontally mirrored line drawings. Lesions are marked with white arrows in the photos of the brain sections and in red in the line drawings. Sectioning artefacts are marked with small black arrows. Locations where a section is partially folded or overlapping are marked with a white star (unit 3 and 5). CC = Corpus cerebelli, LL = Lateral lemniscus, OT = Optic tectum, TL = Torus longitudinalis, TS = Torus semicircularis, VC = Valvula cerebelli.

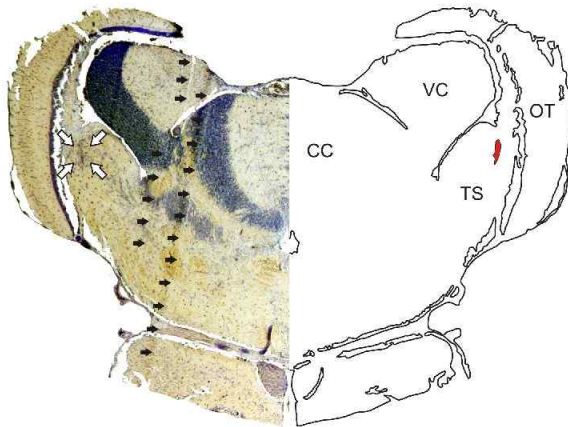
A - Unit 8



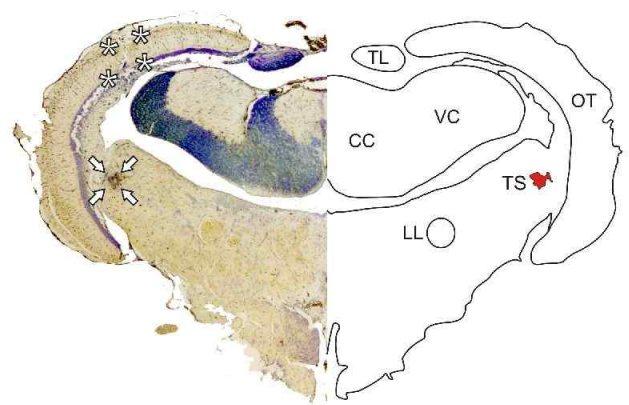
B - Unit 10



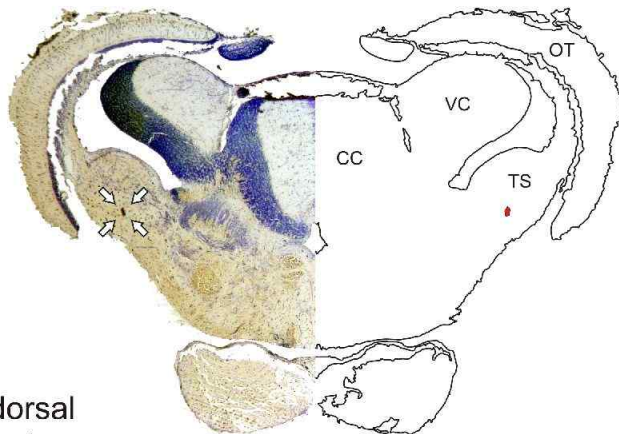
C - Unit 11



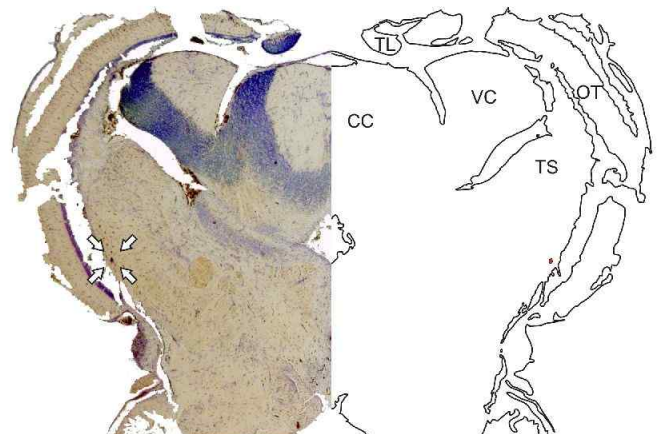
D - Unit 12

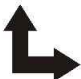


E - Unit 13



F - Unit 14



dorsal

 medial

1.000 μm

Fig. 14, A–F. Electrolytic lesions in the midbrain of goldfish for verification of the recording sites of units 8, 10–14. Lesions for units 7, 9, 15 and 16 could not be recovered. Paraffin-sectioned (15 μm) cresyl-violet stained transverse hemisections and horizontally mirrored line drawings. Lesions are marked with white arrows in the photos of the brain sections and in red in the line drawings. Sectioning artefacts are marked with small black arrows. A part of an electrode track is framed by four white asterisks (unit 12). CC = Corpus cerebelli, LL = Lateral lemniscus, OT = Optic tectum, TL = Torus longitudinalis, TS = Torus semicircularis, VC = Valvula cerebelli.

3.2 Electrophysiology

3.2.1 Ongoing activity

All 16 units showed ongoing activity (mean \pm SD 4.36 \pm 12.57 Hz, median 0.36 Hz, range 0.01–51.72 Hz). 14 of 16 units exhibited average ongoing activities of \leq 0.44 Hz (mean \pm SD 0.44 \pm 0.45 Hz, median 0.32 Hz, range 0.01–1.40 Hz). Unit 12 and unit 3 had average ongoing activities of 12.37 Hz and 51.72 Hz, respectively.

3.2.2 Response patterns of evoked neural activity

All units responded to the vibrating sphere stimulus with an increase in discharge rate (Fig. 15). Response patterns were invariable throughout all positions of a given unit. Unit 12 constituted an exception, as it generally responded to the stimulus with excitation (increase in neural activity relative to the ongoing activity), but showed inhibition (decrease in neural activity relative to the ongoing activity) as a response to stimulation at distinct positions (Fig. 17D). Unit 3 showed a decrease in average ongoing activity during the falling ramp of the stimulus (Fig. 15C). Responses of one unit were phasic, nine units showed phasic-tonic responses and six units responded in a tonic fashion (Fig. 15).

3.2.3 Spatial excitation patterns

112 spatial excitation patterns (SEPs) were plotted, each based on the units responses to stimulation at 42–177 sphere positions. SEPs of ten units were based on a single distance between fish and sphere, while SEPs of six units were mapped for at least two different sphere distances.

SEPs had one (e.g. Figs. 16G₃; 17G₃), two (e.g. Figs. 16E₃; 17H₁), or more peaks of increased neural activity (e.g. Figs. 16F₃). While 15 of 16 units responded to stimulation with excitation only, unit 12 was an exception. It responded with excitation at most sphere positions, but showed inhibition to stimulation at some sphere positions (e.g. Fig. 17D). The variability of the SEPs for different sphere vibration directions recorded from a given unit ranged from low (e.g. Fig. 17C) to high (e.g. Fig. 17D). In all units evoked discharge rates at a given rostro-caudal position generally

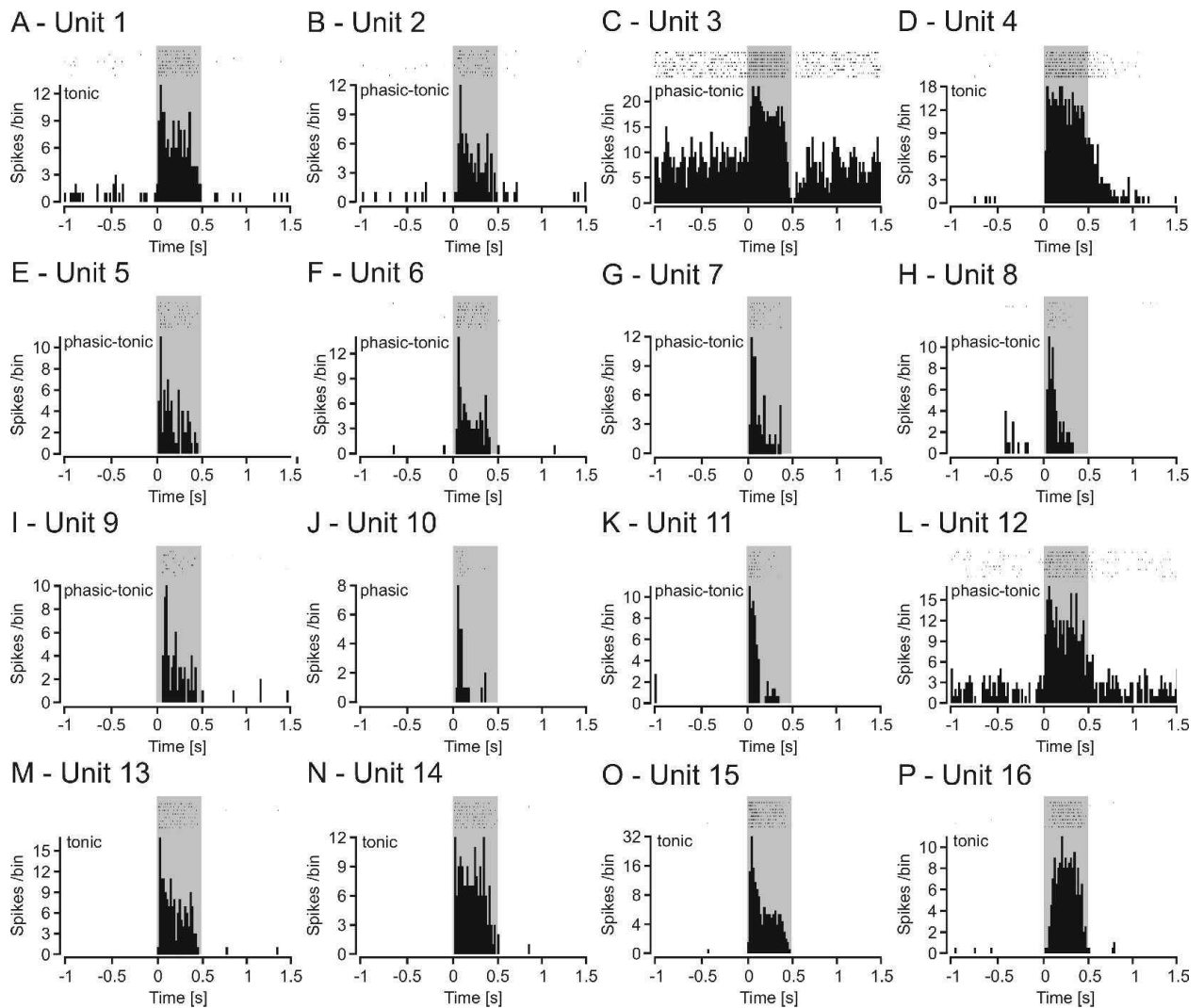


Fig. 15, A–P. Response patterns of units 1–16. Top rows hold raster plots of the spike times of responses to eight successive stimuli. Bottom rows show PSTHs (bin width 20 ms) and the calculated response pattern type (phasic, phasic-tonic or tonic). Time of stimulation is marked in grey.

decreased with increasing stimulus distance. For a given unit and direction of sphere vibration, SEPs for different stimulus distances were therefore similar in shape but differed in spike rate (eg. Figs. 16A₄, E₃; 17C₂, D₁, G₄). Exceptions were SEPs for different stimulus distances that were largely coextensive (e.g. Figs. 16E₄; 17G₂) or SEPs where the excitation pattern for the greater stimulus distance exceeded the pattern for the smaller distance in terms of average evoked activity at certain positions (e.g. Figs. 17G₁, D₂). The rostro-caudal positions of the maxima of the SEPs were located in the snout region (e.g. Figs. 17D₄, E₄) the central region (e.g. Figs. 16E₃; 17G₃) or around the base of the tail fin (e.g. Figs. 16F₁, G₄).

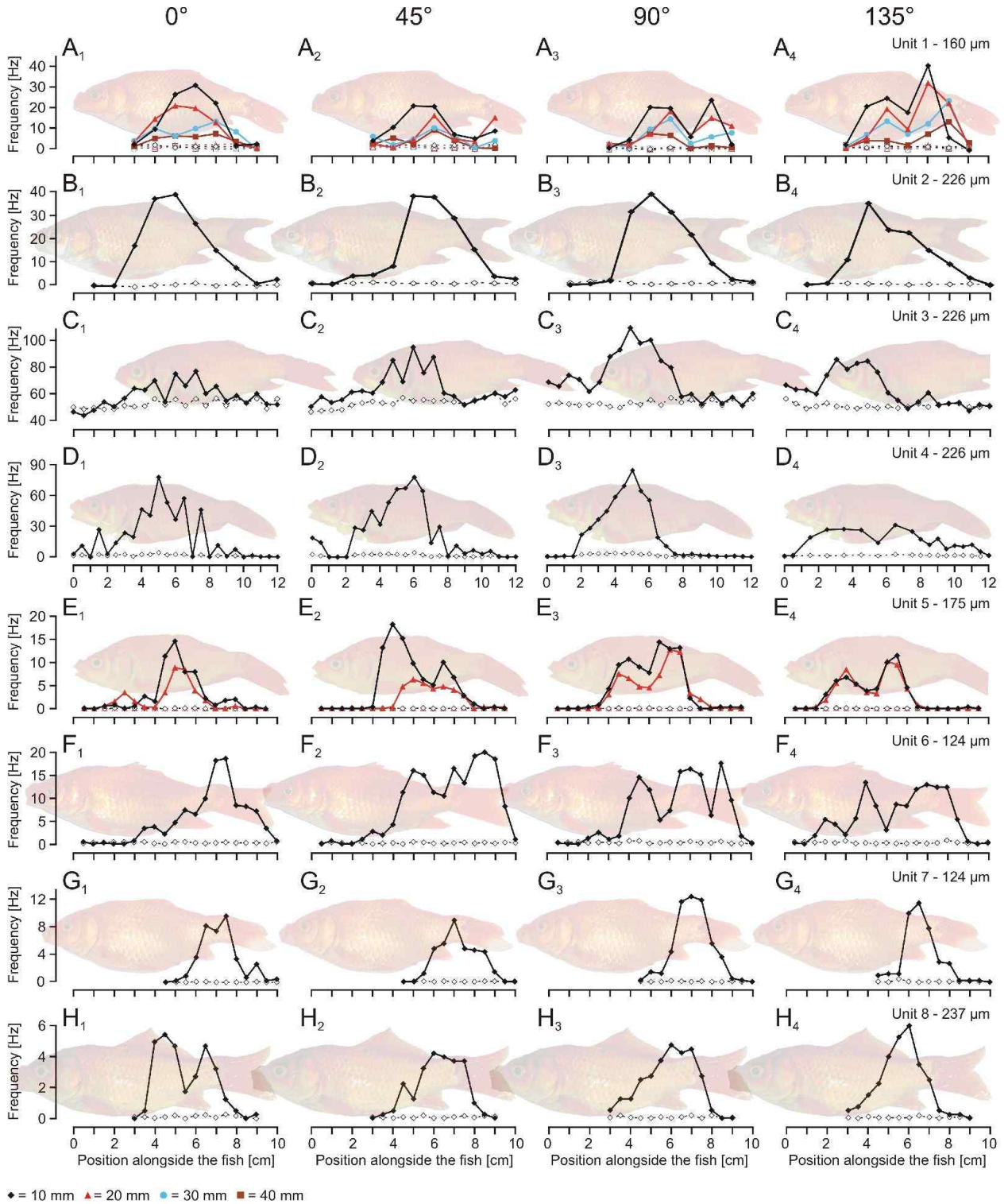


Fig. 16, A–H. SEPs and ongoing activity of midbrain lateral line units 1–8. Ongoing activity (dashed line) and activity evoked by a stationary vibrating sphere (solid line) are plotted as function of sphere position and axis of sphere vibration. The distance between fish and sphere was 10, 20, 30 or 40 mm and is colour-coded (see legend). Axis of sphere vibration was 0° (parallel to the fish), 45°, 90° (perpendicular to the fish) or 135°. The peak-to-peak sphere displacement is given in the top right of each row. Fish size and position are to scale. Please note that the y-axis in C starts at 40 Hz and that the x-axis in D has a maximum of 12 cm, while all other x-axes have a range of 10 cm.

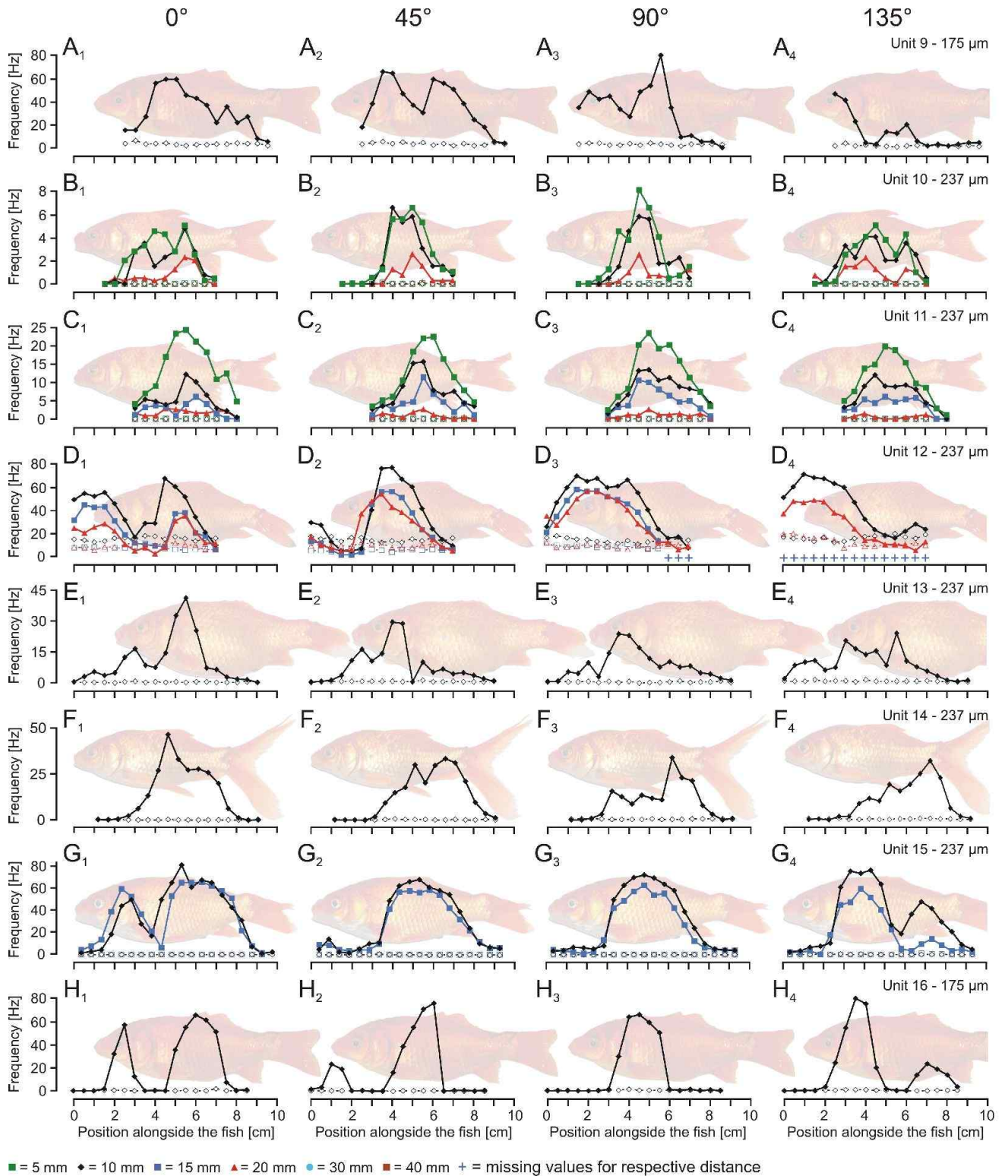


Fig. 17, A–H. SEPs and ongoing activity of midbrain lateral line units 9–16. Ongoing activity (dashed line) and activity evoked by a stationary vibrating sphere (solid line) are plotted as function of sphere position and axis of sphere vibration. The distance between fish and sphere was 10, 20, 30 or 40 mm and is colour-coded (see legend). Axis of sphere vibration was 0° (parallel to the fish), 45° , 90° (perpendicular to the fish) or 135° . The peak-to-peak sphere displacement is given in the top right of each row. Fish size and position are to scale.

HMWs covered 14.9 ± 9.0 % (mean \pm SD; range 1.7–43 %) of the rostral-caudal axis of a 10 cm long fish (Figs. 18; 19; 20; 21). The dimensions of the HMWs that were continuous, i.e. consisted of only one part, ranged from narrow (1.7 %, 4.0 % and 5.1 %; Figs. 21A 135°; 18A 90°; 19C 45°) to broad (31.3 %, 42.2 % and 42.5 %; Figs. 21C 90°; 20D 90°; 19B 90°).

Based on the analysis of HMWs and the peaks of neural activity, units were divided into three groups. The SEPs for sphere vibration directions of 0°, 45°, 90° and 135° were aligned centrally among one another in units 2, 7 and 11 (Figs. 18B; 19C; 20C 30 % max). The positions of the peaks of evoked neural activity in the respective units differed by a maximum of 8.5 mm for a stimulus distance of 10 mm. The SEPs of units 3, 12, 15 and 16 were systematically and continuously displaced towards the snout of the fish with increasing sphere vibration angles (Figs. 18C 30 % max; 20D; 21C, D). The peaks of neural activity were also displaced for at least three of the four sphere vibration directions. The SEPs of the remaining nine units did not show any regularities. The positions of their peaks differed by 13.1–16.7 mm (units 4, 8, 10, 13 and 14)(Figs. 18D; 19D; 20B; 21A, B) and by 29.7–42.1 mm (units 1, 6 and 9)(Figs. 18A; 19B; 20A), respectively.

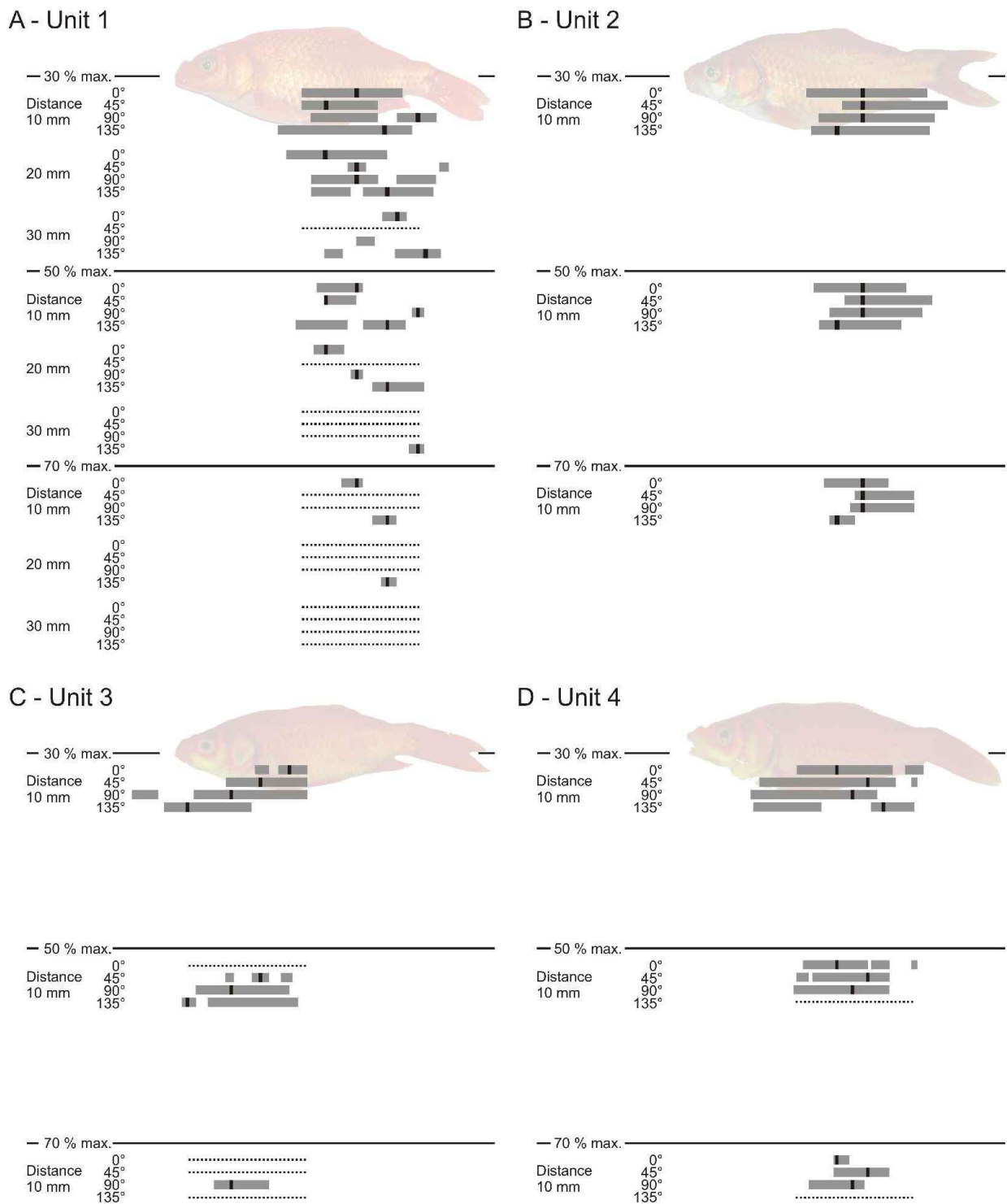


Fig. 18, A-D. Widths of SEPs of units 1–4 for tresholds of 30 %, 50 % (half-maximum width) and 70 % of maximum action potential frequency for different sphere vibration directions. Widths were normalised for a 10 cm long fish. Vertical black bars indicate the positions of the peaks of the SEPs. Stippled horizontal lines indicate positions where neural activity did not exceed the threshold of 30 %, 50 % or 70 % of the maximum action potential frequency.

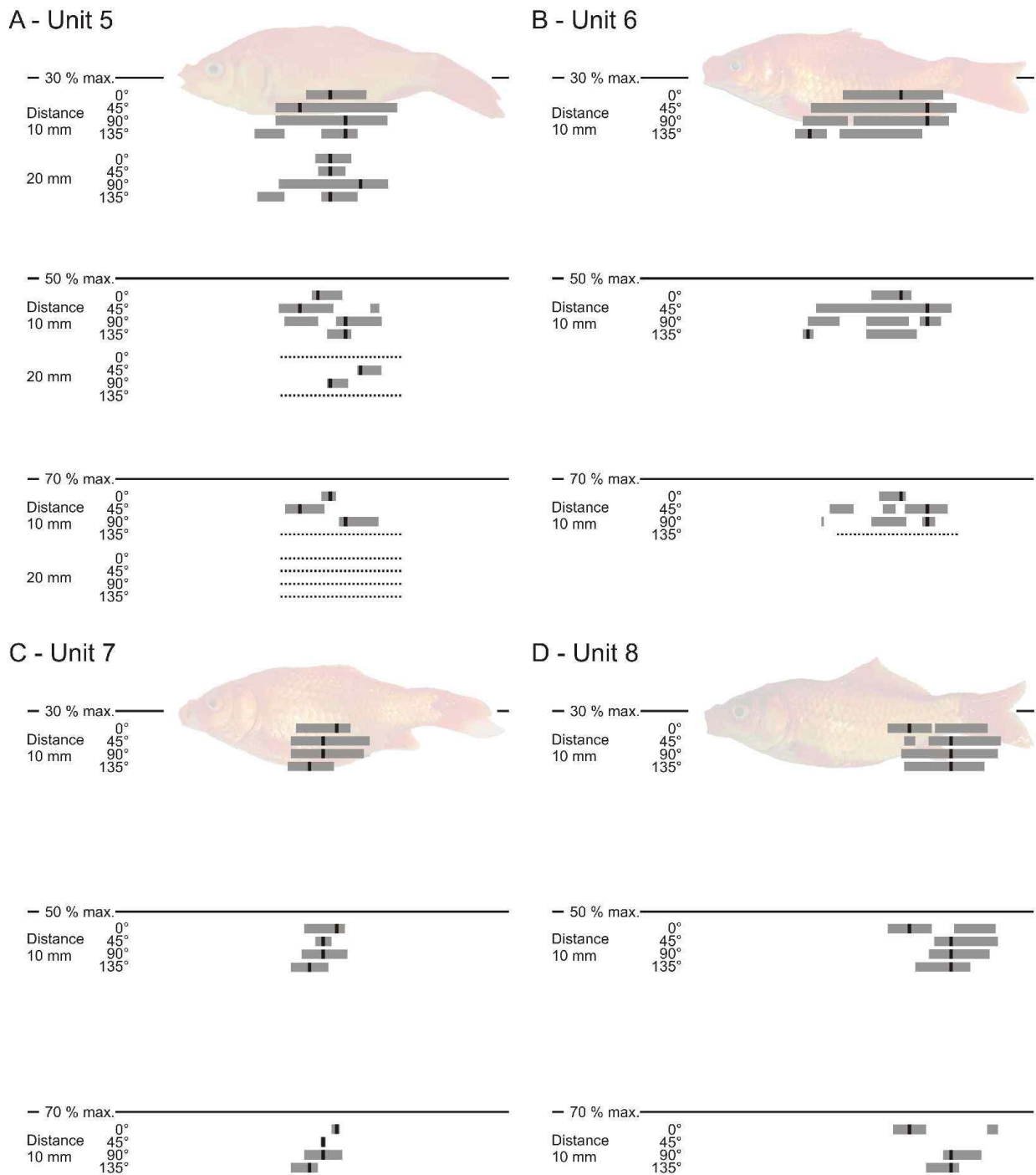
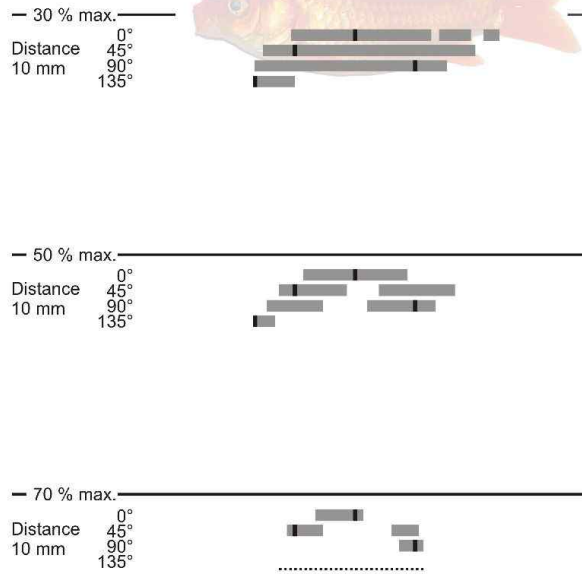
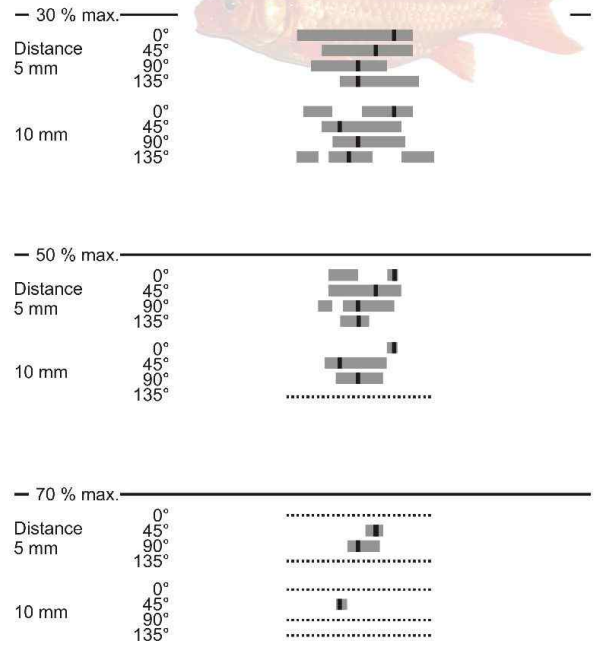


Fig. 19, A–D. Widths of SEPs of units 5–8 for thresholds of 30 %, 50 % (half-maximum width) and 70 % of maximum action potential frequency for different sphere vibration directions. Widths were normalised for a 10 cm long fish. Vertical black bars indicate the positions of the peaks of the SEPs. Stippled horizontal lines indicate positions where neural activity did not exceed the threshold of 30 %, 50 % or 70 % of the maximum action potential frequency.

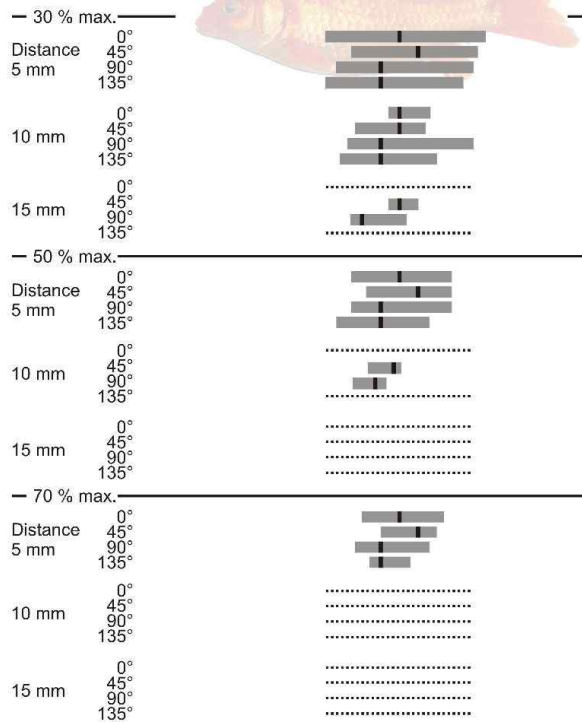
A - Unit 9



B - Unit 10



C - Unit 11



D - Unit 12

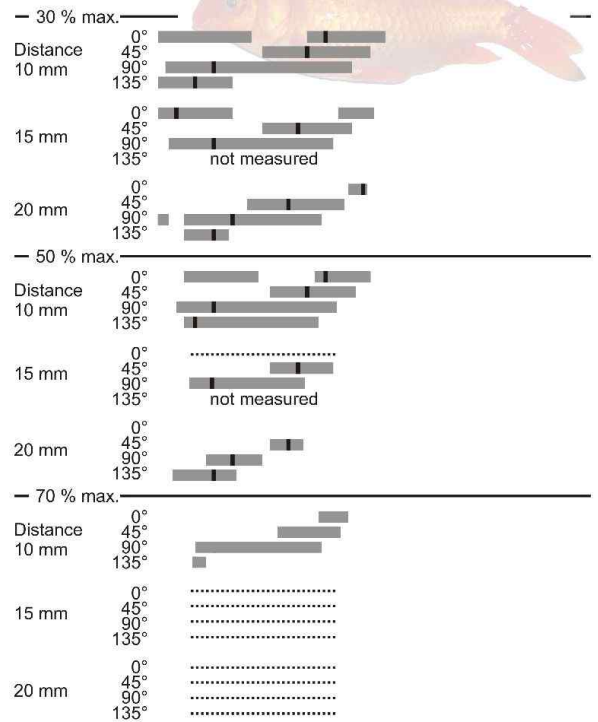


Fig. 20, A–D. Widths of SEPs of units 9–12 for thresholds of 30 %, 50 % (half-maximum width) and 70 % of maximum action potential frequency for different sphere vibration directions. Widths were normalised for a 10 cm long fish. Vertical black bars indicate the positions of the peaks of the SEPs. Stippled horizontal lines indicate positions where neural activity did not exceed the threshold of 30 %, 50 % or 70 % of the maximum action potential frequency.

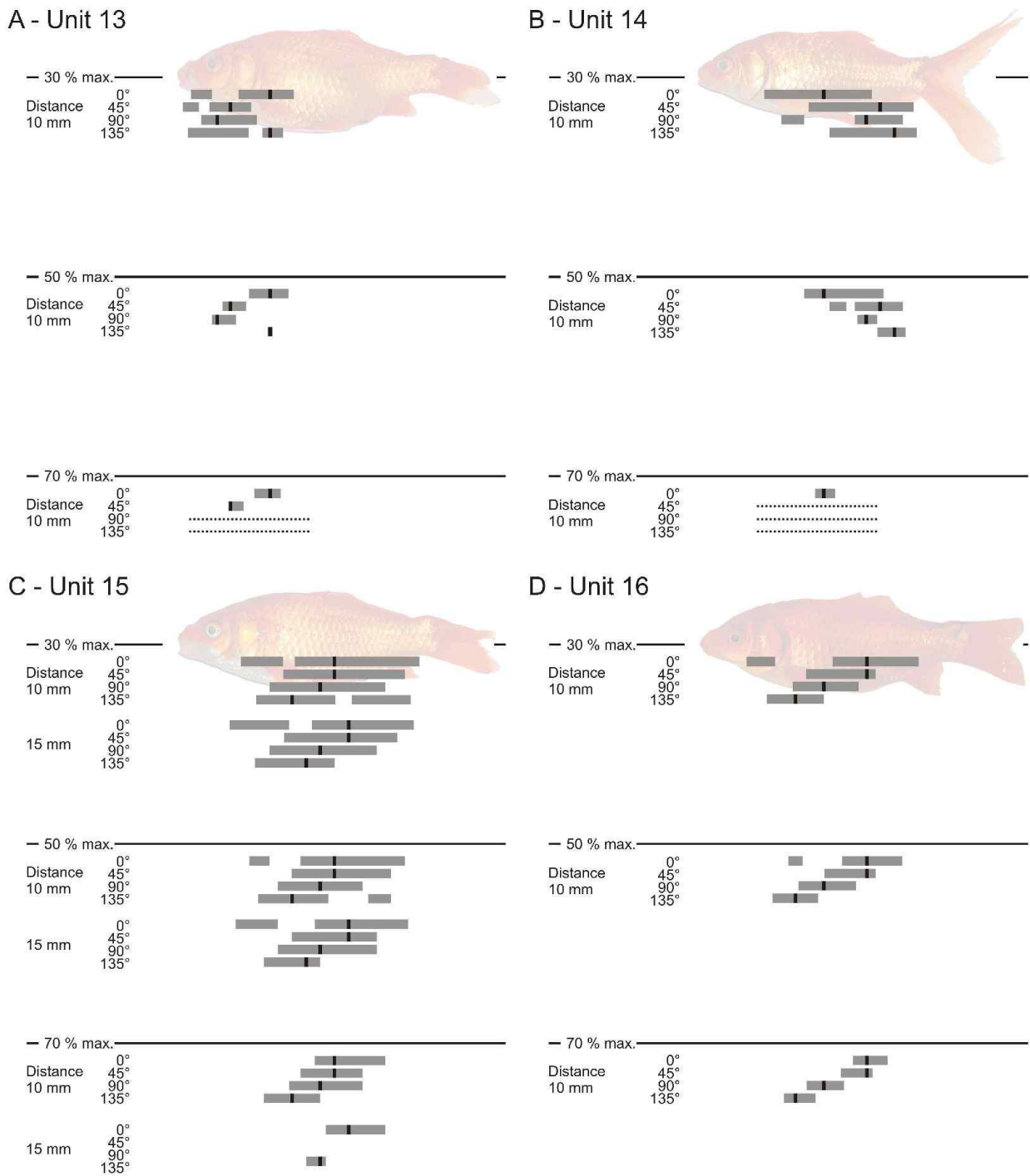


Fig. 21, A–D. Widths of SEPs of units 13–16 for thresholds of 30 %, 50 % (half-maximum width) and 70 % of maximum action potential frequency for different sphere vibration directions. Widths were normalised for a 10 cm long fish. Vertical black bars indicate the positions of the peaks of the SEPs. Stippled horizontal lines indicate positions where neural activity did not exceed the threshold of 30 %, 50 % or 70 % of the maximum action potential frequency.

3.2.4 Phase locking

With the exception of unit 9 all toral lateral line units exhibited significant phase-locking (average Z-values > 4.6) at least at one sphere position (Figs. 24; 25). However, for a stimulus distance of 10 mm only three units (3, 4 and 15) showed significant Z-values for at least six side by side positions of the sphere. Unit 3 had an average Z-value of 82.18 (synchronisation coefficient R was 0.51 ± 0.22 (mean \pm SD)), unit 4 showed an average Z-value of 6.79 (0.35 ± 0.30 (mean \pm SD)) and unit 15 had an average Z-value of 12.80 (0.27 ± 0.20 (mean \pm SD)).

Figure 22 exemplifies phase locked responses of unit 3. Phase histograms revealed that units 3 and 4 phase locked to only one half of a full wave cycle, while unit 15 phase locked to both halves of a full wave cycle (Fig. 23). For phase histograms of all recorded positions of units 3, 4 and 15, see Appendix C.

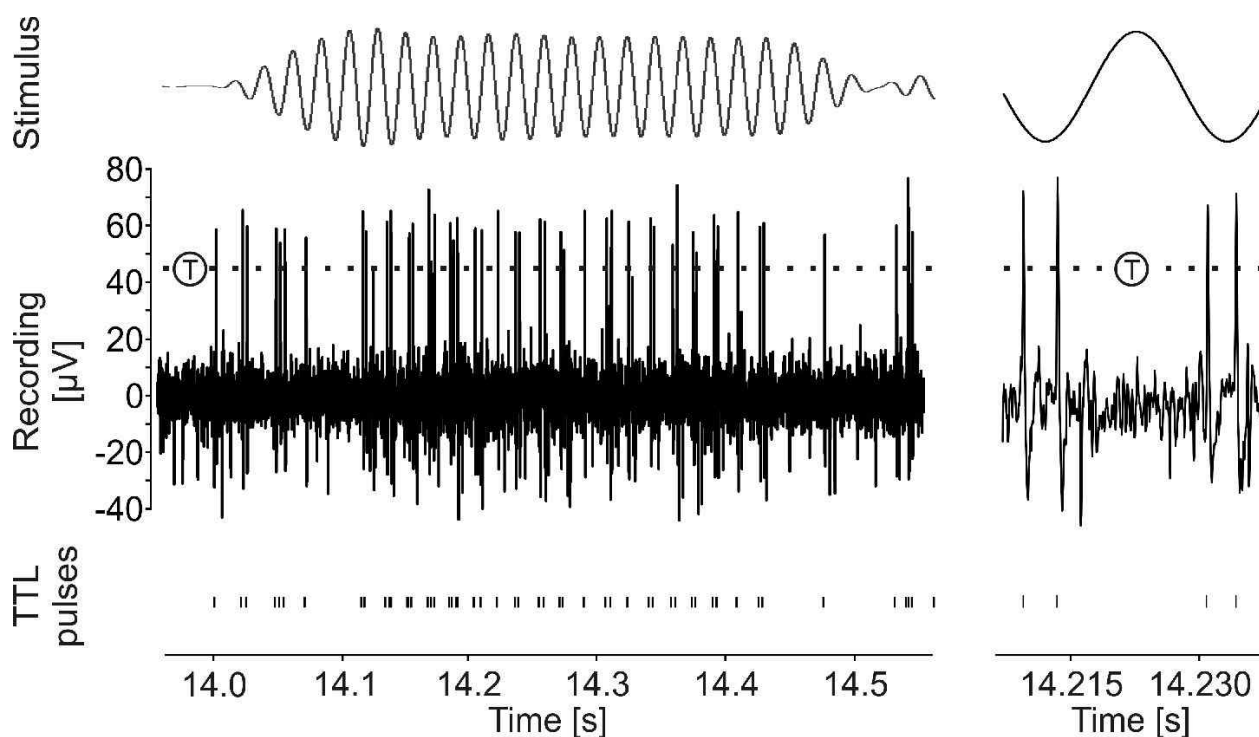


Fig. 22 Phase locked responses of unit 3 (position 1 cm, sphere vibration direction 90° , middle trace) to a vibrating sphere stimulus (voltage input to minishaker, top trace). T marks the threshold used to compute the TTL pulses (bottom trace). The left figure shows the units responses to a full stimulus, the figure on the right shows a magnification of 1.5 full wave cycles. Note that the unit at first responds to the stimulus with bursts of three spikes and thereafter mainly shows two spikes in close succession. The average phase angle for this unit is 229.28° , the average Z-value 264.57. The corresponding phase histogram is depicted in Fig. 23A₂₄.

While certain sphere positions did not lead to a response in the phase histograms of the stimulated unit (e.g. Fig. 23A₁; B₁₁–B₁₃), effects of sphere position and sphere vibration direction on the shape of phase histograms were clearly visible in most of the phase histograms of units 3 and 15 (Fig. 23). Moving the sphere alongside the fish from rostral to caudal or vice versa with a given sphere vibration direction often led to a phase shift. The distance between the sphere positions where a phase shift was evident differed considerably from about 10 mm (e.g. Fig. 23A₆–A₈) to about 30 mm (e.g. Fig. B₂–B₁₀). In some cases a phase shift could also be observed if the sphere position was kept constant but the sphere vibration direction was changed. For example, in one unit, the phase angle shifted from 115.45° to 255.97° if the sphere vibration direction was changed from 0° to 45° (Fig. 23A₆; A₁₆).

In unit 3 and 15, the position where the sphere evoked a characteristic phase histogram shifted rostrally if the sphere vibration angle was increased. For example, for a sphere vibration direction of 0° a response to the second half of a full wave cycle was evident at position A₈ (Fig. 23A₈). If the position of the sphere was left unaltered but the sphere vibration direction was changed to 45°, the same type of response occurred 15 mm more rostral (Fig. 23A₁₅). For the sphere vibration angles 90° and 135° the positions where the sphere caused responses to the second half of a full wave cycle were again shifted towards the head of the fish by 5 and 10 mm, respectively (Fig. 23A₂₃; A₃₂). In unit 15, the position where the unit phase locked to the first half of a full wave cycle also depended on sphere vibration direction. For the sphere vibration direction 0°, the position where the sphere evoked a response only to the first half of a full wave cycle of the stimulus lay 63 mm caudal to the tip of the snout of the fish (Fig. 23B₆). For sphere vibration angles of 45°, 90° and 135°, the positions where the vibrating sphere stimulus resulted in characteristic histograms lay more rostrally, that is 53, 48 and 43 mm caudal to the tip of the snout (Fig. 23B₁₄; B₂₃ and B₃₂).

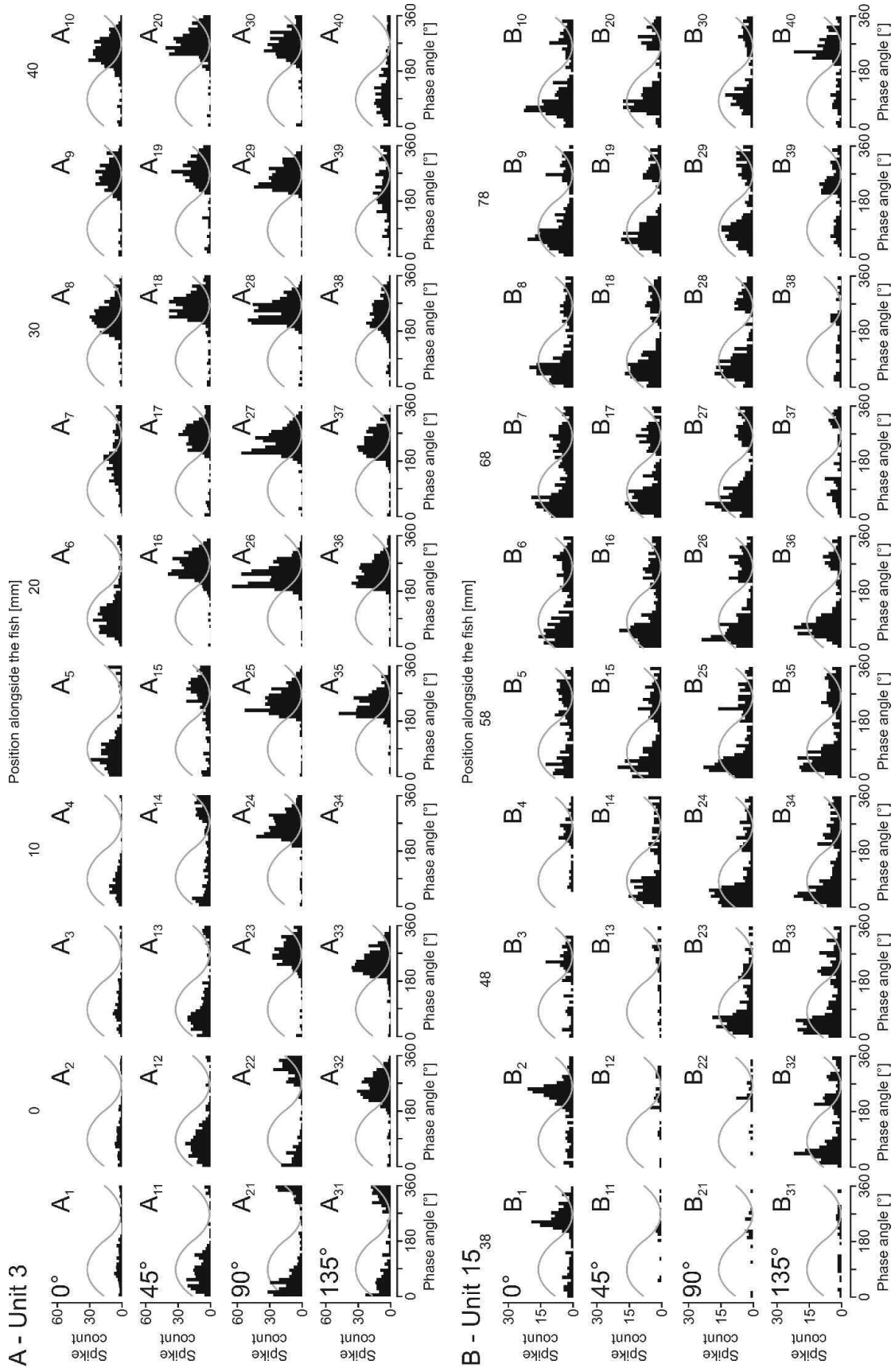


Fig. 23 Selected phase histograms of units 3 (**A**) and 15 (**B**). The distance between two neighbouring sphere positions was 5 mm. Full sinusoidal wave cycles are depicted in grey. Unit 3 responded only to one half of a wave cycle, while unit 15 reacted to both halves of a wave cycle. Note that the phase angle depended on both, the position of the sphere and the direction of sphere vibration. No histogram could be obtained for the sphere position depicted in A_{34} . For all phase histograms of units 3, 4 and 15, see Appendix C.

3.2.5 Plots of average phase angles and average Z-values

The plots of average phase angles and average Z-values of 15 out of 16 units consisted of phase angles that were significant (i.e. Z-value > 4.6) only at single or few sphere positions (Figs. 24A, B, D–H; 25A–F; H). Plots of the two other units are based upon phase angles that are significant for the majority (>50 %) of sphere positions. Unit 3 exhibited significant phase-locking for the vast majority (93 %) of positions for a sphere distance of 10 mm. Especially the positions in the centre of the plots showed highly significant phase-coupling, while the most rostral and caudal positions had lower average Z-values (Fig. 24C). In addition, the shape of the plots of average phase angles of this unit is similar to the shape of the plots of average phase angles of primary lateral line afferents (cf. Fig. 28D). 45 of 80 (56 %) sphere positions of unit 15 showed significant Z-values for a stimulus distance of 10 mm (Fig. 25G). The sphere vibration direction had no systematic or predictable effect on the occurrence or strength of phase-coupling.

Plots of average phase angles and average Z-values of units of which several stimulus distances were examined showed variable characteristics. Plots for a given sphere vibration direction but different stimulus distances of unit 1 and 5 showed strong similarities, but had no consecutive positions where the average Z-values exceeded 4.6 (Fig. 24A, E). The plots for distances of 10 and 15 mm in unit 15 were quite similar to one another, at least in the centers of the plots while its borders showed fluctuations (Fig. 25G). While average Z-values for a stimulus distance of 10 mm were significant for the centers of the plots for all sphere vibration directions, for a distance of 15 mm only positions of the plots for 0° were significant (Fig. 25G). Plots for stimulus distances of 5 and 10 mm in unit 10 were nearly coextensive with significant average Z-values (Fig. 25B).

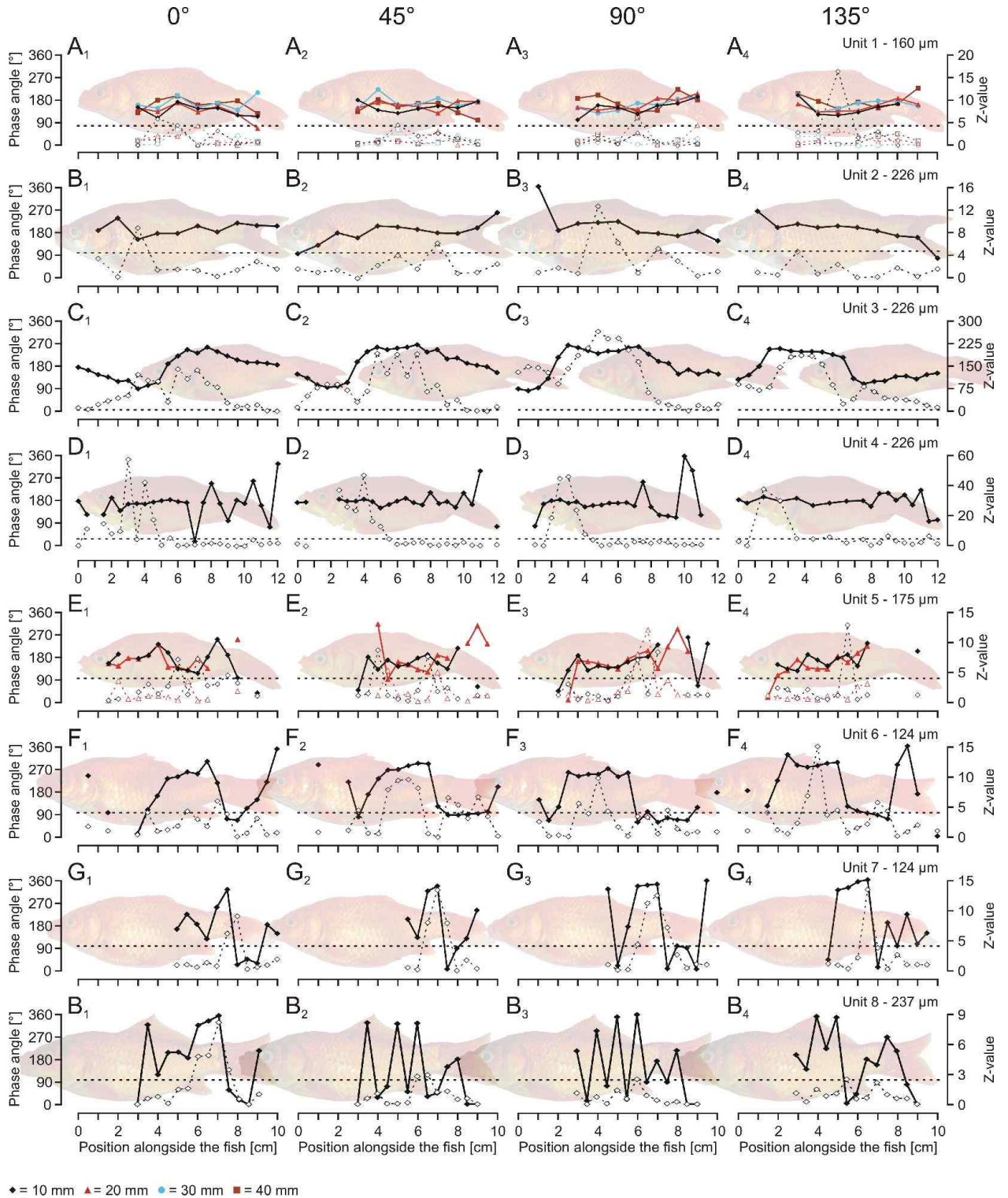


Fig. 24, A–H. Plots of average phase angles and average Z-values of midbrain lateral line units 1–8. Average phase angle (solid line) and average Z-value (dashed line) are plotted as function of sphere position and axis of sphere vibration. The distance between fish and sphere was 10, 20, 30 or 40 mm and is colour-coded (see legend). Axis of sphere vibration was 0° (parallel to the fish), 45°, 90° (perpendicular to the fish) or 135°. The peak-to-peak sphere displacement is given in the top right of each row. Fish size and position are to scale. Please note that the x-axis in D has a maximum of 12 cm, while all other x-axes have a range of 10 cm.

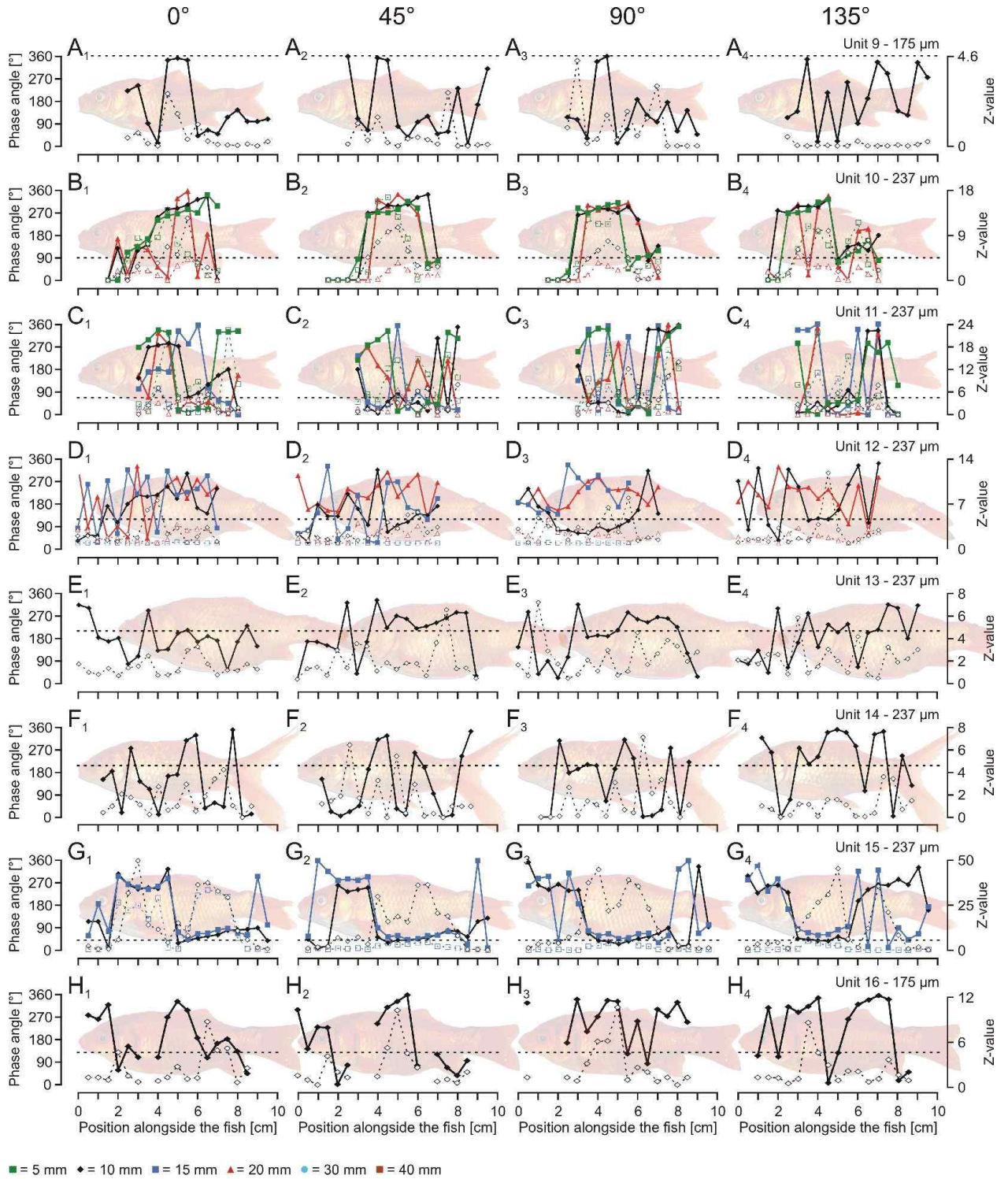


Fig. 25, A-H. Plots of average phase angles and average Z-values of midbrain lateral line units 9–16. Average phase angle (solid line) and Z-value (dashed line) are plotted as function of sphere position and axis of sphere vibration. The distance between fish and sphere was 10, 20, 30 or 40 mm and is colour-coded (see legend). Axis of sphere vibration was 0° (parallel to the fish), 45°, 90° (perpendicular to the fish) or 135°. The peak-to-peak sphere displacement is given in the top right of each row. Fish size and position are to scale.

3.2.6 Topography

A topographic relationship between the the rostro-caudal positions of SEPs and the positions of electrode penetrations on the surface of the OT (cf. Fig. 12) was not evident (Fig. 26). In addition, the rostro-caudal positions of SEPs did not relate to the recording depths (Fig. 27).

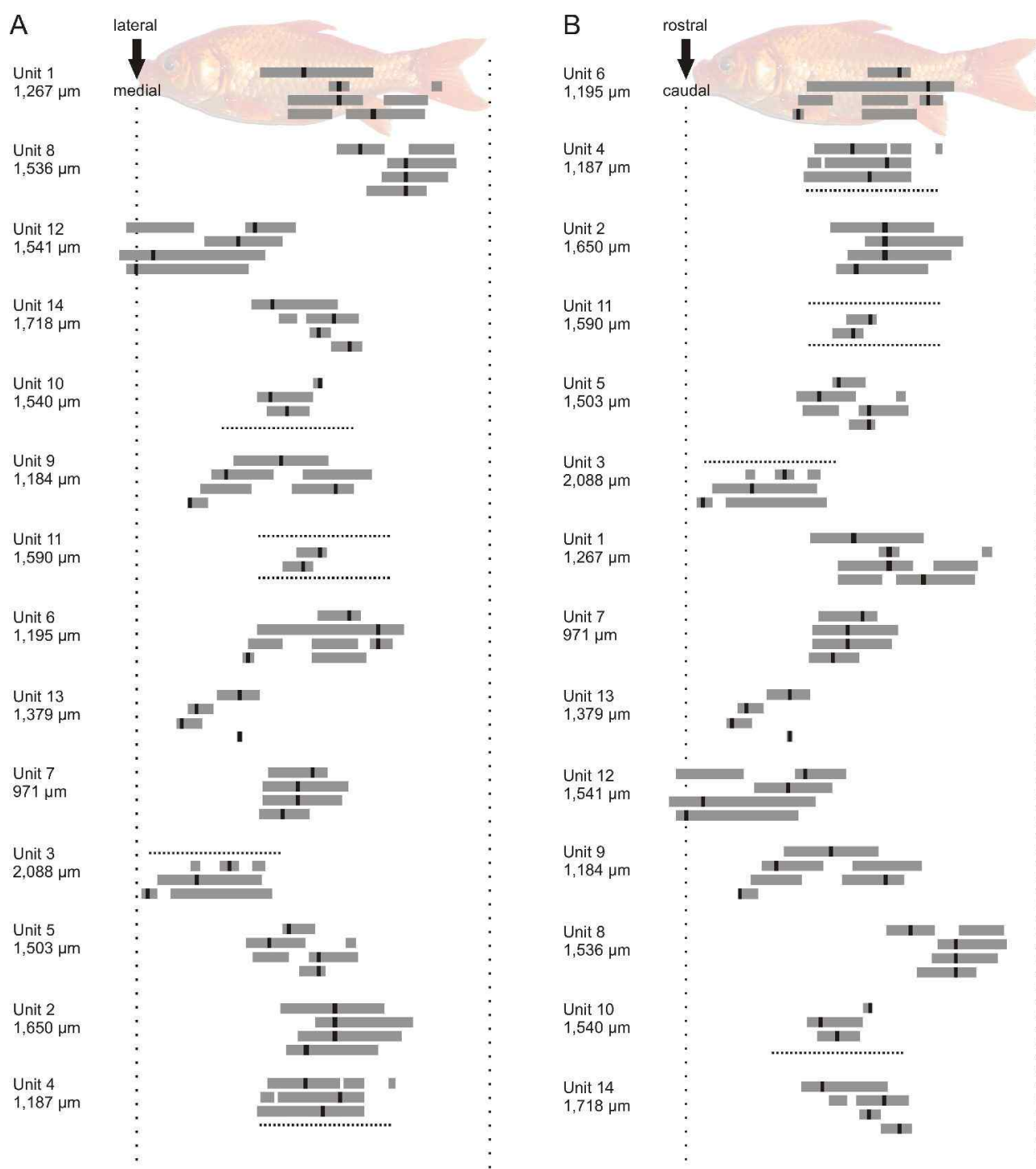


Fig. 26, A, B. Rostro-caudal position of HMWs (sphere distance 10 mm) plotted relative to the medio-lateral (**A**) and the rostro-caudal (**B**) positions of electrode penetrations (cf. Fig. 12). For each unit, HMWs are shown for sphere vibration directions of 0°, 45°, 90° and 135° (from top to bottom), respectively. HMWs were normalised to a 10 cm long fish. Vertical black bars indicate the positions of the peaks of the SEPs. Stippled horizontal lines indicate positions where neural activity of a given unit failed to exceed the threshold of 50 % of the maximum action potential frequency. **41**

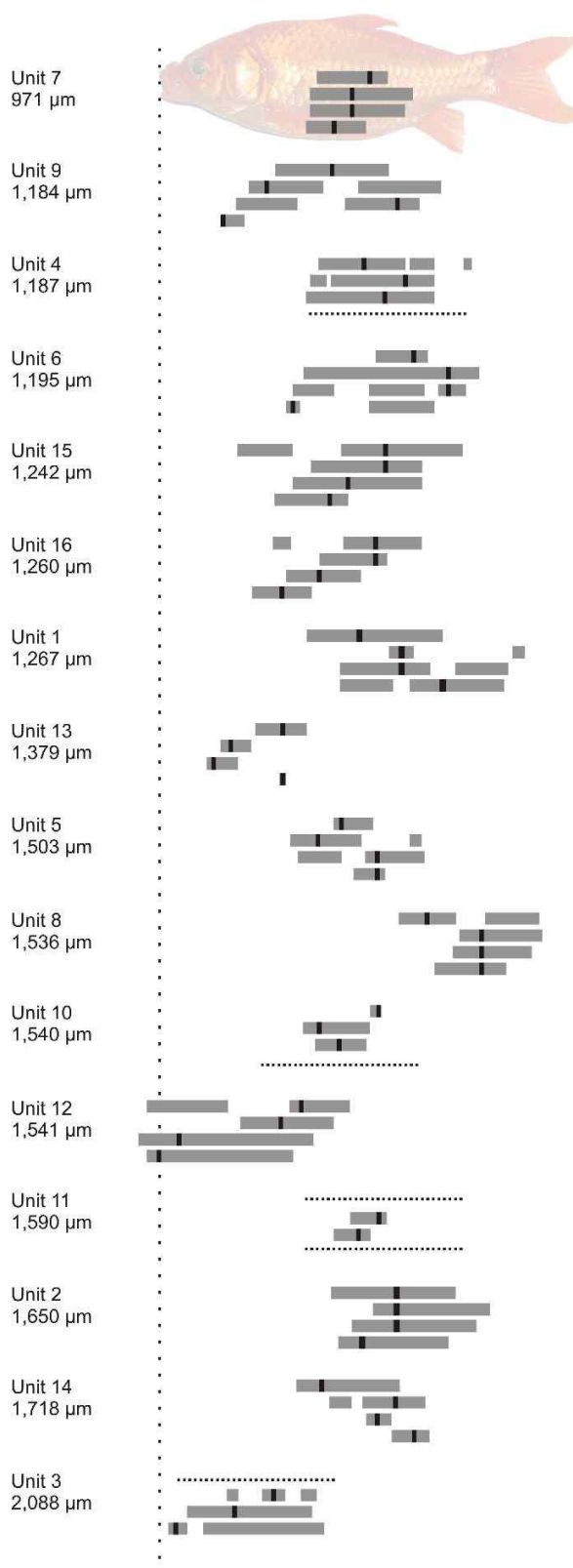


Fig. 27 Rostro-caudal positions of HMWs (sphere distance 10 mm) plotted against recording depths. For each unit, HMWs are shown for sphere vibration directions of 0° , 45° , 90° and 135° (from top to bottom), respectively. HMWs were normalised to a 10 cm long fish. Vertical black bars indicate the positions of the peaks of the SEPs. Stippled horizontal lines indicate positions where neural activity of a given unit failed to exceed the threshold of 50% of the maximum action potential frequency.

4 Discussion

4.1 Aims of research

According to theoretical studies, fish should be able to detect the location of a vibrating sphere and to sense the direction of sphere vibration. This information may be encoded by toral lateral line units. To test this hypothesis, fish were stimulated with a vibrating sphere that was presented at various rostro-caudal positions and distances relative to the fish. In addition, the direction of sphere vibration was varied. Response parameters that were analysed included the ongoing and evoked activity, phase angles, Z-values and the shapes and positions of SEPs.

4.2 Anatomy

The position of the electrode tip was verified for 12 recording sites by lesions, all of which were located in the nucleus ventrolateralis of the TS. This part of the TS receives unimodal lateral line input (McCormick and Hernandez 1996; for review, see McCormick 1989). Four lesions could not be recovered. The dorsal position of the lesions of unit 1, 2 and 5 does not necessarily indicate that these lesions were not located in the nucleus ventrolateralis of the TS. If one analyses the positions of lesions in the TS, it has to be kept in mind that the nucleus ventrolateralis of the TS is located ventrolateral to the nucleus centralis in more rostral parts of the midbrain but is located medial to the nucleus centralis in more caudal parts of the midbrain (McCormick and Hernandez 1996). All units in this thesis were recorded in the caudal half of the midbrain. Hence, dorsal lesions in the TS can, even more if the lesion is located dorso-lateral in the TS, be located in the target brain area – the nucleus ventrolateralis of the TS – of this study.

The longish shape of some lesions possibly results from the fact that the injected DC current flew through fluid that accumulated around the electrode tip inside the electrode penetration canal. Such a lesion would presumably not have a roundish but rather a longish shape. Longish lesions were distinguishable from e.g. blood vessels, fluid filled electrode penetration canals and other structures that might have been stained by cresyl violet under high magnification, basically by the fact that the tissue around a lesion was usually damaged, while the tissue around blood vessels and bleedings

was unaltered. In addition, the boundaries between a blood vessel or a bleeding and the surrounding tissue was quite sharp. In contrast, the boundaries of lesions were diffuse. Artefacts resulting from a notched microtome blade used during the sectioning of the brain can be distinguished from electrode tracks quite well, as the latter usually extend over a majority or even the whole extent of a section.

The recording depths of the twelve units that were verified by lesions varied between 971 and 2,088 μm . The recording depths of the other four units, that were not verified by lesions, were 971 μm , 1.184 μm , 1.242 μm and 1.260 μm . All these recording depths are in accordance with other studies of goldfish. Plachta et al. (2003) and Engelmann and Bleckmann (2004) recorded from toral lateral line units. They recorded units in depths that varied between 700–2,500 μm and 755–1,611 μm , respectively. The recording electrode entered the brain in different angles, as neither the dorso-vental axis of the fish nor the electrode was perfectly oriented parallel to each other. Hence the recording site was not necessarily located exactly ventral to the position of the penetration on the surface of the OT. However, there are indications that units 7 and 9 were recorded roughly in the same region as the other 12 unimodal toral lateral line units. Namely, the positions of the electrode penetrations on the surface of the OT of units 7 and 9, of which no lesions were recovered, were located amidst the penetrations of the 12 units which were recorded in the ventrolateral nucleus of the TS. All 16 units, including units 15 and 16 of which neither lesions nor positions of penetrations on the OT were recovered or determined, were characterised in terms of unit modality and turned out to react to none of the applied stimuli except lateral line stimuli. Taking the recording depths, the positions of electrode penetrations on the OT and the physiological criteria into account, it is likely that all 16 units were recorded in the nucleus ventrolateralis of the TS. However, one can not rule out that all 16 units recorded received lateral line input exclusively, especially against the background that multisensory integration occurs in the TS (for review, see Bleckmann 1994).

4.3 Electrophysiology

The minimal displacement threshold of primary lateral line afferents is about 0.02 μm peak-to-peak water displacement at 100 Hz (for review, see Bleckmann and Zelick 2009). In contrast, the majority of central lateral line units responds only to stimuli with amplitudes that are at least two

orders of magnitude above the amplitudes reported for primary lateral line afferents (for review, see Bleckmann 2008). Thus researchers who recorded from primary lateral line afferents, medullary, midbrain or diencephalic lateral line units used stimuli that varied considerably with respect to sphere displacement amplitude, sphere distance, sphere vibration frequency and stimulus duration. While many studies used goldfish as experimental animals, other species like mottled sculpins (*Cottus bairdi*), catfish (*Ancistrus spec.*), trouts (*Salmo gairdneri*; *Oncorhynchus mykiss*) or thornback guitarfish (*Platyrhinoidis triseriata*) were also used. Furthermore, in different studies multiple types of toral lateral line units were recorded. Engelmann and Bleckmann (2004) and Plachta et al. (2003) recorded from all unimodal lateral line units that they encountered, while the present study is only based on units that responded to a stationary vibrating sphere but not to a sphere that moved alongside the fish. This has to be kept in mind when the present study is compared with other lateral line studies.

4.3.1 Ongoing activity

Ongoing activity typically decreases along the ascending lateral line pathway. Hence the ongoing activity of central lateral line units is usually lower than the ongoing activity of primary lateral line afferents and medullary lateral line units (for review, see Bleckmann 1994). Primary lateral line afferents exhibit high ongoing activities. Mogdans and Bleckmann (1998, 1999) found mean ongoing activities of 1.4–63 Hz (median 21.5 Hz) and 0–85.5 Hz (median 38.7 Hz), respectively. Coombs et al. (1998) reported ongoing activities of 0.4–35.4 Hz (17.4 ± 8.8 Hz (mean \pm SD)). Chagnaud et al. (2007) found mean ongoing activities of 30.8 ± 20.9 Hz (mean \pm SD; median 28.5 Hz). Similar rates were found in other fish species. For the mottled sculpin, *Cottus bairdi*, Coombs and Janssen (1990) reported ongoing rates of 30–40 Hz and Montgomery and Coombs (1998) found ongoing activities of 35 ± 6.1 Hz (mean \pm SD).

In the medulla, i.e. in the first relay station in the ascending lateral line pathway, ongoing activity is much lower. Mogdans et al. (1997) measured mean ongoing activities of 0–16 Hz (mean 1.1 Hz). Coombs et al. (1998) found mean ongoing rates of 0–20 Hz (17.4 ± 8.8 (mean \pm SD)). Künzel (2009) measured mean ongoing activities of 13.8 ± 11.0 (mean \pm SD; median 11.9 Hz).

In the present study, 14 out of 16 units had ongoing rates of 0.01–1.40 Hz (mean \pm SD 0.44 \pm 0.45 Hz, median 0.32 Hz). The two remaining units had average ongoing activities of 12.37 Hz (unit 12) and 51.72 Hz (unit 3), respectively. The median of all 16 units was 0.36 Hz. Unlike primary afferent lateral line units, that respond predictable to stimulation (cf. Fig. 28), all toral lateral line units exhibited firing patterns that did not predictably relate to stimulation. Wojtenek et al. (1998) recorded 27 single unimodal toral lateral line units with a median ongoing activity of 0.16 Hz. 96% (n = 26) of these units had an ongoing activity of \leq 1.3 Hz, one unit had an ongoing activity of 3.9 spikes/s. Plachta et al. (1999) found 54 single unimodal toral lateral line units whose ongoing activity was \leq 1 Hz. Engelmann and Bleckmann (2004) recorded 33 single unimodal toral lateral line units and found a mean ongoing activity of 0.51 \pm 0.93 Hz. Therefore the ongoing activities observed in this study are in agreement with the data from Wojtenek et al. (1998), Plachta et al. (1999) and Engelmann and Bleckmann (2004). The only exceptions are units 3 and 12, that showed higher ongoing frequencies than those reported in literature. Despite the high ongoing activities, the response properties of the two units were similar to the response properties of the other 14 units. The average ongoing activity of unit 3 (51.72 Hz) is reminiscent of the rates reported for primary lateral line afferents (Mogdans and Bleckmann 1998; Coombs et al. 1998; Chagnaud et al. 2007). However, there is no explanation for the high ongoing activity of unit 3, since no direct projections of primary lateral line afferents into the TS are known. The average ongoing activity of units 12 (12.37 Hz) and is similar to the ongoing activity of medullary lateral line units (Mogdans et al. 1997; Coombs et al. 1998; Künzel 2009). Since the TS receives direct input from the medulla (Wullimann 1998; Bleckmann 2008) it may be possible that unit 12 is a secondary lateral line unit that ascended from the medulla into the TS and therefore shows ongoing activity that is typical for medullary units.

4.3.2 Response patterns of evoked neural activity

Responses of midbrain units were either phasic (n = 1), phasic-tonic (n = 9) or tonic (n = 6). 15 out of 16 units responded to sinusoidal water motions with one of the above response patterns, regardless of sphere position. Unit 12 was an exception as it responded with inhibition or excitation, depending on the position of the sphere. This type of response pattern can also been found in the MON (Mogdans and Kröther 2001; Künzel 2009).

Most midbrain and forebrain lateral line units show a phasic response to longlasting sinusoidal hydrodynamic stimuli (for review, see Bleckmann 1994). Engelmann and Bleckmann (2004) characterised unimodal toral lateral line units in terms of their response characteristics. They classified 13 units (76 %) as phasic and two units (12 %) as tonic. The authors also described two toral lateral line units (12 %) whose responses depended on the location of the stimulus. A rostral stimulation site led to an inhibition of neural activity whereas a more caudal stimulation site caused an excitation. These responses are similar to the responses of unit 12 recorded in this study. Engelmann and Bleckmann did not provide parameters for the quantification of the response types. Hence a comparison between the results of this study and the results of Engelmann and Bleckmann (2004) is difficult. While the results of Engelmann and Bleckmann (2004) show a phasic response to longlasting sinusoidal hydrodynamic stimuli, the results of this study are not. This maybe due to different stimulus parameters. Engelmann and Bleckmann (2004) determined the response patterns with stimuli that had a duration of 1,000 ms, whereas I used stimuli with a duration of 500 ms. In addition, Engelmann and Bleckmann (2004) used maximum sphere displacement amplitudes of 1,000 μm and sphere distance was 6–8 mm. The maximum sphere displacement used in the present study was 237 μm with a distance of 10 mm between fish and sphere.

4.3.3 Spatial excitation patterns

For stimulation of primary lateral line afferents with a stationary vibrating sphere only excitatory SEPs are reported (Coombs et al 1996). The shape of SEPs of primary lateral line afferents depends on the orientation of the neuromast(s) the primary lateral line afferent innervates (Coombs et al. 1996).

Sand (review, 1981) was the first to show that the spatial excitation patterns (SEPs) of primary lateral line afferents predictably depend on the direction of sphere vibration. Denton and Gray (1983), Gray (1984) and Gray and Best (1989) stated that the source location can be encoded by the excitation patterns of primary lateral line afferents. Ćurčić-Blake and van Netten (2006) showed that the SEPs of primary lateral line afferents for different directions of sphere vibration are also predictable from the pressure gradient patterns (cf. Fig. 28. The dependencies of sphere distance and sphere vibration direction on pressure gradient patterns was also described (Coombs and Patton 2009).

Coombs et al. (1996) modeled excitation patterns for the lateral line trunk canal based on pressure gradient patterns that were calculated from flow field equations for a dipole source (Kalmijn 1988; for review, see Morse 1948). Their model is based on the assumption that a single neuromast is located between every two pores of the lateral line trunk canal and that each neuromast inside the lateral line trunk canal responds in proportion to the outside pressure gradient. By combining their model with electrophysiological recordings Coombs et al. (1996) proved that the shape of SEPs of primary lateral line afferents is linked to the pressure gradient pattern that contains information about the position, distance and vibration angle of a sphere and that SEPs of evoked activity and plots of Z-values are largely coextensive. Scholze (unpublished) examined the effects of sphere position and sphere vibration direction on the shape of SEPs of primary lateral line afferents. He reproduced the results of Coombs et al. (1996) and, in addition, showed how sphere vibration direction alters the shape of the SEPs for four different sphere vibration directions (Fig. 28). As expected, SEPs of primary lateral line afferents depend on the pressure gradients. The shape of rectified pressure gradient curves is highly similar to curves of the SEPs (Fig. 28A, C). In addition, the plots of calculated and electrophysiologically obtained phase angle plots and Z-values, respectively, are coextensive (Fig. 28B, D).

Medullary lateral line units exhibit four types of SEPs (Mogdans and Kröther 2001). One type is similar to the SEPs of primary lateral line afferents (cf. Fig. 28C). Other SEPs of medullary lateral line units feature one excitatory and one inhibitory area. SEPs with several alternating areas of excitation and inhibition also occur in medullary lateral line units. The last type of medullary lateral line units has SEPs that show only excitation or inhibition. Künzel (2009) found only three types of medullary lateral line SEPs: SEPs were either excitatory, inhibitory or both. Coombs et al. (1998) suggested that primary-like medullary SEPs may result from lateral inhibition. Circuit diagrams for medullary lateral line units are not yet available.

SEPs of toral lateral line units were reported by Plachta et al. (1999) and by Engelmann and Bleckmann (2004). Plachta et al. (1999) examined the SEPs of 19 units and found two types of SEPs. SEPs were either narrow, showing one or two peaks, or had multiple peaks and therefore usually covered large parts of the fish surface. Engelmann and Bleckmann (2004) recorded SEPs

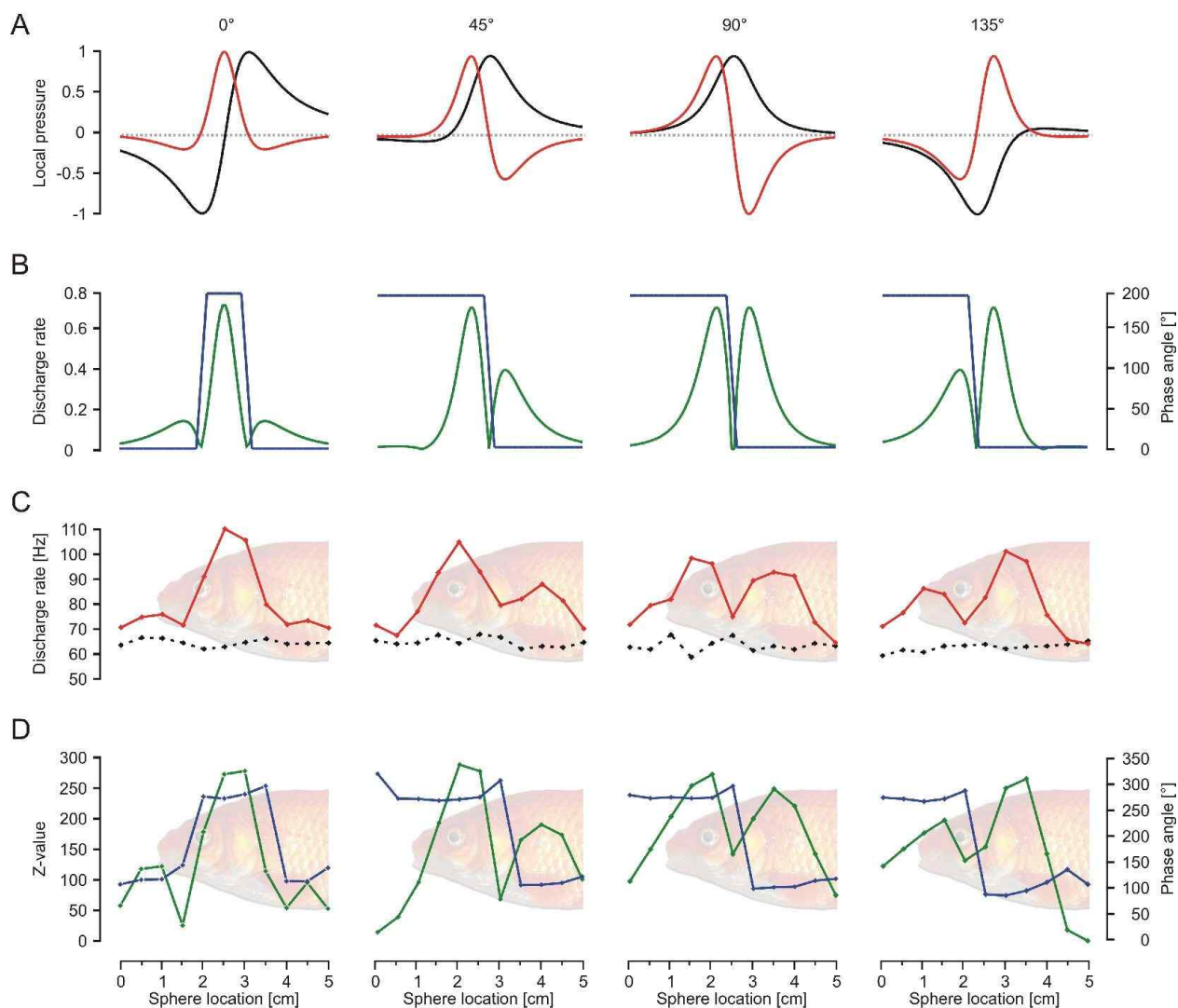


Fig. 28 A–D. **A** Pressure (black) and pressure gradients (red) of a stationary vibrating sphere positioned at different locations along a modelled lateral line canal. The distance between the sphere and the lateral line canal was kept constant. From left to right: Sphere vibration direction is 0° (parallel to the rostral-caudal-axis of the fish), 45°, 90° (perpendicular to the rostral-caudal-axis of the fish) and 135° (cf. Fig. 8). Zero crossings indicate points of phase reversal. **B** Phase angle (blue) calculated from the zero-crossings of the pressure gradients depicted in A. Predicted neural activity (green), derived from the shape of the pressure gradients shown in A. Negative pressure gradients were rectified. **C** SEPs of ongoing activity (black) and evoked activity (red), both constructed from the responses of a primary lateral line afferent to stimulation with a stationary vibrating sphere at positions that were 5 mm apart from one another. Note that the SEPs based on evoked activity (red) show strong similarities with the neural activity (green curve in B) predicted from the pressure gradient curves. **D** Phase angles (blue) and Z-values (green) based on the same PLLN unit as in C. Phase-locking is strong with Z-values up to more than 250. Note that the measured phase angles (blue) are largely in accordance with the calculated phase angles (blue curve in B). The plots of the measured Z-values (green) show strong similarities to the predicted (green curve in B) and measured (red curve in C) neural activity. The data were kindly provided by B. Scholze.

of seven units and distinguished three types. SEPs were either small, discharge rates were not raised above ongoing activity over a width of more than 4 cm. Broad SEPs covered the whole length of the fish. A third type of SEPs had areas of inhibition or excitation, depending on the position

of the vibrating sphere (Bleckmann and Engelmann 2004). These distinctions are not based on a quantitative analysis.

In this thesis even more types of SEPs were obtained. The SEPs of unit 5, 15 and 16 (Figs. 16E; 17G, H) were primary like (cf. Fig. 28C). The SEP of unit 12 (Fig. 17D) showed inhibitory and excitatory areas and therefore was similar to one of the SEPs reported by Engelmann and Bleckmann (2004). Some medullary lateral line units also showed this type of SEP (Mogdans and Kröther 2001; Künzel 2009). This and the high ongoing activity of unit 12 makes it likely, that I recorded the responses of a medullary lateral line unit that projected to the TS. The shape of a SEP of a toral lateral line unit probably depends on the type of medullary units which converge on this unit and/or on the excitatory or inhibitory input of higher brain centres. Unfortunately, physiologically and/or anatomically verified circuit diagrams for the lateral line part of the TS do not yet exist.

According to the criteria of Engelmann and Bleckmann (2004), unit 7 (Fig. 16G₄) and unit 16 (Fig. 17H₃) had small (width ≤ 4 cm) SEPs, provided the direction of sphere vibration was 135° and 90°, respectively. Units with purely excitatory SEPs that covered the whole length of the fish were not found. The large SEPs reported by Engelmann and Bleckmann (2004) may in part be due to the high stimulus amplitude (1,000 μm versus 237 μm used in this study). In the study of Engelmann and Bleckmann (2004) sphere distance was only 6–8 mm. Therefore, the differences between the effective stimulus amplitudes were even larger. Unit 7 had the narrowest SEP of all units, provided sphere vibration direction was 135° (Fig. 16G₄). In rostral-caudal direction, the SEP of this unit covered about 30 mm (fish body length was 117 mm). Assuming that the size of this SEP is independent of stimulus amplitude, this unit can encode the rostral-caudal position of an object with a precision of about 30 mm. This precision is not very high, therefore even this unit shows only a weak (with respect to the rostral-caudal axis of the fish) spatial tuning.

In former studies of toral lateral line units (Plachta et al. 1999; Engelmann and Bleckmann 2004) very few SEPs were plotted. Hence, no comparison between the rostral-caudal positions of SEPs obtained during this study and the former studies is attempted.

In nine out of 16 toral units a systematic change in sphere distance and/or sphere vibration direction did not lead to a systematic change in the location of the SEP. The SEPs of units 3, 12, 15 and 16 were shifted depending on the sphere vibration direction. In units 2, 7 and 11 the positions of the SEP did not depend on sphere vibration direction. This could be the neuronal basis that allows fish to determine the rostro-caudal position of a stationary vibrating sphere regardless of its vibration direction.

No toral lateral line units were encountered that unequivocally encoded the distance or position of a stationary vibrating sphere in terms of evoked neural activity. Such a unit would - irrespective of stimulus amplitude - show maximum excitation at a certain sphere distance or position. Furthermore, no unit sharply encoded the sphere vibration direction by changes in evoked neural activity.

4.3.4 Phase locking

Primary lateral line afferents strongly phase-lock to a vibrating sphere stimulus (e.g. Coombs et al 1996; Scholze, unpublished), up to a 1:1 phase locking of the response at lower frequencies (for review, see Bleckmann 1994). The percentage of central lateral line units that phase-lock to sinusoidal water motions decreases along the neuraxis, i.e. from medulla to telencephalon (for reviews, see Bleckmann 1994, 2008). In addition, the strength of phase-locking also decreases (for reviews, see Bleckmann 1994, 2008).

In the first relay station of lateral line information processing, the MON, phase-locking is already weaker than in primary lateral line afferents but is still present (Z-value mean \pm SD 25.4 \pm 24.0, median 17.4, range 1.0–99.2, Künzel 2009; range 4.2–525.7, Mogdans and Kröther 2001). However, the strength of phase-locking may depend on the response type. For instance, Mogdans and Kröther (2001) and Künzel (2009) found that the majority of excitatory MON units phase locked. In contrast, units that responded to a vibrating sphere stimulus with a decrease in neural activity, did not phase-lock. This is due to the reduced number or the complete absence of spikes.

According to other studies (Plachta et al. 1999; for reviews, see Bleckmann 1994, 2008) toral lateral line units show no or at most a weak phase-locking. For example, Plachta et al. (1999) found that 9

out of 53 toral lateral line units (17 %) phase-locked with Z-values >4.6. In studies done by Plachta et al. (2003) and Engelmann and Bleckmann (2004) phase-locking of toral lateral line units was not examined. The reported low phase-locking of toral lateral line units (Plachta et al. 1999) is not in line with the present study, in which 15 out of 16 units showed significant phase-locking at least at single sphere positions. This may result from the fact that Plachta et al. (1999) calculated the Z-values only for single sphere positions of a receptive field. A calculation of average phase angles for all sphere positions of a receptive field would possibly have shown that an examined toral unit shows significant average Z-values if stimulated at certain sphere positions.

Only unit 3 showed strong phase locking at nearly all sphere positions (average Z-value mean \pm SD 82.18 \pm 70.78, median 66.36, range 0.12–264.57), i.e. Z-values were similar to the Z-values of primary lateral line afferents (mean \pm SD 130.58 \pm 89.29, median 130.58, range 0.18–291.57, Scholze unpublished). In addition, the phase plots of this unit are reminiscent of the phase plots of primary lateral line afferents. This could indicate that I recorded the responses of a primary lateral line afferent that projected to the TS. In contrast, the SEPs of unit 3 show no similarities with the SEPs of primary lateral line afferents (cf. Fig. 28D). However, this is an unlikely, as no direct projections of primary lateral line afferents into the TS are reported. Another explanation could be that I recorded from a medullary lateral line unit that projected into the TS. Furthermore, with average Z-values of 4.2–525.7 only Mogdans and Kröther (2001) reported medullary units that maintained the high Z-values of primary lateral line afferents, while Künzel (2009) found maximum Z-values of medullary units that ranged from 1.0–99.2. The average Z-values of unit 12 (range 0.01–12.18) lie in the lower range of Z-values reported for medullary lateral line units (Mogdans and Kröther 2001; Künzel 2009). Hence, unit 12 is possibly a secondary lateral line unit that ascended from the medulla into the TS. This assumption is supported by the average ongoing activity of unit 12, that is similar to the ongoing activity of medullary lateral line units (see above). Nearly all other units show maximum average Z-values that are reminiscent of the average Z-values of medullary lateral line units. However, most units reach these values only at single sphere positions. Only unit 4 (range 0.00–57.10) and unit 15 (range 0.01–49.61) lie in the range of Z-values reported for medullary lateral line units (Mogdans and Kröther 2001; Künzel 2009) and exhibit respective average Z-values at multiple positions. However, there are no further indications that these units are secondary medullary lateral line units.

Lateral line hair cells are directionally sensitive (Flock and Wersäll 1962). A single lateral line afferent innervates only hair cells which are aligned in the same direction. Therefore, primary lateral line afferents are directionally sensitive and respond only to one half of a full sinusoidal wave cycle (for review, see Bleckmann 1994). Most medullary and midbrain lateral line units also respond only to one half of a full sinusoidal wave cycle (for review, see Bleckmann 1994). This indicates that cells of this type receive only input from one of the two antagonistically oriented hair cell populations. In the present study, however, one unit responded to both halves of a full wave cycle, i.e. this unit received input from antagonistically oriented hair cell populations. To my knowledge, such a unit has never been reported before.

In some cases, both, sphere position and sphere vibration direction strongly influenced the phase histograms. Phase changes can partially be explained by the flow field of a vibrating sphere (Fig. 29). If a sphere is positioned opposite to a neuromast and vibrates perpendicular to the most sensitive axis of the neuromast (Fig. 29A₂), the water movements at the left and the right side of the neuromast are quite similar. Consequentially, the neuromast will not respond since it is exposed to very low pressure gradients. However, if the sphere is moved to either side of the neuromast, the neuromast will be exposed to a strong pressure gradient and consequently will show an excitatory response (Fig. 29A₁, A₃). If, on the other hand, the sphere position is kept constant, a change in sphere vibration direction may also cause strong phase shifts. For example, a change in sphere vibration direction from 45° to 135° may cause a phase shift of 180°. Again, this can be explained by the altered flow field (Fig. 29B₂, B₄).

The effect of sphere distance on phase histograms could only be examined in one of the phase locking units (unit 15), since SEPs for unit 3 and 4 were only acquired for a single sphere distance. Sphere distance had, besides decreased neural activity, if at all, only low influence on phase histograms (Appendix C).

Some of the midbrain lateral line units featured some of the response properties of primary lateral line afferents or medullary lateral line units. However, only unit 12 shows all the response properties (ongoing activity, phase-locking, SEP with inhibitory and excitatory areas) that are reported for medullary lateral line units. The responses of all other toral lateral line units exhibited only some of

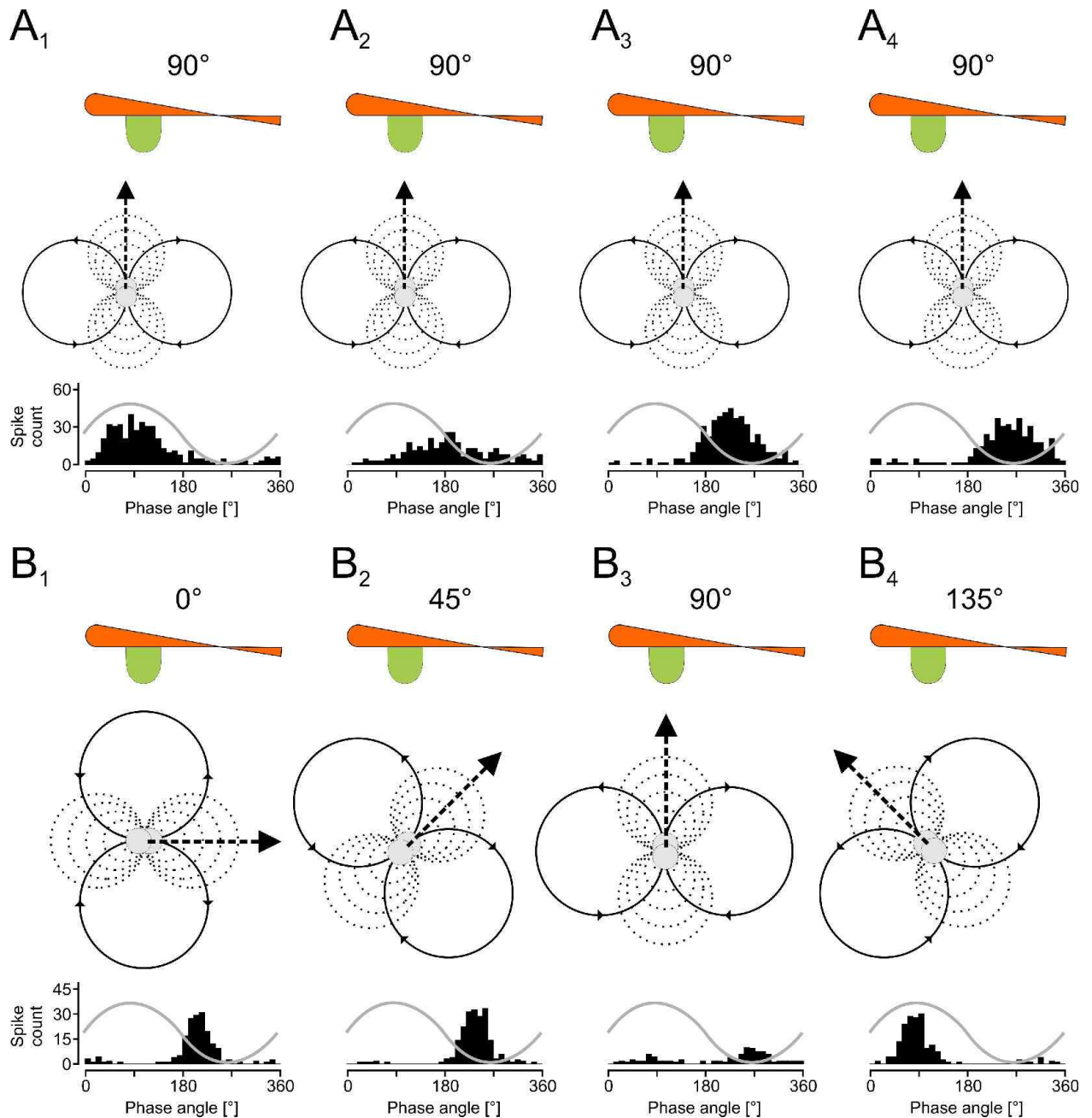


Fig. 29, A–B. Effects of sphere positions (**A**) and sphere vibration directions (**B**) on the shape of phase histograms. In each case the top row shows goldfish with a supersized neuromast (green). Middle rows depict a sphere with iso-pressure contours (dashed lines) and flow lines (solid lines with arrows) around a dipole source. Iso-pressure contours are shown for the plane that bisects the source along its axis of oscillation, indicated by the large arrowheads. The bottom rows show the phase histogram for the respective sphere position. Note that the flow direction of water particles depends on the direction of sphere displacement. **A** Stimulus distance and sphere vibration direction were kept constant. The position of the sphere was changed in steps of 5 mm along the rostral-caudal axis of the fish. A change in the rostral-caudal position of the sphere by only 10 mm (sphere vibration direction of 90°) led to a phase shift of about 180° in the neuronal response. **B** The position of the sphere was unaltered but the sphere vibration direction was changed in steps of 45°. Note that a change in sphere vibration direction from 45° to 135° also caused a 180° phase shift. Note that the unit hardly responded if sphere vibration direction was 90°.

the response properties of peripheral or medullary lateral line units. For example, unit 3 showed high ongoing activity, strong phase-locking and rapid phase changes if the sphere position was altered (Fig. 24C). In addition, the shape of the phase angle plots of unit 3 are similar to the phase angle plots of primary lateral line afferents (cf. Fig. 28D). However, unlike in primary lateral line afferents, high sphere displacements were needed to elicit a neuronal response and the SEPs were different from the SEPs of primary lateral line afferents (cf. Fig. 28C).

In summary, no toral lateral line units were found that unequivocally and sharply encoded the distance, position or sphere vibration direction of a stationary vibrating sphere by changes in phase angles and/or Z-values.

4.4 Topography

In catfish, the rostro-caudal position of the recording site corresponds to the rostro-caudal position of the receptive field of toral lateral line units (Knudsen 1977). Receptive fields of lateral line units recorded in the dorso-medial nucleus of the mesencephalic nuclear complex of *Platyrrhinoidis triseriata* are also somatotopically organised. Rostral receptive fields are represented in rostral parts of the nucleus while caudal receptive fields are mapped in more caudal parts (Bleckmann et al. 1987). Plachta et al. (2003) examined toral lateral line units that responded exclusively to a sphere passing the fish laterally. They found that rostral sphere positions are mapped in rostral and caudal sphere positions are mapped in caudal parts of the TS. In the present study, no topographical relationship between the rostro-caudal positions of SEPs and the rostro-caudal positions of electrode penetrations was found. In addition, no relationship between the rostro-caudal position of a SEP and the medio-lateral position of the recording site was observed. Furthermore, I did not find a relationship between the rostro-caudal position of a SEP and recording depth. There are at least three explanations for this: In goldfish, toral lateral line units that respond exclusively to a stationary vibrating sphere are not topographically organised. If there is a map, it could be distorted or folded. In this case, I probably failed to uncover a toral map. Last, but not least, a topographic map could be concealed by the small sample size of this study.

4.5 Limitations of this study and suggested methodical improvements

In lateral line studies fish are immobilised and artificially respired with fresh water by inserting a tube in their snout. Thus, the water flow which constantly leaves the gills, may interfere with any kind of hydrodynamic stimulus applied. Hence, one can not rule out, that the responses obtained in the present study were altered by artificial respiration.

In nature, fish will rarely (if ever) be confronted with a dipole stimulus that has a constant amplitude and/or frequency (for reviews, see Bleckmann 1994, 2008). Hence, it may well be that many central lateral line units are not optimised for the detection of single frequency, constant amplitude water motions (for review, see Bleckmann 1994). However, this study, like several other studies (e.g. Bleckmann et al. 1987, Engelmann and Bleckmann 2004), clearly shows, that there are central (toral) lateral line units that respond very well to sinusoidal water motions albeit the amplitudes necessary to drive central units were quite high. Nevertheless, in future studies, more natural stimuli (e.g. water jets, vortices or frequency and amplitude modulated dipole stimuli) should be used.

To learn more about the spatial resolution of toral lateral line units and their ability to encode the direction of sphere vibration, researchers should alter sphere position and sphere vibration direction in smaller steps. This especially should be done at positions where a change in sphere position and/or sphere vibration direction leads to marked responses. Intracellular recordings combined with tracing studies would hopefully allow to uncover the circuit diagrams which process lateral line information.

4.6 Conclusion

Based on this study, a single toral lateral line unit neither encodes the position of an object by spike rate nor by phase angle. However, if the responses (spike rates and phase angles) of several toral lateral line units are taken into account, the position and vibration direction of a stationary sphere most likely can be determined. I therefore suggest that the lateral line system uses a population code to do so, possibly as proposed for the electrosensory system in the model of Fujita et al. (2005). Whether spatially tuned lateral line units do exist in other brain areas needs to be shown.

The research reported in this thesis was performed under the guidelines by current German animal protection law. Use of animals and experimental procedures were approved by the Landesamt für Natur, Umwelt und Verbraucherschutz Nordrhein-Westfalen, permission no. 50.203.2-BN 7, 14/05.

This research was supported by the Bioinspired Concepts (BIC) program, funded by the Air Force Office of Scientific Research, the BioSenSE program, funded by the Defense Advanced Research Program Agency (DARPA) and the Cilia program, funded by the EU.

5 Bibliography

Baker CF, Montgomery JC (1999) The sensory basis of rheotaxis in the blind Mexican cave fish *Astyanax fasciatus*. *J Comp Physiol A* 184:519–527

Bartels M, Münz H, Claas B (1990) Representation of lateral line and electrosensory systems in the midbrain of the axolotl, *Ambystoma mexicanum*. *J Comp Physiol A* 167:347–356

Batschelet E (1981) The Rayleigh test. In: Batschelet E (ed) *Circular statistics in biology*. Academic Press, New York, pp 54–55

Behrend O, Branoner F, Zhivko Z, Ziehm U (2006) Neural responses to water surface waves in the midbrain of the aquatic predator *Xenopus laevis*. *Eur J Neurosci* 23:729–744

Behrend O, Branoner F, Ziehm U (2008) Lateral line units in the amphibian brain could integrate wave curvatures. *J Comp Physiol A* 194:777–783

Bensouilah M, Denizot JP (1991) Taste Buds and Neuromasts of *Astyanax jordani*: Distribution and immunochemical demonstration of co-localized substance P and Enkephalins. *Eur J Neurosci* 3:407–414

Blaxter JHS, Fuiman LA (1989) Function of the free neuromasts of marine teleost larvae. In: Coombs S, Görner P, Münz H (eds) *The mechanosensory lateral line: Neurobiology and evolution*. Springer, New York, pp 481–499

Bleckmann H (1980) Reaction time and stimulus frequency in prey localization in the surface-feeding fish *Aplocheilichthys lineatus*. *J Comp Physiol A* 140:163–172

Bleckmann H (1982) Reaction time, threshold values and localization of prey in stationary and swimming surface-feeding fish *Aplocheilichthys lineatus* (Cyprinodontidae). *Zool Jb Abt All Zool Physiol* 86:71–81

- Bleckmann H (1993) Role of the lateral line and fish behavior. In: Pitcher TJ (ed) Behaviour of teleost fishes. Chapman and Hall, London, pp 201–246
- Bleckmann H (1994) Reception of hydrodynamic stimuli in aquatic and semiaquatic animals. Werner Rathmeyer (ed) Progress in Zoology, Gustav Fischer Stuttgart, pp 1–115
- Bleckmann H (2008) Peripheral and central processing of lateral line information. J Comp Physiol A 194:145–158
- Bleckmann H, Bullock TH, Jørgensen JM (1987) The lateral line mechanoreceptive mesencephalic, diencephalic, and telencephalic regions in the thornback ray, *Platyrrhinoidis triseriata* (Elasmobranchii). J Comp Physiol A 161:67–84
- Bleckmann H, Bullock TH (1989) Central nervous physiology of the lateral line system, with special reference to cartilaginous fishes. In: Coombs S, Görner P, Münz H (eds) The mechanosensory lateral line. Neurobiology and evolution. Springer, New York, pp 387–408
- Bleckmann H, Münz H (1990) The physiology of lateral line mechanoreceptors in a teleost with multiple trunk lateral lines. Brain Behav Evol 35: 240–250
- Bleckmann H, Niemann U, Fritsch B (1991). Peripheral and central aspects of the acoustic and lateral line system of a bottom dwelling catfish, *Ancistrus sp.* J Comp Neurol 314:452–466
- Bleckmann H, Weiss O, Bullock TH (1989) Physiology of lateral line mechanoreceptive regions in the elasmobranch brain. J Comp Physiol A 164:459–474
- Bleckmann H, Zelick R (2009) Lateral line system of fish. Integ Zool 4:13–25
- Bullock TH (1982) Electroreception. Ann Rev Neurosci 5:121–170
- Burt de Perera T (2004) Spatial parameters encoded in the spatial map of the blind Mexican cave fish, *Astyanax fasciatus*. Animal Behav 68:291–295

- Caird DM (1978) A simple cerebellar system: the lateral line lobe of the goldfish. *J Comp Physiol A* 127:61–74
- Chagnaud BP, Bleckmann H, Hofmann MH (2007) Lateral line nerve fibers do not code bulk water flow direction in turbulent flow. *Zoology* 111:204–217
- Claas B (1980) Die Projektionsgebiete des Rumpfseitenliniensystems von *Sarotherodon niloticus* L. (Cichlidae, Teleostei): Neuroanatomische und neurophysiologische Untersuchungen. Dissertation, Universität Bielefeld, pp 1–136
- Claas B, Münz H (1996) Analysis of surface wave direction by the lateral line system of *Xenopus*: Source localization before and after inactivation of different parts of the lateral line. *J Comp Physiol A* 178:253–268
- Claas B, Münz H, Zittlau KE (1989) Direction coding in central parts of the lateral line system. In: Coombs S, Görner P, Münz H (eds) *The mechanosensory lateral line: Neurobiology and evolution*. Springer, New York, pp 409–419
- Coombs S, Braun CD, Donovan B (2001) The orienting response of Lake Michigan mottled sculpin is mediated by canal neuromasts. *J Exp Biol* 204:337–348
- Coombs S, Conley RA (1997a) Dipole source localization by mottled sculpin. I. Approach strategies. *J Comp Physiol A* 180:387–399
- Coombs S, Conley RA (1997b) Dipole source localization by mottled sculpin. II. The role of lateral line excitation patterns. *J Comp Physiol A* 180:401–415
- Coombs S, Finneran J, Conley RA (2000) Hydrodynamic image formation by the peripheral lateral line system of the Lake Michigan mottled sculpin, *Cottus bairdi*. *Phil Trans R Soc Lond B* 355:1111–1114
- Coombs S, Hastings M, Finneran J (1996) Modeling and measuring lateral line excitation patterns to changing dipole source locations. *J Comp Physiol A* 178:359–371

- Coombs S, Janssen J (1990) Behavioral and neurophysiological assessment of lateral line sensitivity in the mottled sculpin, *Cottus bairdi*. *J Comp Physiol A* 167:557–567
- Coombs S, Janssen J, Webb JF (1988) Diversity of lateral line systems: evolutionary and functional considerations. In: Atema J, Fay AN, Popper AN and Tavolga WN (eds) *Sensory Biology of Aquatic Animals*. Springer, New York, pp 553–593
- Coombs S, Mogdans J, Halstead M, Montgomery J (1998) Transformation of peripheral inputs by the first-order lateral line brainstem nucleus. *J Comp Physiol A* 182:609–626
- Coombs S, Montgomery J (1992) Fibers innervating different parts of the lateral line system of an Antarctic Nototheniid, *Trematomus bernachii*, have similar frequency responses despite large variation in the peripheral morphology. *Brain Behav Evol* 40:217–233
- Coombs S, New JG, Nelson M (2002) Information-processing demands in electrosensory and mechanosensory lateral line systems. *J Physiol* 96:341–354
- Coombs S, Patton P (2009) Lateral line stimulation patterns and prey orienting behaviors of mottled sculpin (*Cottus bairdi*). *J Comp Physiol A* 195:279–297
- Ćurčić-Blake B, van Netten SM (2006) Source location encoding in the fish lateral line canal. *Comp Exp Biol* 209:1548–1559
- Denton EJ, Gray JAB (1983) Mechanical factors in the excitation of clupeid lateral lines. *Proc R Soc Lond B* 218:1–26
- Denton EJ, Gray JAB (1988) Mechanical factors in the excitation of the lateral lines of fishes. In: Atema J, Fay AN, Popper AN and Tavolga WN (eds) *Sensory Biology of Aquatic Animals*. Springer, New York, pp 595–617
- Denton EJ, Gray JAB (1989) Some observations on the forces acting on neuromasts in fish lateral line canals. In: Coombs S, Görner P, Münz H (eds) *The mechanosensory lateral line: Neurobiology and evolution*. Springer, New York, pp 229–246

- Dijkgraaf S (1952) Bau und Funktionen der Seitenorgane und des Ohrlabyrinths bei Fischen. *Experientia* 8:205–244
- Dowben RM, Rose JE (1953) A metal-filled microelectrode. *Science* 118:22–24
- Ebert J, Schmitz A, Westhoff G (2006) Surface structure of the infrared sensitive pits of the boa *Corallus hortulanus*. In: Vences M, Köhler J, Ziegler T, Böhme W (eds) *Herpetologia Bonnensis II, Proceedings of the 13th Congress of the Societas Europaea Herpetologica*, pp 215–217
- Elepfandt A (1996) Sensory perception and the lateral line system in the clawed frog, *Xenopus*. In: Tinsley RC, Kobel HR (eds) *The biology of Xenopus. Symposia of the Zoological Society of London*. Oxford Univ Press, Oxford, pp 99–104
- Engelmann J, Bleckmann H (2004) Coding of lateral line stimuli in the goldfish midbrain in still- and running water. *Zoology* 107:135–151
- Engelmann J, Hanke W, Bleckmann H (2002) Lateral line reception in still- and running water. *J Comp Physiol A* 188:513–526
- Flock Å (1971) Sensory transduction in hair cells. In: Loewenstein WR (ed) *Handbook of sensory physiology I*. Springer, New York, pp 396–441
- Flock Å, Duvall AJ (1965) The ultrastructure of the kinocilium of the sensory cells in the inner ear and lateral line organs. *J Cell Biol* 25:1–8
- Flock Å, Wersäll J (1962) A study of the orientation of sensory hairs of the receptor cells in the lateral line organ of a fish with special reference to the function of the receptors. *J Cell Biol* 15:19–27
- Fujita K, Kashimori Y, Kambara T (2005) Dynamic population coding for detecting the distance and size of an object in electrolocation. *Neurocomputing* 65-66:243–251

Goldberg JM, Brown PB (1969) Response of binaural neurons of dog superior olivary complex to dichotic tonal stimuli: some physiological mechanisms of sound localization. *J Neurophysiol* 22:613–636

Goulet J, Engelmann J, Chagnaud BP, Fransosch JMP, Suttner MD, van Hemmen JL (2008) Object localization through the lateral line system of fish: theory and experiment. *J Comp Physiol A* 194:1–17

Gray JAB (1984) Interaction of sound pressure and particle acceleration in the excitation of the lateral-line neuromasts of sprats. *Proc R Soc Lond B* 220:299–325

Gray JAB, Best ACG (1989) Patterns of excitation of the lateral line of the ruffe. *J Mar Biol Ass UK* 69:289–306

Harris GG, van Bergeijk WA (1962) Evidence that the lateral-line organ responds to near-field displacements of sound sources in water. *J Acoust Soc Am* 34:1831–1841

Hassan ES (1989) Hydrodynamic imaging of the surroundings by the lateral line of the blind cave fish *Anoptichthys jordani*. In: *The mechanosensory lateral line: Neurobiology and evolution*. Springer, New York, pp 217–228

Hoekstra D, Janssen J (1985) Non-visual feeding behaviour of the mottled sculpin, *Cottus bairdi* in Lake Michigan. *Env Biol Fish* 12:111–117

Hudspeth AJ (1983) Mechanoelectrical transduction by hair cells in the acousticolateralis sensory system. *Annu Rev Neurosci* 6:187–215

Kalmijn AJ (1988) Hydrodynamic and acoustic field detection. In: Atema J, Fay RR, Popper AN, Tavolga WN (eds) *Sensory biology of aquatic animals*. Springer, New York, pp 83–130

Kalmijn AJ (1989) Functional evolution of lateral line and inner-ear sensory systems. In: Atema J, Fay AN, Popper AN and Tavolga WN (eds) *Sensory Biology of Aquatic Animals*. Springer, New York, pp 187–215

- Kaus S, Schwartz E (1986) Reaction of young *Betta splendens* to surface waves of the water. In: Bath FG, Seyfarth EA (eds) Verh Dtsch Zool Ges, Gustav Fischer, Stuttgart, pp 218–219
- Knudsen EI (1977) Distinct auditory and lateral line nuclei in the midbrain of catfishes. J Comp Neurol 173:417–432
- Knudsen EI (1982) Auditory and visual maps of space in the optic tectum of the owl. J Neurosci 2:1177–1194
- Knudsen EI, Konishi M (1978) A neural map of auditory space in the owl. Science 200:795–797
- Kroese ABA, Schellart NAM (1992) Velocity- and acceleration-sensitive units in the trunk lateral line of the trout. J Neurophysiol 68:2212–2221
- Kroese ABA, van Netten SM (1989) Sensory transduction in lateral line hair cells. In: Coombs S, Görner P, Münz H (eds) The mechanosensory lateral line: Neurobiology and evolution. Springer, New York, pp 265–284
- Kröther S, Mogdans J, Bleckmann H (2002) Brainstem lateral line responses to sinusoidal wave stimuli in still- and running water. J Exp Biol 205:1471–1484
- Künzel S (2009) Characterisation of brainstem lateral line neurons in goldfish, *Carassius auratus*: frequency selectivity, spatial excitation patterns and flow sensitivity. PhD thesis, Institute of Zoology, University of Bonn, pp 1–149
- Liao JC (2006) The role of the lateral line and vision on body kinematics and hydrodynamic preference of rainbow trout in turbulent flow. J Exp Biol 209:4077–4090
- Liao JC (2007) A review of fish swimming mechanics and behaviour in altered flows. Phil Trans R Soc Lond B 362:1973–1993
- Lohmann KJ (2000) The neurobiology of magnetoreception in vertebrate animals. T Neurosci 23:153–159

- Manger PR, Pettigrew JD (1995) Electroreception and the feeding behaviour of platypus (*Ornithorhynchus anatus*: Monotremata: Mammalia). *Phil Trans R Soc London* 347:359–381
- Martin J, Jessell T (1996) Die sensorischen Systeme. In: Kandel ER, Schwartz JH and Jessell TM (eds) *Neurowissenschaften*. Spektrum Akademischer Verlag GmbH, Heidelberg, pp 376–392
- McCormick CA (1982) The organisation of the octavolateralis area in Actinopterygian fishes: a new interpretation. *J Morphol* 171:195–181
- McCormick CA (1989) Central lateral line mechanosensory pathways in bony fish. In: Coombs S, Görner P, Münz H (eds) *The mechanosensory lateral line: Neurobiology and evolution*. Springer, New York, pp 341–364
- McCormick CA, Hernandez DV (1996) Connections of the octaval and lateral line nuclei of the medulla in the goldfish, including the cytoarchitecture of the secondary octaval population in goldfish and catfish. *Brain Behav Evol* 47:113–138
- Meek J, Schellart NAM (1978) A golgi study of the goldfish optic tectum. *J Comp Neur* 182:89–122
- Mogdans J, Bleckmann H (1998) Responses of the goldfish trunk lateral line to moving objects. *J Comp Physiol A* 182:659–676
- Mogdans J, Bleckmann H (1999) Peripheral lateral line responses to amplitude-modulated sinusoidal wave stimuli. *J Comp Physiol A* 185:173–180
- Mogdans J, Bleckmann H, Menger N (1997) Sensitivity of central units in the goldfish, *Carassius auratus*, to transient hydrodynamic stimuli. *Brain Behav Evol* 50:261–283
- Mogdans J, Kröther S (2001) Brainstem lateral line responses to sinusoidal wave stimuli in the goldfish, *Carassius auratus*. *Zoology* 104:153–166
- Montgomery JC, Coombs S (1992) Physiological Characterization of Lateral Line Function in the Antarctic Fish *Trematomus bernacchii*. *Brain Behav Evol* 40:209–216

- Montgomery JC, Coombs S (1998) Peripheral encoding of moving sources by the lateral line system of a sit-and-wait predator. *J Exp Biol* 201:91–102
- Montgomery JC, Coombs S, Baker CF (2001) The mechanosensory lateral line system of the hypogean form of *Astyanax fasciatus*. *Env Biol Fish* 62:87–96
- Montgomery JC, Hamilton AR (1997) Sensory contributions to nocturnal prey capture in the dwarf scorpion fish (*Scorpaena papillosus*). *Mar Freshwater Behav Physiol* 30:209–223
- Montgomery JC, Baker CF, Carton AG (1997) The lateral line can mediate rheotaxis in fish. *Nature* 389:960–963
- Morse PM (1948) *Vibration and sound*. McGraw Hill, New York, pp 1–468
- Münz H (1979) Morphology and innervation of the lateral line system in *Sarotherodon niloticus* (L.) (Cichlidae, Teleostei). *Zoomorphol* 93:73–86
- Münz H (1985) Single unit activity in the peripheral lateral line system of the cichlid fish *Sarotherodon niloticus* (L.) *J Comp Physiol A* 157:555–568
- Münz H (1989) Functional organization of the lateral line periphery. In: Coombs S, Görner P, Münz H (eds) *The mechanosensory lateral line: Neurobiology and evolution*. Springer, New York, pp 285–298
- Nederstigt LJA, Schellart NAM (1986) Acousticolateral processing in the torus semicircularis of the trout *Salmo gairdneri*. *Pflügers Arch* 406:151–157
- Nelson JS (2006) *Fishes of the world*, Fourth Edition. John Wiley & Sons, New York, p 3
- Northcutt RG (1989) The phylogenetic distribution and innervation of craniate mechanoreceptive lateral lines. In: Coombs S, Görner P, Münz H (eds) *The mechanosensory lateral line: Neurobiology and evolution*. Springer, New York, pp 17–78
- Northcutt RG (1997) Evolution of gnathostome lateral line ontogenies. *Brain Behav Evol* 50:25–37

- Oakley B, Schafer R (1978) *Experimental Neurobiology: A Laboratory Manual*. The University of Michigan Press, Ann Arbor. pp 352–357
- Palmer LM, Mensinger AF (2004) Effect of the anesthetic tricaine (MS-222) on nerve activity in the anterior lateral line of the oyster toadfish, *Opsanus tau*. *J Neurophysiol* 92:1034–1041
- Partridge BL, Pitcher TJ (1980) The sensory basis of fish schools: Relative roles of lateral line and vision. *J Comp Physiol A* 135:315–325
- Plachta D (2000) Responses of toral lateral line units of the goldfish, *Carassius auratus*, to dipole and complex water wave stimuli. PhD thesis, Institute of Zoology, University of Bonn, pp 1–50
- Plachta D, Mogdans J, Bleckmann H (1999) Responses of midbrain lateral line units of the goldfish, *Carassius auratus*, to constant-amplitude and amplitude modulated water wave stimuli. *J Comp Physiol A* 185:405–417
- Plachta D, Hanke W, Bleckmann H (2003) A hydrodynamic topographic map in the midbrain of goldfish *Carassius auratus*. *J Exp Biol* 206:3479–3486
- Pohlmann K, Atema J, Breithaupt T (2004) The importance of the lateral line in nocturnal predation of piscivorous catfish. *J Exp Biol* 207:2971–2978
- Pohlmann K, Grasso FW, Breithaupt T (2001) Tracking wakes: The nocturnal predatory strategy of piscivorous catfish. *Proc Nat Acad Sci* 98:7371–7374
- Piechocki R (1990) *Der Goldfisch und seine Varietäten (Carassius auratus auratus)*, 6. durchgesehene Auflage, Ziemsen, Wittenberg Lutherstadt, pp 12–34
- Puzdrowski RL (1989) Peripheral distribution and central projections of the lateral-line nerves in goldfish, *Carassius auratus*. *Brain Behav Evol* 34:110–131
- Rupp B, Wullmann MF, Reichert H (1996) The zebrafish brain: a neuroanatomical comparison with the goldfish. *Anat Embryol* 194:187–203

Sand O (1981) The lateral line and sound perception. In: Tavalga WN, Popper AN, Fay RR (eds) Hearing and sound communication in fishes. Springer, New York, pp 459–446

Schellart NAM, Wubbels RJ (1998) The auditory and mechanosensory lateral line system. In: Evans DH (ed) The physiology of fishes, 2nd edition, CRC press, Boca Raton, pp 283–312

Schellart NAM, Kamermans M, Nederstigt LJA (1987) An electrophysiological study of the topographical organization of the multisensory torus semicircularis of the rainbow trout. *Comp Biochem Physiol* 88:461–469

Schmitz A, Mogdans J, Bleckmann H (2008) Organization of the superficial neuromast system in goldfish, *Carassius auratus*. *J Morphol* 269:751–761

Schmitz A, Sehrbrock A, Schmitz H (2007) The analysis of the mechanosensory origin of the infrared sensilla in *Melanophila acuminata* (Coleoptera; Bupestridae) adduces new insight into the transduction mechanism. *Arth Struct Develop* 36:291–303

Simmons DM, Swanson LW (2009) Comparing histological data from different brains: Sources of error and strategies for minimizing them. *Brain Res Rev* 60:349–367

Späth M, Schweickert W (1977) The effect of metacaine (MS-222) on the activity of the efferent and afferent nerves in the teleost lateral-line system. *Naunyn Schmiedebergs Arch Pharmacol* 297:9–16

Sterba G (1990) Süßwasserfische der Welt. Weltbild GmbH, Augsburg, pp 271–274

Teyke T (1989) Learning and remembering the environment in the blind cave fish *Anoptichthys jordani*. *J Comp Physiol A* 164:655–662

van Netten SM and Kroese ABA (1987) Laser interferometric measurements of the dynamic behaviour of the cupula in the fish lateral line. *Hear Res* 29:55–61

van Trump WJ, McHenry MJ (2008) The morphology and mechanical sensitivity of lateral line receptors in zebrafish larvae (*Danio rerio*). *J Exp Biol* 211:2105–2115

- von Campenhausen C, Riess I, Weissert R (1981) Detection of stationary objects in the blind cave fish *Anoptichthys jordani* (Characidae). *J Comp Physiol A* 143:369–374
- von der Emde G (1990) Discrimination of objects through electrolocation in the weakly electric fish, *Gnathonemus petersii*. *J Comp Physiol A* 167:413–421
- Weisstein EW (1998) The CRC Concise Encyclopedia of Mathematics, CRC Press, Boca Raton, p 1120
- Wiltschko W, Wiltschko R (2005) Magnetic orientation and magnetoreception in birds and other animals. *J Comp Physiol A* 191:675–693
- Wojtenek W, Mogdans J, Bleckmann H (1998) The responses of midbrain lateral line units of the goldfish *Carassius auratus* to moving objects. *Zoology* 101:69–82
- Wubbels RJ (1992) Afferent response of head canal neuromast of the ruff (*Acerina cernua*) lateral line. *Comp Biochem Physiol A* 102:19–26
- Wubbels RJ and Schellart NAM (1998) An analysis of the relationship between the response characteristics and topography of directional- and non-directional auditory neurons in the torus semicircularis of the rainbow trout. *J Exp Biol* 201:1947–1958
- Wubbels RJ, Schellart NAM, Goossens JHHLM (1995) Mapping of sound direction in the trout lower midbrain. *Neurosci Letters* 3:179–182
- Wullimann MF (1998) The central nervous system. In: Evans DH (ed) *The physiology of fishes*, 2nd edn. CRC Press, Boca Raton, pp 245–282
- Zittlau KE, Claas B, Münz H (1986) Directional sensitivity of lateral line units in the clawed toad *Xenopus laevis* Daudin. *J Comp Physiol A* 158:469–477

Appendix A

Physiological salt solution

Physiological salt solution for fresh water fish (Oakley B, Schafer R 1978).

Dissolve in 700 ml distilled water:

NaCl	5.902 g
KCl	0.261 g
NaHCO ₃	2.1 g
Na ₂ HPO ₄	0.179 g
Tris-Buffer (C ₄ H ₁₁ NO ₃)	0.121 g
MgSO ₄	0.296 g

Fill up with distilled water to 750 ml, set pH to 7.2. Add 0.277 g dehydrated CaCl₂, fill up with distilled water to 1,000 ml and set pH to 7.2.

Phosphate buffer

For 1,000 ml phosphate buffer dissolve in 1,000 ml distilled water:

KH ₂ PO ₄	2.72 g
Na ₂ HPO ₄ · 2 H ₂ O	14.24 g

Paraformaldehyde solution, 4 %

Dissolve 40 g Paraformaldehyde in 1,000 ml phosphate buffer.

Paraffine embedding

Wash brain in phosphate buffer (3 x 30 min).

Dehydration of brain:

70 % ethanole	30 minutes
80 % ethanole	30 minutes
85 % ethanole	30 minutes
90 % ethanole	30 minutes
96 % ethanole	30 minutes
96 % ethanole	15 minutes
Isopropanole	30 minutes
Isopropanole/paraffine (1:1)	60 minutes at 60° C
Let isopropanole evaporate	approx. 8 hours at 60° C
Transfer brain to fresh paraffine	3 x 15 min

Cresyl violet staining of paraffine sections

Cresyl violet solution, 0.4 %, pH 3.5

Dissolve in 937 ml distilled water:

Cresyl violet	5 g
100% CH ₃ COOH	5.71 ml
0.1 M NaOH	57.1 ml

Stir at 50° until cresyl violet is solved.

Acetate buffer, pH 5.4, 0.1 M

Stock solution A - Sodium acetate, 0.1 M:

Dissolve 8.2 g CH₃COONa in 1,000 ml distilled water.

Stock solution B - Acetic acid, 0.1 M:

Dissolve 5.8 ml 100% CH₃COOH in 1,000 ml distilled water.

Mix 1,710 ml of stock solution A with 290 ml of stock solution B for 2 l of acetate buffer.

Cresyl violet staining

Xylene	2 x 15 minutes
100 % ethanole	2 minutes
90 % ethanole	2 minutes
70 % ethanole	2 minutes
50 % ethanole	2 minutes
30 % ethanole	2 minutes
Distilled water	5 minutes
Cresyl violet solution	2 minutes
Acetate buffer	10 minutes
Acetate buffer	10 minutes
70 % ethanole, 1 drop of 100 % CH ₃ COOH	5 minutes
90 % ethanole	5 minutes
100 % ethanole	5 minutes
Isopropanole	5 minutes
Xylene	15 minutes

Mount with Roti[®]- Histokitt (Carl Roth GmbH + Co. KG, Karlsruhe).

Appendix B

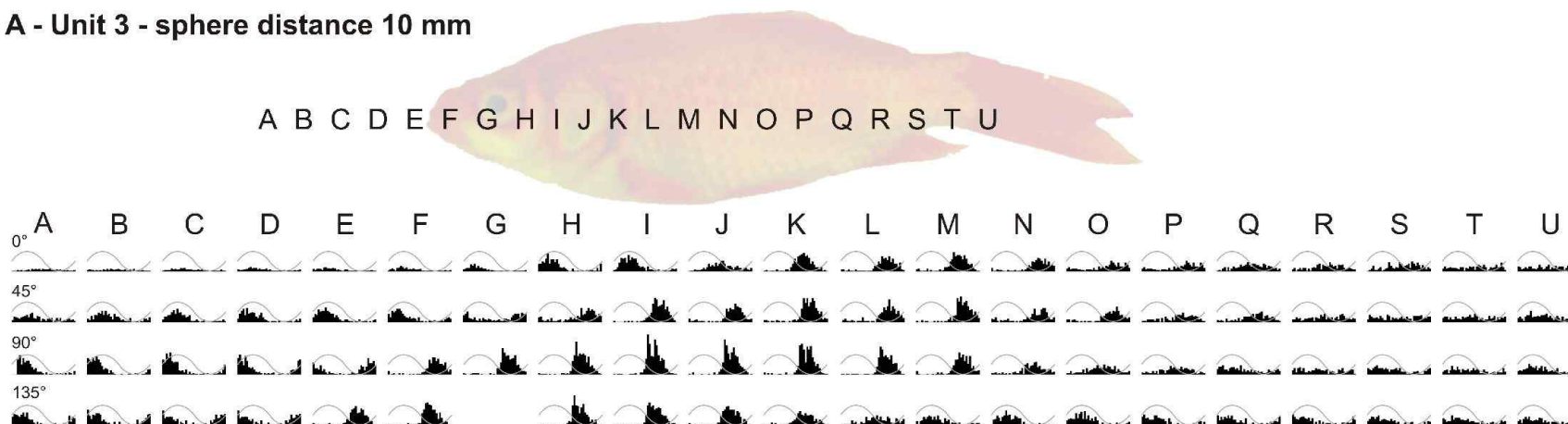
Unit	Fish length [cm]	Recording depth [μm]	Sphere displ. [μm]	Recorded sphere positions	Mean OA [Hz]	SD of OA [Hz]	Median of OA [Hz]	Range of OA [Hz]	Response pattern	Lesion recovered
1	10.1	1,267	160	42	0.80	0.69	1.14	0.16–3.05	tonic	yes
2	12	1,650	226	80	0.97	0.39	0.94	0.30–2.30	phasic-tonic	yes
3	10.6	2,088	226	96	51.72	2.75	51.64	45.15–59.00	phasic-tonic	yes
4	10	1,187	226	100	1.40	1.02	1.14	0.12–4.37	tonic	yes
5	10.5	1,503	175	144	0.01	0.02	0	0–0.09	phasic-tonic	yes
6	12	1,195	124	84	0.29	0.17	0.26	0–0.74	phasic-tonic	yes
7	11.7	971	124	61	0.05	0.11	0.06	0–0.44	phasic-tonic	no
8	11.5	1,536	237	82	0.09	0.08	0.05	0–0.56	phasic-tonic	yes
9	9.5	1,184	175	61	0.56	0.19	0.55	0–1,16	phasic-tonic	no
10	10.5	1,540	237	162	0.01	0.02	0	0–0.02	phasic	yes
11	10.2	1,590	237	177	0.03	0.03	0.02	0–0.16	phasic-tonic	yes
12	10.2	1,541	237	162	12.37	3.90	11.75	5.44–20.85	phasic-tonic	yes
13	12	1,379	237	76	0.51	0.23	0.49	0.16–1.30	tonic	yes
14	11.2	1,718	237	70	0.37	0.16	0.35	0.12–0.86	tonic	yes
15	11.2	1,242	237	159	0.22	0.15	0.19	0.02–1.14	tonic	no
16	11.1	1,260	175	73	0.34	0.28	0.30	0.02–1.72	tonic	no

Tab. 1. Overview of fish body lengths, recording depths, peak-to-peak sphere displacements, number of recorded sphere positions, average ongoing activities, standard deviations (SD) of ongoing activities, mean ongoing activities, ranges of ongoing activities, types of response patterns and recovered lesions of all recorded units.

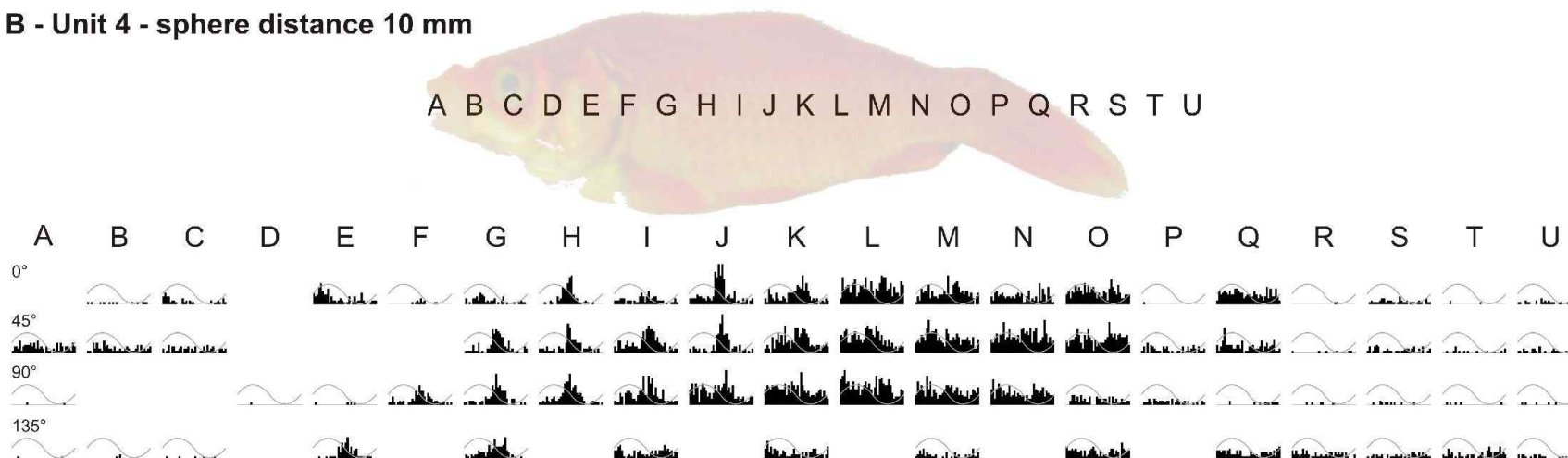
Unit	Mean R	SD R	Median R	Minimum R	Maximum R	Mean Z	SD Z	Median Z	Minimum Z	Maximum Z
1	0.21	0.12	0.20	0.02	0.54	2.06	3.58	1.72	0.03	18.42
2	0.34	0.28	0.26	0.03	1.00	2.25	2.46	1.47	0.02	12.48
3	0.51	0.22	0.52	0.02	0.79	82.18	70.78	66.36	0.12	264.57
4	0.35	0.30	0.23	0.00	1.00	6.79	12.25	1.76	0.00	57.10
5	0.27	0.34	0.13	0.00	1.00	1.27	2.26	0.35	0.00	12.64
6	0.32	0.26	0.27	0.00	1.00	2.57	2.96	1.15	0.00	14.82
7	0.42	0.33	0.34	0.00	1.00	2.52	3.72	1.00	0.00	13.40
8	0.51	0.30	0.45	0.04	1.00	1.47	1.60	1.00	0.00	8.16
9	0.28	0.21	0.21	0.00	0.98	1.23	1.02	0.95	0.00	4.39
10	0.76	0.22	0.79	0.25	1.00	2.93	3.91	1.62	0.00	16.52
11	0.35	0.16	0.33	0.08	0.85	3.39	2.98	2.47	0.00	19.71
12	0.11	0.07	0.09	0.02	0.34	2.12	2.22	1.43	0.01	12.18
13	0.32	0.24	0.24	0.06	1.00	1.67	1.41	1.31	0.00	7.62
14	0.34	0.38	0.20	0.00	1.00	1.43	1.51	1.04	0.00	7.19
15	0.27	0.20	0.24	0.01	0.88	12.80	13.72	6.81	0.10	49.61
16	0.44	0.37	0.30	0.05	1.00	1.83	2.30	1.00	0.00	10.23

Tab. 2. Overview of the means, standard deviations (SDs), medians, minima and maxima of the synchronisation coefficient R and the Z-values of all recorded units.

A - Unit 3 - sphere distance 10 mm



B - Unit 4 - sphere distance 10 mm



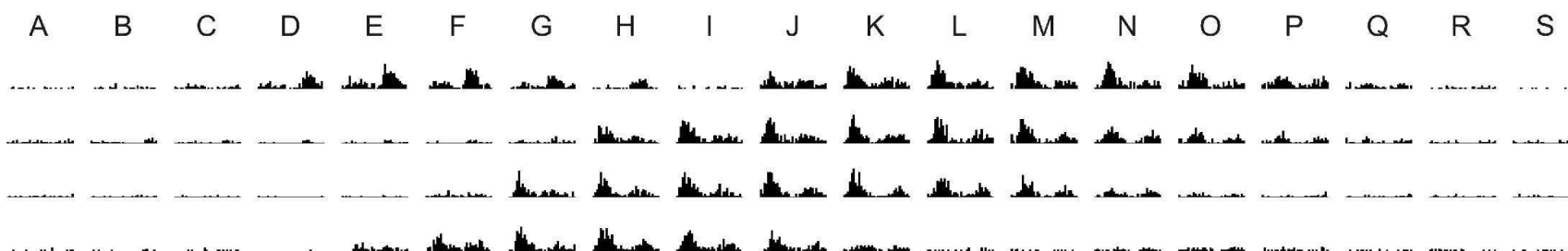
Phase histograms (bin width 10°) of responses of the toral lateral line units 3 (**A**) and 4 (**B**) to sinusoidal water motions generated by a stationary vibrating sphere at a distance of 10 mm. The x-axis (°) ranges from 0 to 360 in A and B. The y-axis (spikes/bin) in A ranges from 0 to 65 and from 0 to 25 in B. Letters A to U denote sphere positions that were altered in 5 mm steps. Fish are depicted in actual size. Sphere vibration direction was 0° (parallel to the long axis of the fish), 45°, 90° (perpendicular to the long axis and the surface of the fish), and 135°. At the positions of missing histograms no neural activity could be recorded. Note that both units responded only to one half of a full wave cycle and that the phase angles of the responses depended on both, the position of the sphere and the direction of sphere vibration.



A - Unit 15 - 10 mm sphere distance



B - Unit 15 - 15 mm sphere distance



Phase histograms (bin width 10°) of responses of the toral lateral line unit 15 to sinusoidal water motions generated by a stationary vibrating sphere at a distance of 10 (**A**) and 15 mm (**B**). mm. The x-axes (°) range from 0 to 360. The y-axes (spikes/bin) range from 0 to 30. Letters A to S denote sphere positions that were altered in 5 mm steps. Fish is depicted in actual size. Sphere vibration direction was 0° (parallel to the long axis of the fish), 45°, 90° (perpendicular to the long axis and the surface of the fish), and 135°. Note that the unit responded to both halves of a full wave cycle and that the phase angles of the responses depended on both, the position of the sphere and the direction of sphere vibration.

Erklärung

Hiermit erkläre ich, dass ich die vorliegende Arbeit eigenständig und nur unter Zuhilfenahme der angegebenen Hilfsmittel erstellt habe.

Bonn, den 10.02.2010